A Thesis Submitted for the Degree of PhD at the University of Warwick

Permanent WRAP URL:

http://wrap.warwick.ac.uk/91143

warwick.ac.uk/lib-publications

Mathematical modelling and simulation of the foot with specific application to the Achilles tendon

A thesis submitted to the University of Warwick for the degree of
Doctor of Philosophy

by

Nefeli Chatzistefani

Department of Engineering

January 2017

Table of Contents

iii

List of Tables

List of Figures

Acknowledgements

A gratifying part of this thesis is the ability to recall the course of my studies and acknowledge the support, guidance and experiences that have been bestowed upon me throughout my academic aspirations. Therefore, I would like to express my sincere gratitude to those who have influenced and supported me throughout my research the past four years.

First and foremost, I would like to thank my family for their patience, love and support during my studies. My mother's sacrifices and prayers was what sustained me thus far.

Special thanks to my supervisors Dr. Michael J. Chappell and Dr. Neil D. Evans for their support and guidance over the course of the project. Their encouragement, advice and constructive criticism helped me grow as a research scientist. Their reassurance, patience and motivation fortified me to proceed with my research goals irrespective of the size of the obstacles placed before me.

I would also like to thank all of my friends, life-long and new ones, who supported me during the writing up period of my thesis. Their friendship, love and encouragement made my experience at Warwick very memorable. A sincere thank you to my colleagues from the Biomedical Engineering department for the stimulating discussions we had, for the sleepless nights we were working together and for all the good times we have had in the last four years.

Finally, I would like to thank the School of Engineering at the University of Warwick for the Victoria Fernandes scholarship awarded to me, without which I would not be able to carry out my research.

Declaration

I, the author of this thesis titled 'Mathematical modelling and simulation of the foot with specific application to the Achilles tendon', declare that the work presented in this thesis is original and my own. The work was performed in the Department of Biomedical Engineering at the School of Engineering at the University of Warwick. This thesis was conducted under the supervision of Dr Michael J. Chappell and Neil D. Evans.

I declare that the work presented in this thesis has only been submitted to the University of Warwick for the degree of Doctor of Philosophy and has not been submitted for any other degree at any other university.

Ethical approval complying with the research code of practice of the University of Warwick has been granted by the University's Biomedical and Scientific Research Ethics Committee (BSREC) for:

i) all Gait Laboratory experiments and Ultrasound sessions at UHCW that will be mentioned in this thesis and

ii) handling and publishing all measured data from human volunteers that participated in the experiments

(BSREC full approval *Simulation of the Achilles tendon*, BSREC reference: REGO-2013-578AM01).

Parts of this thesis have been published by the author:

1. N. Chatzistefani, M.J. Chappell, C. Hutchinson, S. Kletzenbauer, N.D. Evans, <u>A mathematical model characterizing Achilles tendon dynamics in flexion,</u> Original Research Article, *Mathematical Biosciences, Volume 284, February 2017, Pages 92-102*. Journal paper explaining the full mathematical/musculoskeletal model of the Achilles tendon-

gastrocnemius muscle. Analysis and results introduced and verified by mathematicians and biomedical engineer reviewers.

2. N. Chatzistefani, M.J. Chappell, C. Hutchinson, N.D. Evans, <u>A Mathematical Model of the Achilles tendon in humans</u>, Original Research Article, *IFAC-PapersOnLine, Volume 48, Issue 20, 2015, Pages 429-434*. Journal research article introducing the full mathematical/musculoskeletal model of the muscle-tendon model. Initial results from experiments presented.

3. N. Chatzistefani, M.J. Chappell, C. Hutchinson, N.D. Evans, <u>Parameter Estimation and Structural Identifiability model of the Achilles tendon,</u> Proceedings of the 21st Congress of the European Society of Biomechanics, Prague, 5-8 July 2016. Conference paper explaining the structural identifiability and the parameter estimation of the mathematical model of the Achilles tendon-gastrocnemius muscle.

4. N. Chatzistefani, M.J. Chappell, N.D. Evans, <u>Mathematical modelling of the Achilles tendon,</u> Proceedings of PGBIOMED/ISC 2014, University of Warwick, School of Engineering, Coventry, UK, 15th-17th July 2014. Peer reviewed conference paper where the initial mathematical model of the Achilles tendon and the gastrocnemius muscle was introduced. This model was also presented to orthopedic doctors, was validated and ultrasound sessions were suggested to implement the model.

Abstract

In this thesis, the development of an anatomically meaningful musculoskeletal model of the human foot with specific application to the Achilles tendon is presented. An in vivo experimental method of obtaining parameter values for the mechanical characteristics of the Achilles tendon and the gastrocnemius muscle is presented incorporating a Hill-type muscle model. The incentive for this work has been to enable the prediction of movement with regard to Achilles tendon motion of healthy volunteers, in order to then compare it with the movement of a pathologic gait and help in preventing Achilles tendon injuries.

There are relatively few mathematical models that focus on the characterisation of the human Achilles tendon as part of a muscle-tendon unit in the literature. The mechanical properties of the Achilles tendon and the muscles connected to the tendon are usually calculated or predicted from muscle-tendon models such as the Hill-type muscle models. A significant issue in model based movement studies is that the parameter values in Hill-type muscle models are not determined by data obtained from in vivo experiments, but from data obtained from cadaveric specimens. This results in a complication when those predictive models are used to generate realistic predictions of human movement dynamics.

In this study, a model of the Achilles tendon-gastrocnemius muscle is developed, incorporating assumptions regarding the mechanical properties of the muscle fibres and the tendinous tissue in series. Ultrasound images of volunteers, direct measurements and additional mathematical calculations are used to determine the initial lengths of the muscle-tendon complex as well as the final lengths during specific movements of the foot and the leg to parameterise the model. Ground reaction forces, forces on specific joints and moments and angles for the ankle are obtained from a 3D motion capture system. A novel experimental marker placement for the Achilles tendon is developed and generated in the 3D motion capture system.

Movement dynamics of the foot are described using Newton's laws, the principle of superposition and a technique known as the method of sections. Structural identifiability analyses of the muscle model ensured that values for the model parameters could be uniquely determined from perfect noise free data. Simulated model dynamics are fitted to measured movements of the foot. Model values are obtained on an individual subject basis. Model validation is performed from the experimental data captured for each volunteer and from reconstruction of the movements of specific trajectories of the joints, muscles and tendons involved in those movements.

The major output of this thesis is a validated model of the Achilles tendon-gastrocnemius muscle that gives specific parameters for any individual studied and provides an integral component in the ultimate creation of a dynamic model of the human body. A new approach that was introduced in this thesis was the coupling of the Achilles tendon force from the musculoskeletal model to the muscle-tendon model and the non-linearity approach studied through a motion capture system. This approach and the new Achilles tendon marker placement is to the best of the authors knowledge, novel in the field of muscle-tendon research.

Abbreviations

Abbreviation	Meaning
2D	Two-dimensional
3D	Three-dimensional
AT	Achilles tendon
ADC	Analog to digital converter
BSREC	Biomedical and scientific research ethics committee
CE	Contractile Element
COP	Centre of pressure
CSV	Comma separated files
CT	Computed tomography
DV	Digital video
EDL	Extensor digitorium longus
EHL	Extersor hallucis longus
EMG	Electromyogram
FBD	Free body diagram
FDL	Flexor digitorum longus
FE	Finite element
FHL	Flexor halluces longus
GCS	Global coordinate system
GRF	Ground reaction force
HAT	Head arms trunk
IR	Infra-red
MRI	Magnetic resource images
MUAPs	Motor unit action potentials

NOC	Nuffield orthopaedic centre
OFM	Oxford food model
PB	Peroneus brevis
PEC	Parallel elastic component
PL	Peroneus longus
ROM	Range of motion
RMSE	Root Mean Square Error
SEC	Series elastic component
TA	Tibialis anterior
TP	Tibialis posterior
UHCW	University hospitals Coventry and Warwickshire
US	Ultrasound

Chapter 1. Introduction

1.1 Context and Motivation

The first pioneer of scientific gait analysis was Aristotle with his work titled *De Motu Animalium* (On the Gait of Animals) to be followed in 1680 by Giovanni Alfonso Borelli with his script also called *De Motu Animalium* (*I* et *II*). From the earliest days, it has been the hope of researchers in the field of biomechanics that gait measurements and analysis could assist in managing patients with walking disorders. During the late 1970s and early 1980s, development of computer based and video camera systems that could generate detailed studies of individuals within realistic cost and time constraints began [1, 2]. The improvements in measurement and analytical techniques have led to the production of high-quality data. The aspiration that drives most researchers nowadays is how best to use these data for the benefit of patients.

The history and evolution of clinical gait analysis has been reviewed by Sutherland [3, 4]. He stated that early investigators understood that very little could be said about the dynamic action of muscles without electromyography, so that was the initial field of investigation. Next came kinematics to be followed by kinetics and energy. There is still not an accepted general theory of why individuals walk so differently. Many explanations discuss that the cause of these differences lies in the way that particular muscles achieve specific movements [5]. Methodologies are being developed in order to determine the functions of individual muscles. A particular requirement is the development of subject specific models that combine three-dimensional imaging data of the musculoskeletal anatomy with kinematic and kinetic data.

There has been observed an increase in Achilles tendon pathologies in recent years. When overused, the Achilles tendon is one of the two most commonly injured tendons and is the most frequently ruptured one. Changes in activity such as sudden increases in the duration or intensity

1

of athletic training, or individuals engaging in irregular strenuous physical activities may cause overuse injuries and ruptures. Rupture can occur at any age and any group of individuals. However, it has been observed to occur mainly in recreational athletes aged 30-50 years and non-athletes aged 40-65 [6].

In the earlier years, it was believed that Achilles tendon ruptures and pathologies were more common in men than in women. It was suggested that oestrogen protects tendons and thus women were not as prone to injuries as men. However, a study by Longo et al., that was performed on athletes aged over 40, proved that there is no gender difference [3]. In addition, Jonge et al. in a Dutch GP-based cohort study also found that there was no gender difference present in Achilles tendon injuries [7]. They found that the incidence rate of Achilles tendinopathy is 1.85 per 1000 Dutch GP registered patients. The adult population that they investigated was between 21 to 60 years old. In 35% of the cases, a relationship with sports activity was recorded [7]. Achilles tendon rupture is commonly observed in football, basketball, tennis, running, diving, and other sports that involve a forceful push off of the foot. Achilles tendon rupture is increasing in incidence and has become one of the most disastrous sports injury since it can alter or end the career of the athlete if not treated properly [8]. Lantto et al. investigated the epidemiology of Achilles tendon ruptures and the complications that appear after operative and non-operative treatments over a 33-year period in Finland. They observed that the overall incidence per 100,000 person/years increased from 2.1 in 1979 to 21.5 in 2011 [9]. Incidence increase was observed in all age groups. In contrast to the previous studies, Lantto et al. found that the mean annual increase in incidence was 2.4% higher for non-sports related ruptures than for sports-related ruptures. Sports-related ruptures escalated during the second 11-year period of the study while non-sports-related ruptures had a gradual increase over the entire study period. Infection and re-rupture after operative treatment was found to be four times higher than in non-operative treatment [9]. Lastly, reported incidence is 7 injuries per 100,000

2

in the general population and 12 per 100,000 in competitive athletes in the UK [6]. Therefore, it is very important to investigate what cause Achilles tendon pathologies and try to find ways to prevent them from happening.

1.2 Aims and Objectives

The basic aim of this PhD project is to develop a mathematical/musculoskeletal model of the Achilles tendon using motion capture, plantar pressure analysis, parameter estimation and identifiability analysis so that it could potentially become a useful clinical tool that could evaluate gait pathologies, could help in preventing foot injuries and could assist in the rehabilitation of Achilles tendon injuries. The purpose of this study is to acquire mechanistic knowledge of the gastrocnemius muscle-Achilles tendon complex behaviour during specific movements in humans through mathematical modelling. Accurate model outcomes can be used to study how particular muscles contribute to movement coordination and propose or assess interventions to prevent foot injuries. Therefore, a validated model of the Achilles tendon that could provide specific parameters for a specific person studied, could be a first step towards creating a dynamic model of the human body.

The main objective of this project is a better understanding of the Achilles tendon, ways to prevent its injuries and how rehabilitation works through modelling of the tendon and its locality. This will help many individuals with Achilles tendon disorders that undergo short or long term therapies to i) understand the function of a healthy Achilles tendon ii) realise what limitations they have due to their injuries or disorders and iii) assist their gradual and painless rehabilitation.

1.3 Structure of the thesis

This thesis comprises of six chapters. At the beginning of each chapter a summary of the main points covered in included.

- Chapter 1 is the introductory chapter, illustrating the motivation and the main focus of this research, as well as the aims, objectives and the structure of this thesis.

- Chapter 2 forms the literature review, presenting the anatomy and physiology of the Achilles tendon and the connecting muscles, the cause of Achilles tendon injuries and an explanation of the movements studied, i.e. dorsiflexion, plantar flexion and gait. It also provides a description of the Hill muscle model and its modifications and gives a review of the musculoskeletal modelling regarding the foot that is found in the literature.

- Chapter 3 describes the instrumentation used to perform the experiments of the thesis. It explains the basic concepts of accelerometry, electromyography, motion capture, plantar pressure analysis and imaging. In this chapter, the creation of my own marker placement model appropriate for the Achilles tendon and the gastrocnemius muscle is introduced. Since this project required a novel modelling approach, this section follows the development process and is in itself a result of this research.

- Chapter 4 describes the method followed to derive the mathematical/mechanical model of this thesis. The system equations are presented and the definitions of the parameters of the equations are given.

- Chapter 5 presents the model validation and the simulation of the model. The experimental design, methodology and analysis is described. The structural identifiability, the parameter estimation and the results of the simulations are given.

- Chapter 6 presents the main conclusions of the research conducted. The results and the main concluding points are summarised, while recommendations for future research are provided.

This thesis also includes an Appendix section containing the ethics approval granted for the experiments by the University of Warwick Biomedical and Scientific Research Ethics Committee (BSREC).

Chapter 2. Literature review

Biomechanics is the science that studies the internal and external forces that act on the human body and the effects produced by these forces. Knowledge of the anatomy and physiology of the human body is thus a key, a crucial aspect of biomechanical modelling, since it helps in understanding the mechanisms responsible for human movement. In this chapter, the anatomy and physiology of the Achilles tendon, the skeletal muscles and the human skeleton are illustrated. Human gait as well as dorsiflexion and plantar flexion of the foot are described in detail since these are the movements studied in this thesis. The classic Hill-type muscle model and its modifications are introduced. Causes of Achilles tendon injuries and disorders are presented, in order to understand how easily a tendon can be injured and how important it is to develop an accurate mathematical and mechanical model of the Achilles tendon, the foot and the human body and thus dynamics in general. Lastly, already existing models of the foot and the Achilles tendon are presented along with their shortcomings in order for the reader to obtain a full picture of the field of foot kinematics and kinetics.

2.1 Anatomy and physiology of the Achilles tendon, the skeletal muscles and the human skeleton

The Achilles tendon (AT), also known as calcaneal tendon or heel cord, is a fibrous tissue that connects the *calcaneus bone* (heel) to the *plantaris*, *gastrocnemius* (calf) and *soleus* muscles of the lower leg (Figure 2.1). Tendons connect muscle to bone and are located all over the human body. The Achilles tendon begins at the middle of the gastrocnemius muscle at the level of the lower margins of the heads of the calf muscle and is located superficially along almost the entire length of the *triceps surae* muscle (the soleus and gastrocnemius muscles). At its beginning, near the middle of the calf, it receives fleshy fibres on its inner surface, almost to its lower end. Moving downwards from the calf to the heel, the Achilles tendon becomes

gradually thinner and it inserts into the middle part of the back of the calcaneus bone. The Achilles tendon is inserted into the calcaneal tuberosity with usually two additional "slips" extending medially and laterally past its apex. However, it is justified to say that it mainly inserts into the proximal aspect of the calcaneal tuberosity. The tendon spreads out slightly at its lower end, so that its narrowest part is about 4 centimetres above its insertion [10, 11].
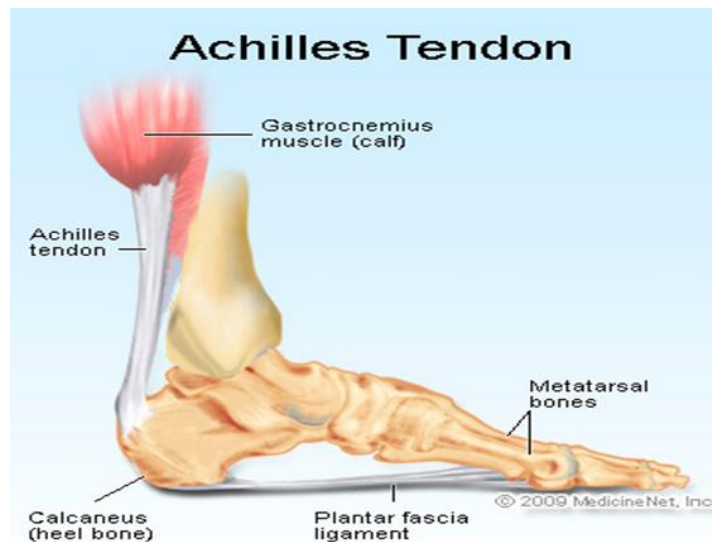
Figure 2.1. The Achilles tendon connects the heel to the calf and the soleus muscles of the leg. Image taken from [12] and used with permission of WebMD manager.

Generally, tendons have a multi-unit hierarchical structure composed of collagen molecules, fibrils, fibre bundles and tendon units [13]. The smallest structural unit of a tendon is the fibril that consists of collagen molecules aligned end-to-end in a quartet-staggered array. The next level of the structure is formed by fibres that are composed of collagen fibrils and are bound by a thin layer of connective tissue which contains blood vessels, lymphatics and nerves, the *endotenon*. Then fascicles are formed from the fibre bundles. All fascicle bundles are enclosed by the *epitenon*, which is a fine, loose connective tissue sheath containing the vascular, lymphatic and nerve supply to the tendon [13, 14]. The Achilles tendon also has a *paratenon* which is an array of thin, firmly fibrous tissue that provides protection, nutrition and stability

[10, 11, 13, 15, 16]. Tendons consist of small quantities of proteoglycans, collagen fibres, elongated cells and minimal ground substance which is an amorphous gel-like substance surrounding the cells. The collagen fibres are packed closely together and are parallel to the direction of force (Figure 2.2) [14, 17]. The Achilles tendon has a mean length of 15 cm, an average width of 20 mm and an average thickness of 5 to 6 mm at ankle level [11, 17-19].
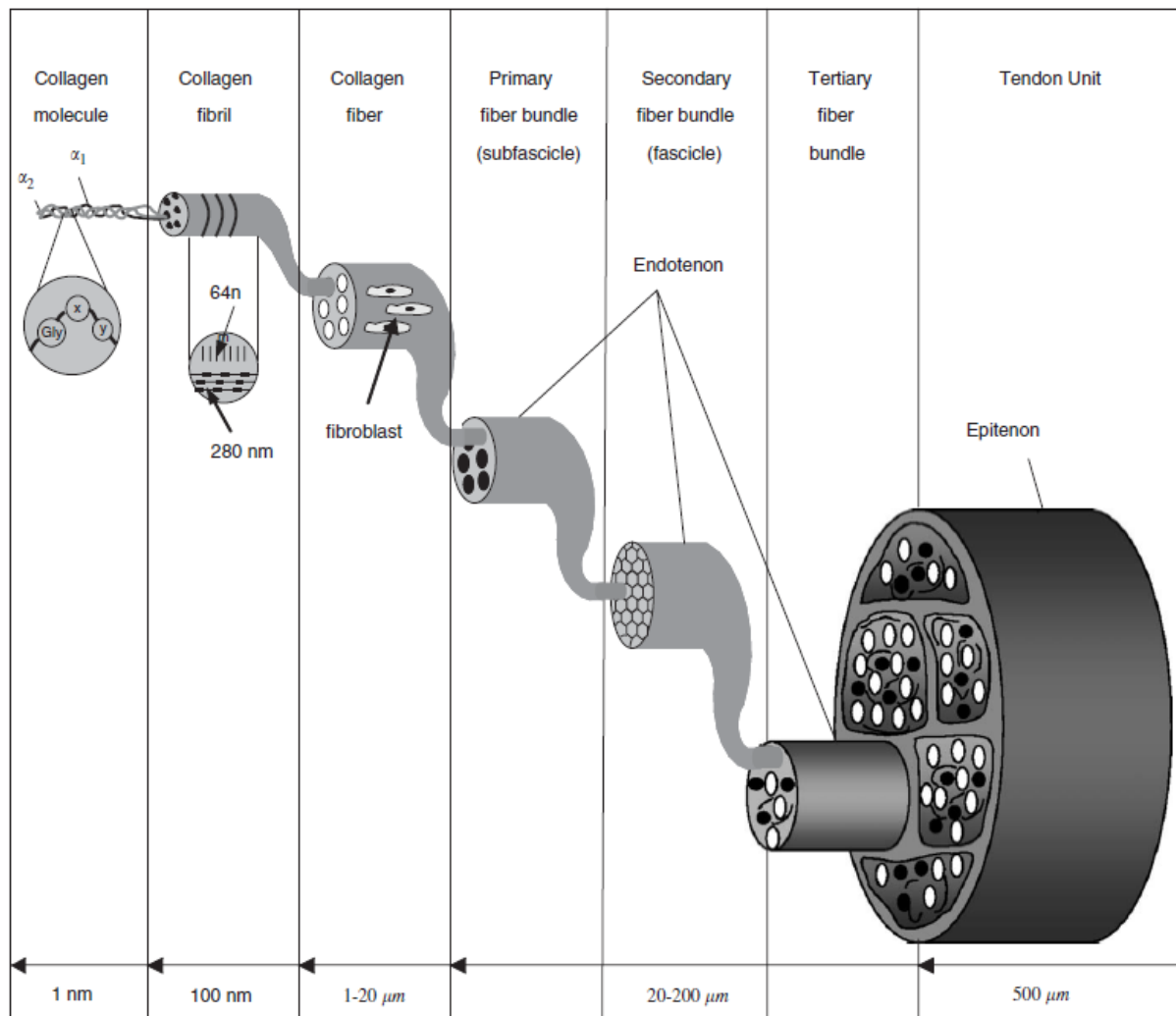
Figure 2.2. A schematic of a multi-unit hierarchical structure of the tendon. Image taken from [13].

The fascicles and the fibres of the Achilles tendon have a very specific arrangement, since the Achilles tendon is not a homogenous structure, but is built up of fascicles originating from the different parts of the triceps surae muscle. Proximally they run parallel and then rotate

distally. This means that as it descends its fibres spiral up to 90° so that the lateral fibres become surface fibres and the medial ones turn to become deep fibres (Figure 2.3) [11, 17, 18]. The Achilles tendon gains its vascular supply through: i) mainly the blood supply that reaches the tendon from the blood vessel of the paratenon; ii) the blood vessels from the muscle belly that continue into the endotenon; and iii) the bone insertion periosteal vessels that enter the endotenon, approximately up to 2 cm [15-17].
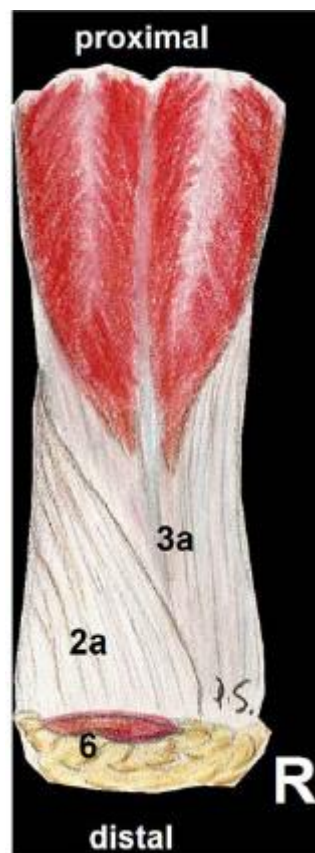
Figure 2.3. Fibre distribution of the Achilles tendon. Image taken form [11].

The skeletal system of the human body consists of the bones and their cartilages, together with tendons and ligaments. The skeleton supports the soft tissues, provides attachment points for the tendons of most skeletal muscles and therefore serves as a structural framework to the human body [20]. The skeleton is divided into the *axial skeleton*, that consists of the skull, the vertebral column and the thoracic cage, and the *appendicular skeleton*, which consists of the

pectoral (shoulder) girdle, the upper limb, the pelvic (hip) girdle and the lower limb. In this study the interest lies in the lower limbs that carry the entire weight of the body and are subject to forces when people carry out everyday movements such as standing, walking, running etc. [21]. The bones of the lower limbs are thicker and stronger than those of the upper limbs and are divided into three segments: the thigh, the leg and the foot. However, since bones are too rigid to bend without being damaged, flexible connective tissues form joints that hold the bones together while still allowing some degrees of movement [20].

Joints are categorized by structure and function. The *structural classification* depends on whether or not a joint cavity is present and on the material that binds the bones together. Structurally, there are *fibrous*, *cartilaginous* and *synovial* joints. In this thesis the term joints will be used to refer to synovial joints unless stated differently. The *functional classification* focuses on the amount of movement allowed at the joint. Based on this classification, joints are divided into *synarthroses*, which are immovable joints, *amphiarthroses*, which are slightly movable joints and *diarthroses*, which are freely movable joints [21]. Since the structural categories are more easily recognizable, structural classification will be used to describe the joints and functional properties will be specified where appropriate.

The ankle joint is the one considered in this thesis. It is a synovial, hinge, diarthrotic and uniaxial joint. A *synovial* joint has a unique characteristic that distinguishes it from other joints; namely the *synovial cavity* that exists between the articulating bones that it connects. The synovial cavity is a space between the connecting bones that allows considerable movement at the joint and that is why functionally it is considered as a freely movable joint. Figure 2.4 shows a typical ankle joint.

Plane or *planar* joints are joints where the articulating surfaces of bones are essentially flat or slightly curved. Plane joints permit only short gliding or translational movements. For

example, they permit back-and-forth or side-to-side movements. Many plane joints are biaxial,

meaning that they permit movement in two axes, or triaxial, permitting movement in three axes.

Plane joints are the intertarsal joints between the tarsal bones at the ankle.
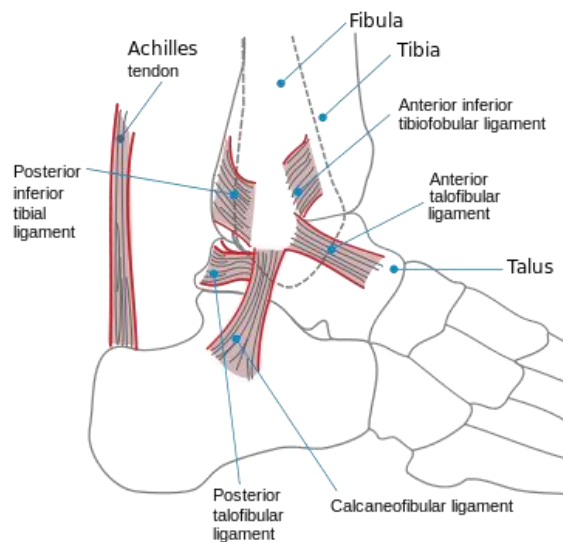
Figure 2.4. Schematic representation of the ankle joint. Image taken from [22].

In *hinge* joints the convex surface of one bone (the cylindrical projection of one bone) fits

into the concave surface (the through-shaped surface) of another bone. Hinge joints produce an

opening and closing motion like that of a hinged door where the motion is along a single plane

or a single axis and that is why they are named *uniaxial* joints. Hinge joints permit only flexion

and extension. Examples of hinge joints are the knee, the elbow, the ankle etc. However, the

knee isn't strictly just a hinge joint. Whilst it provides predominantly flexion and extension, it

is capable of up to 20 degrees of axial rotation during flexion and extension, and indeed has to

axially rotate during the last few degrees of extension (this is called the screw home

mechanism). Therefore, the predominant angular rotation of the knee occurs in thee sagittal

plane; although axial rotation needs to occur during end point of extension for stability.

In a *pivot* joint, the rounded end of one bone protrudes/fits into a "sleeve" or ring composed of bone and possibly ligaments that are part of another bone. Pivot joints are *uniaxial* since they allow rotation only around their own longitudinal axis. The atlanto-axial joint is a pivot joint, in which the atlas rotates around the axis and allows the head to turn from side to side.
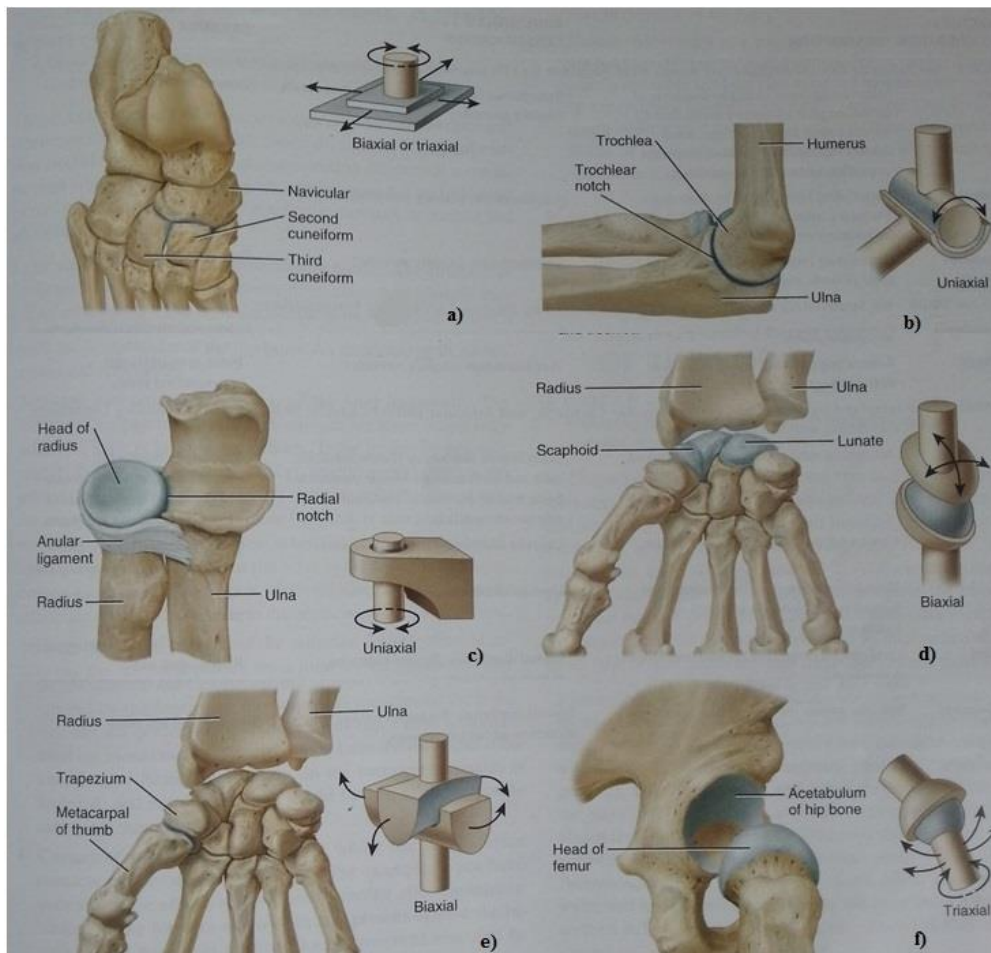
Figure 2.5. a) Plane joint b) Hinge joint c) Pivot joint d) Condyloid joint e) Saddle joint f) Ball-and-socket joint. Image taken from [20].

In *condyloid* joints or *ellipsoidal* joints, the oval surface of one bone fits into the complementary oval depression of another. Condyloid joints are *biaxial* since they permit movement around two axes, giving flexion-extension and abduction-adduction. The radiocarpal (wrist) joints and the metacarpophalangeal (knuckle) joints are typical condyloid joints.

Saddle joints resemble condyloid joints where the articular surface of one bone is saddle shaped and the surface of the other bone fits into the saddle as a sitting rider would. Saddle joints are biaxial but allow greater freedom of movement than the condyloid; they permit flexion-extension and abduction-adduction plus limited circumduction. The most well-known saddle joints are the carpometacarpal joints of the thumbs.

In *ball and socket* joints, the spherical or hemispherical head of one bone articulates with the cuplike socket of another. Such joints are *triaxial (uniaxial)* permitting movements around three axes; allowing flexion-extension, abduction-adduction and rotation. The shoulder and the hip joints are examples. Figure 2.5 shows examples of different types of joints and their freedom of movement [20, 21]. In more detail: a) shows a plane joint between navicular and second and third cuneiforms of the tarsus in foot, b) represents a hinge joint between trochlea of humerus and trochlear notch of the ulna at the elbow, c) demonstrates a pivot joint between head of radius and radial notch of the ulna, d) presents a condyloid joint between the radius and scaphoid and lunate bones of carpus (wrist), e) shows a saddle joint between the trapezium of the carpus (wrist) and metacarpal of the thumb and f) ball-and-socket joint between the head of the femur and the acetabulum of the hip bone.

Even though bones form the framework of the body and provide stabilization, they cannot move body parts by themselves. Motion and movement come from the alternation of contraction and relaxation of muscles. Most skeletal muscles attach to the bones and they produce movement when contracting by pulling the bones down. In more detail, every skeletal muscle of the body is attached to bone or other connective tissue structures at, at least, two points. The anatomy of a skeletal muscle is shown in Figure 2.6. On the left side of the figure the muscle is connected to the bone via a tendon. On the right side, the muscle is illustrated. Each muscle fibre is wrapped with a connective tissue sheath, the endomysium. Bundles of muscle fibres are bound by a collagenic sheath, the perimysium, and the entire muscle is

strengthened and wrapped by a coarse epimysium sheath. The muscle's origin is usually attached to the immovable, or less movable bone and its insertion is attached to the movable bone. Consequently, body movement happens when muscles contract across joints and their insertion moves toward their origin.
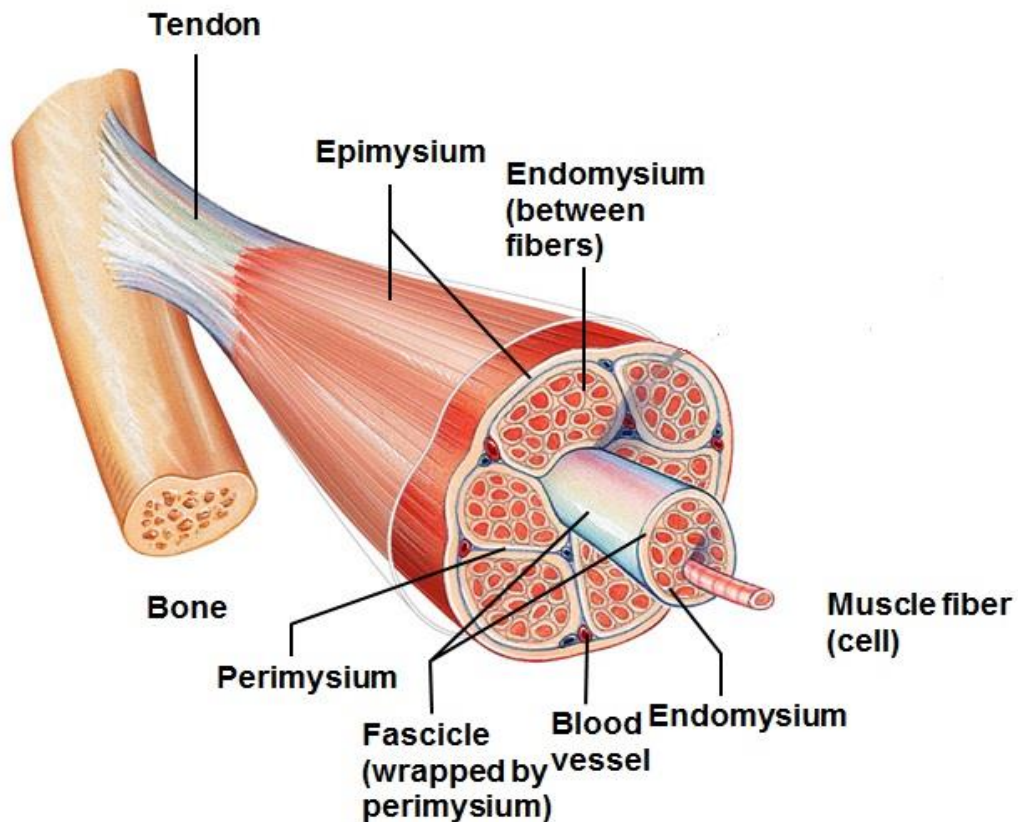
Figure 2.6. Anatomy of the skeletal muscle. Image taken from [21].

Each skeletal muscle is a distinct organ made up of hundreds of thousands of cells, the *muscle fibres*. Skeletal muscle also contains blood vessels, nerves and connective tissues surrounding muscle fibres and whole muscles. These connective tissues are the *epimysium*, the *perimysium* and the *endomysium* that attach the skeletal muscle to other muscles or to the bone. In some cases, the three connective tissue layers extend beyond the muscle fibres and create a tendon that attaches the muscle to the bone. The Achilles tendon is such a tissue that attaches the

gastrocnemius (calf) muscle to the calcaneus (heel bone). The connective tissue is called *aponeurosis* when it extends as a flat and broad sheet [21].

Muscles perform four important functions for the body: they generate heat, stabilise joints, maintain posture of the body and produce movements. Almost all movements of the human body are a result of muscle contraction. Muscle fibres, transform chemical energy into mechanical thus providing the contractile tension to maintain muscle length under load, or shorten the muscle. The skeletal muscles have natural resting lengths. When they are extended beyond this length, they produce a passive spring force. When they are released, this force returns the muscle to its natural resting length.

The muscle components that are responsible for producing the contractile force are the actin and myosin filaments of the myofibrils within the muscle fibre cells illustrated in Figure 2.7. Myofibrils are made up of three different proteins. The *contractile* proteins that generate force during contraction, the *regulatory* proteins that help switch on and off the contraction process and the *structural* proteins that keep the thin and thick filaments of the myofibrils in alignment, give the myofibril elasticity and extensibility and link the myofibril to the sarcolemma and extracellular matrix. The two contractile proteins in a muscle are actin and myosin which are thin and thick filaments respectively. Myosin is a *motor* protein that converts chemical energy to mechanical energy and produces force. When the muscle is activated, the bonding and releasing action of the actin and myosin filaments act as a mechanical ratchet system, attempting to shorten the length of the sarcomere. Muscle contraction occurs because myosin heads attach to and move along the thin filaments at both ends of a sarcomere and pull the thin filaments progressively. As a result, the thin filaments slide inward and meet at the centre of a sarcomere. Subsequently the sarcomere shortens as the Z disks, which are the ends of the thin filaments, come closer. Shortening of the sarcomere causes shortening of the whole muscle fibre which leads to shortening of the entire muscle. When the muscle length shortens, the ratio of the

overlap between the actin and myosin filaments increases, providing more bonding sites between the actin and myosin filaments, thus permitting a stronger contractile force. The maximum possible force drops when the actin filaments are pushed against the Z disc. When the muscle relaxes and returns to its natural resting length, the bonds between the actin and myosin break and the filaments are allowed to slide away to their natural position [20, 21]. Further analysis of the function of the muscles is given in Section 2.5.
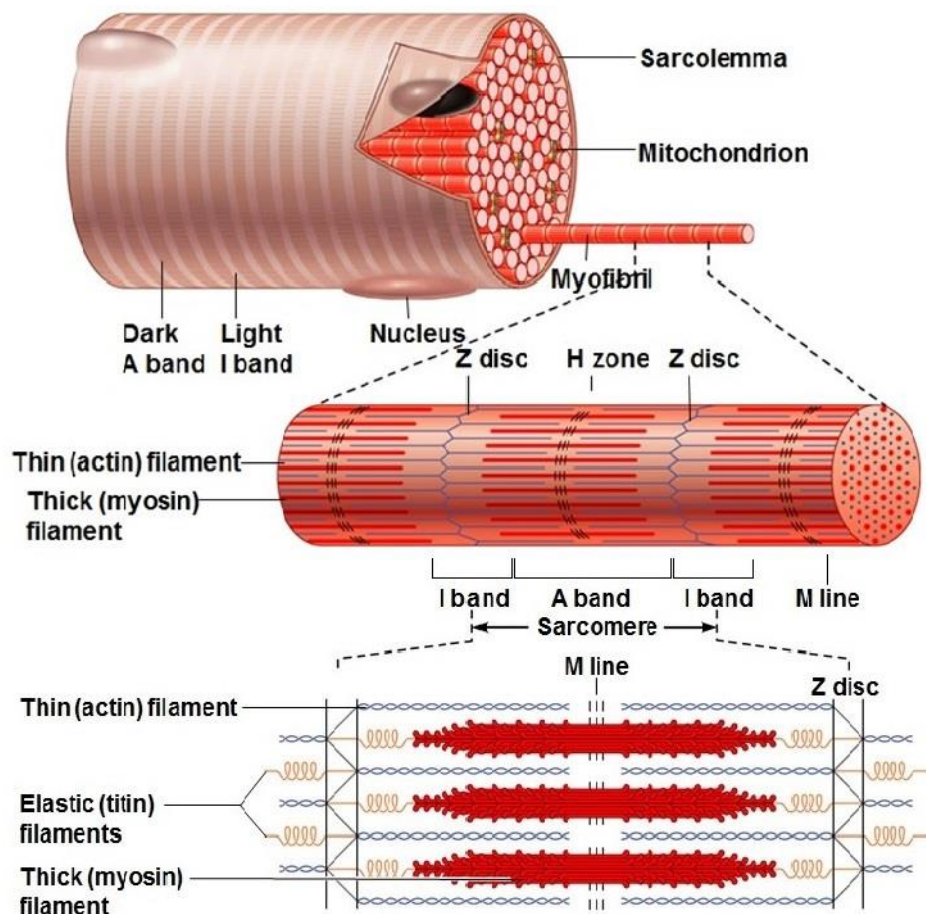
Figure 2.7. Micro anatomy of a muscle fibre. Image taken from [20].

The most powerful muscle group in the body is the leg muscles where the Achilles tendon forms the thickest and strongest tendon [16]. Its primary role is to plantar flex the ankle and therefore the Achilles tendon is essential for normal propulsion and gait. Any contraction of the calf muscles pulls the Achilles tendon, which results in pushing the foot downwards [18]. This contraction enables walking, jumping, running and standing on the toes. During a sprint or push

off the Achilles tendon may be subject to 3-12 times a person's body weight, depending upon stride, speed and any additional weight being carried or pushed. Experiments have shown that in twisting, the tendon is wrung, causing contraction of the vascular networks [17]. This results in less deformation of individual components when under tension and less fibre buckling when the tendon is lax, thus decreasing both inter-fibre friction and fibre distortion and therefore increasing strength. Studies have confirmed that torsion in the human Achilles tendon certainly exists, ranging from 11° to 65°, but never reaching 90° [17, 18]. The direction of Achilles tendon torsion primarily occurs in the distal two-thirds component of the tendon and is medial to lateral. No sexual difference in the degree of torsion has been observed [18]. Trying to explain torsion in the human Achilles tendon in a functional way has led researchers to consider in their experiments movement about the oblique axes of the ankle and subtalar joints. The Achilles tendon transmits tensile forces from the leg to the foot. These forces pass through the two joints and produce inversion of the heel accompanied by plantar flexion. Consequently, movement in both ankle and subtalar joints is produced [17, 18].

2.2 Achilles tendon injuries and disorders

Achilles tendon injuries can be caused by misalignment, overuse, medication side-effects, accidents and sometimes by the use of improper footwear [23]. The Achilles tendon, when overused, is one of the two most commonly injured tendons and is the most frequently ruptured one. Tendons are dynamic structures that respond to stresses - tensile loads - by increasing their collagen synthesis [15]. However, mechanical loading imposed on the Achilles tendon during physical activity is related to its injuries and ruptures. Changes in activity such as sudden increases in the duration or intensity of athletic training, or individuals engaging in irregular strenuous physical activities may cause overuse injuries and ruptures. More often these injuries are noticed after the subject's third decade of life. Most of Achilles tendon ruptures are found where its avascular zone is situated, approximately 2-6 cm above the point of insertion [24].

Depending on its course, an Achilles tendon rupture can be defined as acute or chronic and according to its extent it can be complete or incomplete. 75% of acute, complete ruptures appear during sporting activities especially during the 30th-50th year of age of the person involved. Acute Achilles tendon rupture can be caused by direct impact or indirect injury of the Achilles tendon while landing, taking off or falling on the foot abruptly. Chronic Achilles tendon rupture may be a result of a missed or mistreated acute rupture, or as a result of an overuse syndrome or a slow tendinosis syndrome [15]. There are two main theories concerning the factors leading to rupture:

a) the degenerative theory where a combination of hypovascularity of a part of the Achilles tendon and repeated trauma together prevent the regeneration of the tendon and lead to rupture, and

b) the mechanical theory which states that malfunction of inhibitory mechanisms of the musculo-tendinous unit decrease the tendon's threshold and lead to rupture [15].

There are two types of treatment of Achilles tendon rupture: a non-operative (closed repair) treatment and an operative (open repair) treatment. They are both effective when applied sufficiently, however in both cases there are potential dangers. Any of these two treatments should be chosen for each patient individually and only after careful consideration of the risks and benefits involved [15, 25, 26]. Supporters of non-operative treatment underline the ability of the Achilles tendon to repair itself. They stress the fact that this method is relatively risk-free and a patient can avoid problems caused by anaesthesia, wound complications like necrosis of the skin and tendons, scars and deep infections caused by open surgery. The advocates of an open repair treatment have stressed the biomechanical benefits that the patients gain. They emphasise the fact that after reconstructing the tendon and closing the gap, the normal length of the Achilles tendon is restored. They have observed that there is a great improvement in the

17

return of strength, endurance and athletic performance of the patient if the operative method has been used [15, 25]. It has been observed that there is a small rate of re-rupture in surgically repaired tendons (0% to 5%) in comparison with the larger rate (20% to 30%) of re-ruptures observed in non-operative treatments. This is cited as a major factor in the recommendation of an operative treatment in active individuals [25].

Figure 2.8. Achilles tendon disorders. Image taken from [27].

The evolution of the Achilles tendon includes: i) it is the strongest tendon in the body, ii) it has an energy-saving mechanism for fast locomotion, iii) it allows humans to walk, jump and run and iv) it is a spring and shock absorber during gait. A disadvantage is that the causes of its pathology are complicated [28]. Since the Achilles tendon is poorly vascularised for its size, it can endure long periods of relative ischaemia during physical activity. It also needs long pauses to generate its energy and has little ability to adapt to training. This causes an imbalance between the force that the muscle is able to exert and the force that the tendon is able to transmit without suffering any damage [29]. So many inflammations, disorders and ruptures occur because of its large size, its poor blood supply and its continuous functional demands during

gait [15]. Chronic Achilles tendon pathology is typified by paratendonitis, paratendonitis with tendinitis, tendinitis with rupture, insertional tendinitis, tendinosis, haglung deformity inflammation and chronic disruption (Figure 2.8) [13, 15, 16, 24, 26, 28, 29].

According to clinical and experimental studies, a normal tendon fails under extreme stress. Nevertheless, many ruptures occur due to destructive changes of the texture of tendons. Degeneration of the tendon results more commonly from mechanical overstress than from metabolic or systemic inflammatory diseases [30]. In order to evaluate acute or chronic foot and ankle disorders as well as acute or chronic ruptures and pathologies of the Achilles tendon, an overview of non-invasive imaging is given [31]. Almost every patient with a foot and ankle disorder will undergo conventional radiography in order to assess quickly and easily any acute bone injury [32]. A detailed description of the imaging techniques used to evaluate the physiology of the Achilles tendon is given in Chapter 3.

2.3 Dorsiflexion and Plantar flexion of the foot

As mentioned in Section 2.1, the ankle joint is a hinge joint located between the tibia, the fibula and the talus. Even during a simple motion such as gait, the ankle joint is continuously exposed to extreme mechanical conditions. When the foot contacts the ground, forces are generated due to the dissipation of kinetic energy [33, 34]. The ankle joint is subject to those forces and the weight of the entire body. It assists the foot in rotating about an axis of rotation with respect to the centre of the joint. The predominant movement of the ankle joint, in normal function and anatomical position, occurs in the sagittal plane. However, its movement can be triplanar which means that it can move simultaneously in the sagittal, coronal and transverse planes about the mediolateral, anteroposterior and vertical axes, respectively [2, 33]. Thus, the ankle has the ability to create flexion and extension freely in the sagittal plane and controls the

movement of the leg relative to the foot. These movements are essential for walking on any surface.

Dorsiflexion and plantar flexion are the sagittal plane motions of the foot about the ankle joint that refer to flexion and extension of the foot at the ankle respectively. Abduction and adduction are the transverse plane motions and eversion and inversion are the coronal plane motions (Figure 2.9). The muscles that activate during those motions are divided into two categories: i) *intrinsic* muscles, muscles that are located entirely within the foot and therefore have their origins and insertions within the foot and ii) *extrinsic* muscles, muscles that have their origins in the lower leg and their insertions in the foot, i.e. across the ankle joint [33]. This PhD focuses only on the sagittal plane motions, the muscles involved in flexion and extension of the ankle and the part the Achilles tendon plays in those motions.
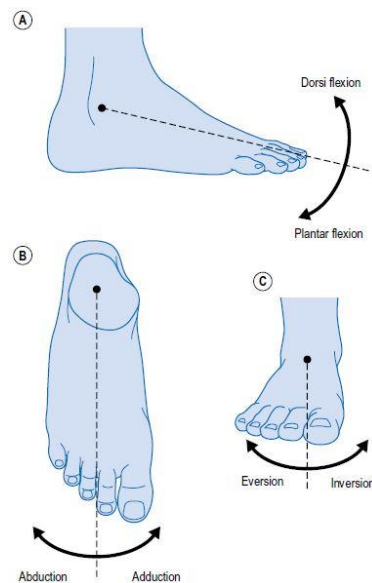
Figure 2.9. Dorsiflexion, plantar flexion, abduction, adduction, eversion and inversion of the foot about the ankle joint. Image taken from [33].

Dorsiflexion is the flexion between the foot and the body's dorsal (superior) surface where the foot moves closer to the shin. Thus, the dorsum of the foot is lifted towards the anterior surface of the leg [33, 34]. The muscles engaged in dorsiflexing the foot are the following:

i)   the *tibialis anterior*, a muscle that originates from the upper two-thirds of the lateral tibia and its insertion point is anterior to the ankle joint via the medial aspect of the foot. It attaches onto the plantar aspects of the first cuneiform and the base of the first metatarsal. The tibialis anterior is the most important muscle that creates dorsiflexion of the foot but also plays a role in inverting the foot [33, 34].

ii)   the *extensor digitorum longus*, a muscle that originates from the anterior lateral aspect of the condyle of the tibia and the upper two-thirds aspect of the fibula. Its insertion point is anterior to the ankle joint and its tendon passes under the musculature in the foot. The tendon splits into four individual tendons that attach onto the superior aspects of the bases of the middle and distal phalanges of the lateral 4 toes thus inserting on toes 2 through 5. The extensor digitorum longus creates dorsiflexion of the foot and dorsiflexion of toes 2 through to 5 [33, 34].

iii)   the *extensor hallucis longus*, a muscle that originates from the medial two-thirds of the anterior-medial aspect of the fibula and the interosseous membrane, passes under the musculature of the foot and inserts onto the superior aspect of the base of the distal phalanx of the hallux (i.e. the great toe). It creates dorsiflexion of the ankle and dorsiflexion of the hallux [33, 34].

iv)   the *peroneus tertius*, is a muscle that forms part of the extensor digitorum longus. This muscle does not reach the toes. It originates from the distal third of the anterior fibula and the interosseous membrane and its insertion point is at the dorsal base of the fifth metatarsal. The peroneus tertius acts mainly in everting the foot but also plays a small part in dorsiflexing the ankle [34].

Plantar flexion, also denoted as extension of the ankle, is the flexion between the foot and the body's plantar surface, where the foot moves away from the shin and the toes are pointed.

Therefore, when plantar flexing the ankle, the dorsum of the foot lengthens in line with the leg and points downward [33, 34]. The muscles that contribute in plantar flexion are:

i) the *gastrocnemius*, a muscle that consists of the medial and lateral heads of the gastrocnemius. The medial and lateral heads both originate from the superior aspect of the medial condyle of the femur, just superior to the femoral condyles. The two heads attach onto the upper Achilles tendon, which in turn is inserted onto the upper half of the posterior aspect of the calcaneus. Thus the gastrocnemius muscle inserts on the posterior calcaneus via the Achilles tendon. The gastrocnemius muscle plays a very large role in plantar flexing the foot. It also assists in flexing the ankle [33, 34].

ii) the *soleus*, a muscle that originates from the upper one-third of the fibula and the adjoining soleal line of the upper one-third of the tibia. The soleus muscle merges with the gastrocnemius to insert on the posterior calcaneus via the Achilles tendon as mentioned in ii). The main function of the soleus muscle is to plantar flex the foot during gait [33, 34].

iii) the *plantaris*, a muscle that has its origin at the lateral femoral condyle. It passes medially around the tibia between the soleus and the gastrocnemius and has a common insertion with the gastrocnemius. Therefore, the plantaris also inserts into the posterior calcaneus via the Achilles tendon. It assists very weakly in plantar flexing the ankle and flexing the knee and that is why it is generally considered as a redundant muscle [34].

iv) the *flexor hallucis longus*, a muscle that originates from the lower two-thirds of the posterior-medial aspect of the fibula and interosseous membrane. It goes along a channel on the posterior talus, posterior to the medial malleolus, behind the sustentaculum tali (i.e. the prominent projection on the calcaneus), and along the

medial plantar surface of the foot. Its insertion point is under the medial malleolus where it attaches onto the inferior aspect of the base of distal phalanx of the hallux. The flexor hallucis longus assists in plantar flexing the hallux, plantar flexing the foot, supporting the medial arch of the foot and creating inversion of the foot. It also plays an important role in the propulsion phase during walking where it provides anterior support when balancing on tiptoe [33, 34].

v)   the *flexor digitorum longus*, a muscle that originates from the lower two-thirds of the posterior aspect of the tibia. It runs posterior to the medial malleolus and sustentaculum tali and along the plantar surface of the foot and its insertion point is under the medial malleolus on the second through the fifth distal phalanges. The muscle's tendon splits into four branches, one for each of the lateral 4 toes. The tendons attach onto the bases of distal phalanges of the lateral 4 toes. The flexor digitorum longus plays the most important role in plantar flexing the lateral 4 toes, i.e. toes 2 to 5. It also supports the arches, inverts the foot and plantar flexes the ankle [33, 34].

vi)   the *tibialis posterior*, the origin of this muscle commences at the posterior aspect of the upper half of the interosseous membrane and adjoining borders of the tibia and fibula. It runs posterior to the medial malleolus and anterior to the sustentaculum tali. Its insertion point is under the medial malleolus. Its tendon slits into six branches that attach onto the plantar aspects of the navicular, first cuneiform and the bases of the 2nd–5th metatarsals. The tibialis posterior not only plantar flexes and inverts the foot, but also raises the longitudinal and transverse arches of the foot. It lies medially to the long axis of the ankle joint and along with the flexor digitorum longus and the flexor hallucis longus produce adduction and supination [33, 34].

vii)   the *peroneus longus*, a muscle that originates from the head and upper two-thirds of the lateral aspect of the fibula. Its insertion point is under the lateral malleolus. Its tendon splits into two branches that travel behind the lateral malleolus and under the peroneal retinaculum (foot muscle) and attach onto the plantar aspects of the first cuneiform and the base of the 1st metatarsal. Its role is to plantar flex and evert the foot as well as raise the longitudinal and transverse arches of the foot [33, 34].

viii)   the *peroneus brevis*, is a muscle that lies just beneath the peroneus longus. It originates from the lower two-thirds of the lateral aspect of the fibula. Its tendon passes behind the lateral malleolus, beneath the peroneal retinaculum and superior to the peroneal tubercle and its insertion point is under the lateral malleolus where it attaches onto the tuberosity of the 5th metatarsal. Like the peroneus longus, the peroneus brevis lies on the lateral side of the fibula and laterally to the long axis of the ankle joint, is an extrinsic muscle and produces plantar flexion and eversion of the foot as well as raises the lateral aspect of the longitudinal arch [33, 34].

Figure 2.10 shows the muscles described above and their role in the movement of the foot. The tendons of the muscles of the three compartments of the leg are shown, as well as the neurovascular bundles related to the hallucis and digitorum tendons. The plantaris muscle is seen joining the medial side of the calcaneal tendon. An indication of the muscles contributing in some important muscular functions, such as dorsiflexion, plantar flexion, eversion and inversion, is provided. Table 2.1 shows the names of the muscles from Figure 2.10 along with their abbreviations in parenthesis.
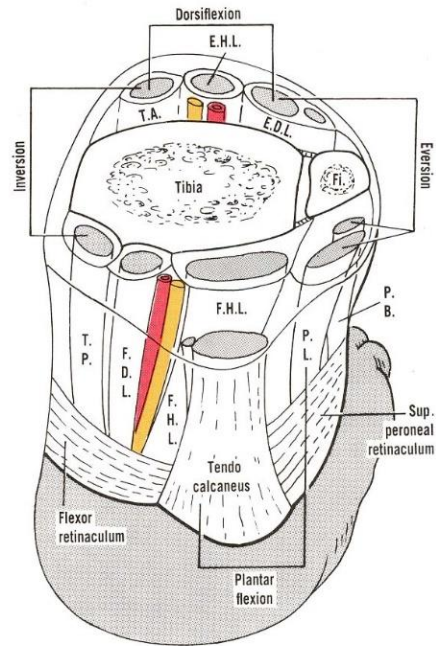
Figure 2.10. Representation of the horizontal section of the lower end of the tibia and fibula along with the abbreviations of muscles in that area. Image taken from [35].

Table 2.1. Definition of muscles shown in Figure 2.10

(T.A.)	Tibialis anterior
(E.H.L.)	Extensor hallucis longus
(E.D.L.)	Extensor digitorum longus
(P.B.)	Peroneus brevis
(P.L.)	Peroneus longus
(F.H.L.)	Flexor hallucis longus
(F.D.L.)	Flexor digitorum longus
(T.P.)	Tibialis posterior
(Tendo calcaneus)	Achilles tendon

2.4 Gait Analysis

Gait can be defined as walking, a method of movement that uses the two legs alternately and provides both propulsion and support [2]. Gait analysis in general helps us study different kinds of movement patterns as well as the forces involved in producing those movements and permits measurement and interpretation of kinematics and kinetics [36]. In order to study "normal" gait it is necessary to define what "normal" means. The term "normal" indicates the guideline, the standard against which the gait of a subject can be compared and against which pathologies, injuries and abnormalities can be observed. When defining "normal" gait a wide range of ages, a wide range of body geometries and both sexes are covered so that a suitable standard is chosen that is appropriate and adequate for all the individuals studied [2]. For example, if normal data from the gait of an elderly male subject or a child are compared with normal data obtained from fit young subjects, there will undoubtedly be large differences. However, when comparing data from healthy elderly men with those from healthy elderly women, the results may show similarities and the subject's gait may be well within normal limits that are appropriate to sex and age differences. Another aspect to be considered when describing "normal" gait is that even though a subject's gait may differ in some way from what one thinks is normal, it does not mean that it is wrong, undesirable or that it should be altered into a 'normal' gait. Many gait abnormalities compensate for some problem experienced by the subject and even though they may look abnormal, they are nevertheless not an issue.

A "normal" gait cycle begins with the initial contact of one foot with the walking surface and ends with the re-contact of that foot with the surface [36]. Sometimes the cycle is called a stride which comprises of two steps where each step is made by each foot respectively. The starting point of the gait cycle could happen at any event of the cycle. However, the most often mentioned starting point in the literature and in experiments is the heel strike, also called initial

contact, since the instant at which one foot contacts the ground is an event that can be defined very clearly and distinctively [36]. Each gait cycle is divided into two periods: i) the stance period or phase (60% of a typical gait cycle) and ii) the swing period or phase (40% of a typical gait cycle). During the stance phase most of the time the foot is in contact with the ground surface and around 25% of the typical gait cycle includes double limb support where both feet touch the ground. During the swing phase the foot is usually not in contact with the ground since the subject is moving forwards [37, 38]. As seen in Figure 2.11 a complete gait cycle comprises of: the heel strike or initial contact, the opposite toe off, the heel rise, the opposite initial contact, the toe off, the feet adjacent and the tibia vertical after which the cycle repeats itself starting again from the initial contact.
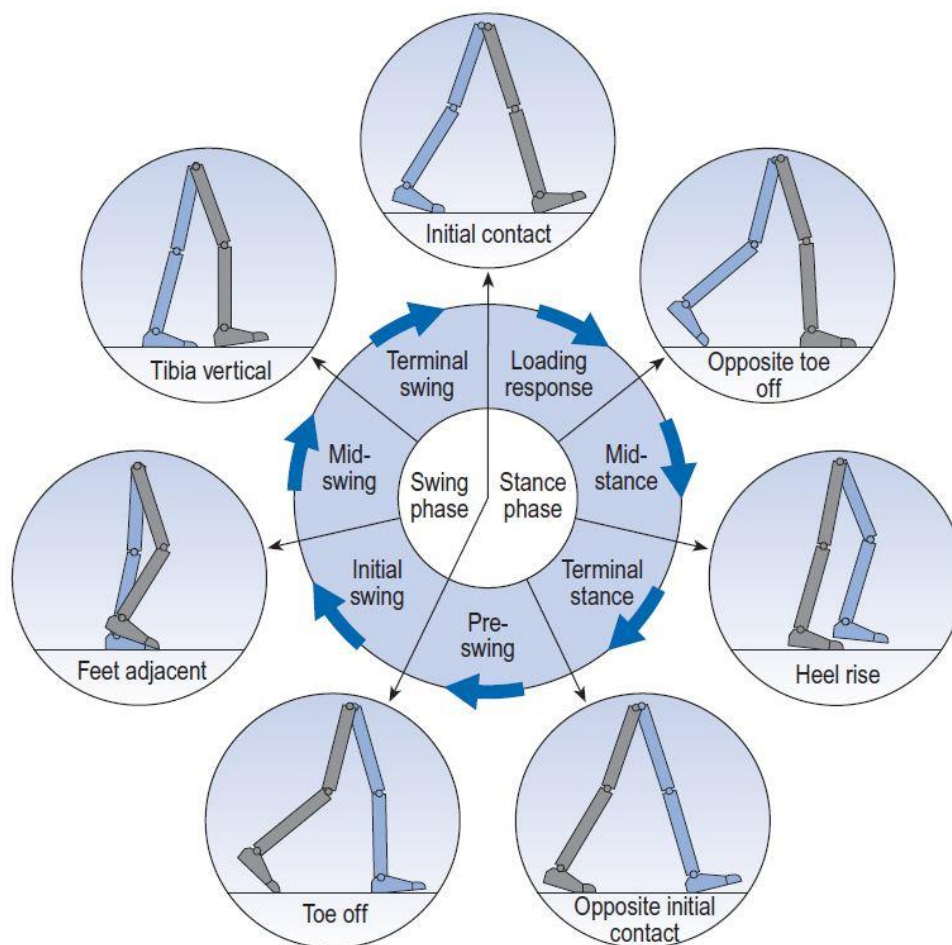
Figure 2.11. Different phases and leg positions of a complete gait cycle of the right foot. The right foot is represented by the grey colour and the left foot by blue. Image taken from [2].

The seven events represented in Figure 2.11, subdivide the gait cycle into seven periods. Four of them happen during the stance phase also called the "support phase" or "contact phase", when the foot is on the ground and three of them occur during the swing phase, when the foot is moving forwards. The stance phase takes place from heel strike until toe off and is subdivided into: loading response, mid-stance, terminal stance and pre-swing. The swing phase occurs from toe off to the next heel strike and is subdivided into: initial swing, mid-swing and terminal swing [2, 36].

The Achilles tendon contributes mainly in plantar flexing the foot about the ankle joint and less in dorsiflexing the foot. That is why it is important to know the movement of the ankle and the changes in its position during the different stages of a gait cycle. The starting point of the loading response is the initial contact which indicates the first period of the stance phase. The ground reaction force changes direction usually from upwards during the heel strike transient to upwards and backwards in the loading response directly afterwards. The ankle lies usually within a few degrees of the neutral position in dorsiflexion/plantar flexion at the time of initial contact. The tibia tilts backwards making the foot slope upwards and the only contact with the ground is maintained through the heel. Most of the time the food is somewhat supinated at this instant which causes a wear pattern to appear on the lateral side of the heel of the shoe for many people. The tibialis anterior is responsible of maintaining dorsiflexion during the swing phase and therefore is active throughout the swing and in the early stance phase. A slight moment or power exchange occurs at the ankle joint until just after initial contact. An absorption of energy by the elastic tissues of the heel, such as the Achilles tendon, and by specific materials in the footwear αre involved in the heel strike, very little of which can be recovered later in the stance phase. However, the energy lost to the environment as sound and heat is relative size [2, 33].

The next point after initial contact is the loading response of the gait cycle, also called the 'initial rocker', 'heel rocker' or 'heel pivot' which is the double support period between initial

contact and the opposite toe off. During this period the ankle plantar flexes and the foot is lowered to the ground. The plantar flexion is caused by an eccentric contraction of the tibialis anterior muscle. Plantar flexion is followed by pronation of the foot and internal rotation of the tibia. An automatic coupling between pronation/supination of the foot and any internal/external rotation of the tibia occurs. The ground reaction force increases rapidly in magnitude and its direction becomes upward and backwards. The posterior placement of the force vector produces an external plantar flexor moment at the ankle joint. During normal gait an internal dorsiflexor moment resists the external plantar flexor moment. It is produced by the tibialis anterior which contracts eccentrically, absorbing power and permitting the foot to be lowered moderately to the ground. In a pathologic gait, the tibialis anterior fails to generate sufficient moment thus allowing the foot to dorsiflex rapidly, producing an audible 'foot slap' [2, 33].

The "opposite toe off" marks the end of the double support period identified as a loading response and the beginning of the mid-stance phase which is the first period of single support. The forefoot after being lowered due to plantar flexion of the ankle, contacts the ground at 'foot flat' which normally occurs about the time of "opposite toe off". Since the tibia moves forward over the now stationary foot, the direction of ankle motion changes from plantar flexion to dorsiflexion. Foot pronation and internal tibial rotation are coupled, which means that they always occur together because of the geometry of the ankle and the subtalar joints. Both reach a peak around opposite toe off and begin to reverse. The tibialis anterior stops its contraction just as the triceps surae muscles start to contract. The ground reaction force begins to move forward along the foot, reducing the internal dorsiflexor moment at the ankle joint until it reverses and becomes a plantar flexor moment. A slight power exchange occurs at the ankle during this period of the gait cycle [2, 33].

The period of the gait cycle between opposite toe off and heel rise is called mid-stance. The 'mid-stance rocker', also called the 'ankle rocker' or 'second rocker', happens during mid-

stance and terminal stance. During this period the tibia rotates forward about the ankle joint as the triceps surae contract eccentrically, the ankle angle changes from plantar flexion to dorsiflexion and the foot remains flat on the floor. The line of the ground reaction force moves forward along the foot from the instant of foot flat and onwards moving into the forefoot prior to heel rise. The ankle presents an internal plantar flexor moment that increases throughout mid-stance and into terminal stance as the force vector moves into the forefoot. This moment is generated due to the absorption of power caused by the eccentric contraction of the triceps surae [2, 33].

The transition between mid-stance and terminal stance is called the heel rise or 'heel off'. At this point the heel starts to lift from the walking surface. How fast this transition happens varies significantly between individuals and due to differences in their speed of walking. Contraction of the gastrocnemius not only enhances the action of the soleus as far as the ankle joint is concerned, but also initiates the flexion of the knee while preventing hyperextension. The ankle dorsiflexes and reaches its peak at some point after heel rise. As the knee starts to flex, the triceps surae maintains the ankle angle. Plantar flexion begins only late in the terminal stance phase. The tibia rotates externally and the foot supinates, both increasing with time and they are coupled due to the motion at the subtalar joint. As the heel starts to lift from the ground, the toes remain flat on the surface and extension at the metatarsophalangeal (MTP) joints along an oblique line across the foot occurs. This movement is called the 'metatarsal break' or 'toe break'. After the heel rises, hind-foot inversion appears. If the ankle joint was free, unattached to tendons and muscles, then the forward motion of the body would purely dorsiflex the ankle. However, contraction of the triceps surae decelerates the forward movement of the tibia. As the femur moves forwards, an external extensor moment is generated at the knee which is opposed by an internal flexor moment. During heel rise only minor and variable power exchanges occur at the knee. At the ankle joint, the internal dorsiflexor moment continues to increase. At the

beginning the soleus muscle and then the soleus and gastrocnemius muscles combined (triceps surae) contract in an increasingly strong manner. This contraction is eccentric at first, with power absorption [2, 33].

Opposite initial contact in symmetrical normal gait occurs at approximately 50% of the gait cycle. It indicates the end of the single support period and the beginning of the pre-swing period. Pre-swing is considered to be the second period of double support. During the opposite initial contact, also called the 'opposite foot contact', the ankle is plantar flexing, the knee is flexing and the hip begins to flex. The triceps surae contract concentrically and cause the ankle to plantar flex during the period from before opposite initial contact until the foot leaves the ground at toe off. The toes at the MTP joints continue to extend which leads to a tightening of the plantar fascia. The foot then reaches its maximal supination, with hind foot inversion and external tibial rotation present. Due to all of these factors, the mid-tarsal joints lock and produce high stability of the foot for load bearing. During opposite initial contact at the ankle joint, the force vector is well in front of the joint. The concentric contraction of the triceps surae produce a high external dorsiflexor moment that is opposed by a similarly high internal plantar flexor moment. This results in the highest power generation of the entire gait cycle that accelerates the limb forward into the swing phase [2, 33].

The period that follows is toe off that usually occurs at about 60% of the gait cycle. It distinguishes pre-swing from the initial swing and is the period of time when the stance phase ends and the swing phase begins. Immediately after toe off appears the peak of the ankle joint plantar flexion. The magnitude of plantar flexion depends on the method of measurement and the ability of each individual to flex their feet. Just before toe off, the triceps surae ceases to contract. During the swing phase, the tibialis anterior begins to contract in order to bring the ankle up into a neutral or dorsiflexed position. During pre-swing, at the ankle joint the internal plantar flexor moment decreases rapidly while the magnitude of the ground reaction force

31

reduces. The moment at the ankle joint as well as the power generation peak reach zero as the foot leaves the ground at toe off [2, 33].

Feet adjacent distinguishes initial swing (lift off) from *mid-swing*. It is the period of the gait cycle when the swinging leg succeeds the stance phase leg and the two feet are found side by side. The swing phase lasts for about 40% of the gait cycle and the feet become adjacent at about the half of this time. At the point when the feet are adjacent, the ankle joint changes again from a plantar flexed position that it maintains around toe off to a neutral or dorsiflexed position at terminal swing. The knee flexes and shortens the swing phase leg which then produces toe clearance. The plantar flexion of the ankle is achieved by the contraction of the anterior tibial muscles even though the force of contraction is much less than that required to control foot lowering following initial contact. During the period of time that the feet are adjacent, the toes approach the ground very closely. Although the degree of foot supination decreases following toe off, the foot remains supinated to a small extent until the next initial contact. Only very small moments and power exchanges are seen at the ankle joint, since only the weight of the foot is involved and only weight bearing conditions apply [2, 33].

Tibial vertical, is the point in time that separates the periods of mid-swing and terminal swing. It is named such since the tibia of the swinging leg becomes vertical, which happens at around 86-90% of the gait cycle. After toe clearance, and usually before the tibia becomes vertical, the ankle position becomes less important as it may be anywhere between a few degrees of dorsiflexion and a few degrees of plantar flexion prior to the next initial contact. The ankle joint is held in position by the continuous contraction of the tibialis anterior. However, this contraction increases before the initial contact, in anticipation of the greater contraction forces which will be needed during the loading response. The ankle moment continues to be negligible with very little power exchange. The gait cycle in a normal gait ends at the next initial contact

of the same foot. Since it is confusing to denote the end of the cycle as 'initial contact', sometimes it is called 'terminal foot contact' [2, 33].
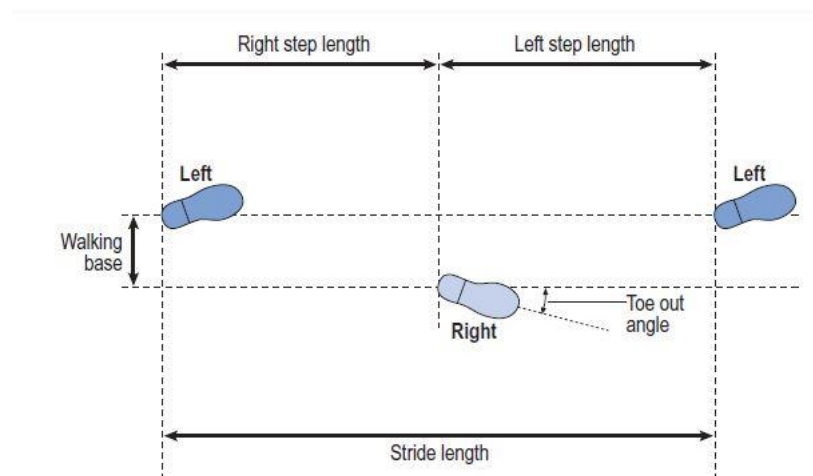
Figure 2.12. Representation of the step length, the stride length and the walking base during gait. Image taken from [2].

Apart from the stance and swing phases of the gait cycle there are also other important gait parameters that a researcher should recognise when analysing gait such as: step length, stride length, walking base and cadence. Step length is defined as the distance from the initial contact of one foot with the surface to the initial contact of the other foot with the surface, i.e. the left step length is the distance from one heel strike of the right foot to the first consecutive heel strike of the left foot as seen in Figure 2.12. The step length has a maximal length for each individual since it results from the leg length, height, and overall abilities of the individual. Stride length is determined as one complete gait cycle, as the distance between two successive placements of the same foot. So the stride length is the horizontal distance covered along the plane of progression during one stride and is equal to the sum of the two step lengths, i.e. it is the distance covered from the first heel strike of the right foot to the second heel strike of the right foot as seen in Figure 2.12. The walking base, that is also known as 'stride width' or 'base of support', is defined as the side-to-side distance between the line of the two feet. It is generally measured at the midpoint of the back of the heel or sometimes below the centre of the ankle

joint of each foot (Figure 2.12). The preferred unit for stride length and step length is metres and for the walking base is millimetres. Cadence is the number of steps that occur during normal gait at a given period of time that is generally considered to be around a minute, so its units are steps per minute. Cadence varies between individuals and between men and women. Women usually take smaller steps, and thus have a natural cadence of six to nine steps per minute more than men [2, 36]. When one starts running an increase in cadence appears since the initial step length increases. As mentioned above, step length has a finite maximal length. Up to that point, an increase in step length correlates with an increase in speed. However, after attaining that maximal step length, an increase in speed can only occur due to an increase in cadence [1, 2, 36].

2.4.1 Applications of Gait Analysis

Gait analysis has been practiced for more than a century, but has only recently become available and hands-on for an office setting and the non-elite athlete due to the development of technology. Before the arrival and use of technology, gait analysis was observed and interpreted without the assistance of computers, motion capture methods or videography, but depended only on the clinical experience of the researcher/expert who performed the experiments, the observations and the further analysis of the gait studied [36]. The advance of technology over the last 20 years has considerably benefitted the practice of gait analysis as it has aided the progress and practice of many disciplines in medicine. Gait analysis nowadays is more reliable since it uses computers and videography to capture, observe and interpret the different possible kinds of movements [36, 39]. The measurements are now more accurate and the observations more reliable since videography allows the analyst to break a movement of a subject frame by frame and study it thoroughly. Also, the rapid development of computer technology helps the analyst to interpret intricate data through analysis and the automatic calculation of complex measurements of angles, forces, moments, powers, electromyograms etc. of the movements

studied. Thus, motion capture systems and videography aids in obtaining better observations and measurements of a subject's gait, assists in analysing and interpreting kinetics, kinematics and movement patterns as well as the forces involved in producing those movements, such as ground reaction forces, joint forces and muscle forces [36].

Motion capture and videography have been used broadly in modern medicine not only to observe gait analysis, but also to assist in different disciplines. For example, they have been employed in rehabilitation clinics to assist in developing and monitoring rehabilitation programmes for patients that have suffered strokes, that have had accidents or suffer from other pathologies affecting their gait and for children with genetic muscular abnormalities. They have also been used in order to identify subtle patterns of kinematic or kinetic abnormalities during dynamic periods that are not visible in static examinations. This helps clinicians to diagnose injuries in early stages, to treat ongoing injuries more effectively and to prevent injuries from happening. Another field that has used motion capture systems and videography is the field of orthotics and prosthetics in order to improve orthotic design prescriptions and to assess the progress of a patient using orthotics during a therapy programme. Also the military uses the above mentioned methods to monitor and assess patients that have sustained traumatic limb amputations and have prostheses. Motion capture systems are also widely used with the assistance of pressure monitors, such as insole pressure sensors, in order to examine and evaluate specific abnormalities and pathologies of the foot such as foot drop [36].

In this thesis, dorsiflexion and plantar flexion movements as well as gait analysis experiments were conducted in the University of Warwick Gait Laboratory to support and validate the simulation of the Achilles tendon models developed with the help of a motion capture system.

2.5 Classic Hill-type muscle models and modifications

For a full understanding of normal gait, it is necessary to know which muscles are active during the different parts of the gait cycle. When describing and creating a muscle-tendon model, Hill-type muscle models are commonly used [40]. In the early 1930's Hill developed a simple, but widely accepted, model of muscle function that can describe in a satisfactory way skeletal and cardiac muscles. The original Hill muscle model is suitable for defining the basic mechanics of the muscles and for modelling specific beaviours of muscles during voluntary human movements [40, 41].

In Figure 2.13 the classical Hill muscle model is represented. The Hill muscle model consists of three elements: the contractile element (CE) and two non-linear spring elements, one in series (SE) and one in parallel (PE). It is a mechanical model that describes the mechanical characteristics of the anatomical components of the main part of the muscle that are connected to a free tendon. The muscle and its main internal components are described by the l_{m} part in Figure 2.13 and the free tendon is portrayed by the l_{t} part in the Figure.
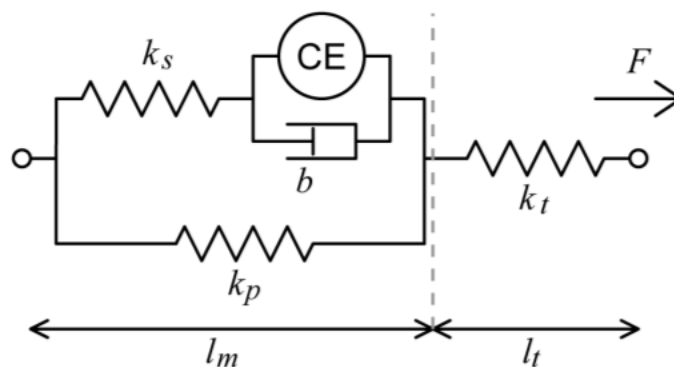
Figure 2.13. Representation of the classical Hill muscle model. Image taken from [42].

The contractile element (CE) denotes the contractile force produced by the actin-myosin cross bridges that were described in Section 2.1 and can be seen in Figure 2.13. A damping element b is connected in parallel with the CE, which represents the resistance to movement

when fluid is moving in and out between the actin-myosin filaments when the sarcomere lengthens or shortens [40]. The damping element denotes the ability of the muscle to resist the shortening or lengthening of the muscle depending on the movement studied. A spring element k_s is linked in series with the CE and damping element and represents the elasticity in the Z-disc, titin filaments, actin filaments and myosin filaments. Another spring element k_p is connected in parallel with all of the above mentioned components. It characterises the elastic properties of the epimysium, perimysium and endomysium that wrap around the muscle fibre fascicles. The elasticity that the parallel component provides, gives the muscle its ability to return to its natural resting length once it has been released from a stretched length that lays beyond its natural resting length. Lastly, there is a spring component k_t that is linked in series with the classical Hill muscle and belongs to the l_t part of the model as seen in Figure 2.13. This component represents the free tendon that connects to the muscle. This muscle-tendon model is connected to the bones at the point of origin and point of insertion and exerts tension force at these two points. The mathematical equations describing the damping and spring elements shown in Figure 2.13 are presented below.

The force of the serial spring element is given by the following equation:

$$F_{ks} = -k_s (x_{ks} - x_{ks0}) \qquad\qquad \text{(Eqn. 2.1)}$$

where x_{ks0} is the natural resting length of the serial spring element when no force is generated.

The force of the damping element b is given by:

$$F_b = -b \frac{dx_b}{dt} \qquad\qquad \text{(Eqn. 2.2)}$$

where dx_b/dt is the lengthening or shortening velocity of the damping element and the contractile element.

The force of the parallel spring element k_p is given by:

$$F_{kp} = -k_p(x_{kp} - x_{kp0}) \tag{Eqn. 2.3}$$

where x_{kp0} is the natural resting length of the parallel spring element when no force is generated.

The length of the whole muscle as presented in Figure 2.13 is l_m which is equal to the length of the parallel spring element x_{kp} and we can name it $x(\mathrm{t})$. When the muscle exerts no force, the length the muscle has it its natural resting length x_0 which is the same as x_{kp0}.

The relationship governing elements k_s, b and the contractile element CE is the following:

$$\vec{F}_{ks} = -\vec{F}_b - \vec{F}_{CE} . \tag{Eqn. 2.4}$$

The total muscle force $F(\mathrm{t})$ equals to the sum of the serial and the parallel spring force shown by:

$$\vec{F}(t) = \vec{F}_{ks}(t) + \vec{F}_{kp}(t) . \tag{Eqn. 2.5}$$

The total length of the muscle is given by:

$$x(t) = x_{kp}(t) = x_{ks}(t) + x_b(t) . \tag{Eqn. 2.6}$$

The derivation of Equation 2.6 along with the use of Equations 2.1 to 2.5, gives the model equation that relates the muscle's total force $F(\mathrm{t})$ to the muscle's total length $x(\mathrm{t})$. Therefore, the model equation for the classical Hill muscle model is given by:

$$F(t) - \frac{b}{k_s}\frac{dF(t)}{dt} + F_{CE}(t) = b(1 + \frac{k_p}{k_s})\frac{dx(t)}{dt} - k_p(x(t) - x_0) . \tag{Eqn. 2.7}$$

As seen in Equation 2.7, the Hill muscle model equation includes time derivatives of both the overall muscle force $F(t)$ and the length $x(t)$. However, an equation that includes the time derivatives of both the force and length of a muscle is difficult to be incorporated in a musculoskeletal model as a subsystem. Usually, musculoskeletal models based on in vivo

experiments, can only describe the muscle force as a function of muscle length and the muscle lengthening or shortening velocity without the derivatives of the muscle force appearing in the equation. That is why alterations of the Hill muscle model have been studied.

Since this early work, progress had been made towards the understanding of muscular structure and its function and new Hill-type muscle models have been created [43, 44]. In all Hill-type muscle models there is an *active* element that converts neural signals into force, the *contractile element* (CE). The amount of the force the contractile element produces is determined by the mechanical characteristics of the element and can be represented by four relationships: stimulation-activation, force-activation, force-velocity and force-length [45].

The stimulation-activation is a mechanical property of the CE that describes how the nervous system signal, that could be either an excitation or a stimulation, is related to the activation of the muscle's intrinsic force capability [41]. From a physiological point of view, this property indicates the excitation-contraction coupling process. During this process, alpha motor neuron action potentials trigger motor unit action potentials (MUAPs) that travel along muscle fibres. These MUAPs are then transferred to the sarcoplasmic reticulum through the transverse tubule system where they release calcium ions into individual sarcomeres. This part of the excitation-contraction coupling sequence is considered to be the stimulation since it is independent of the actual force production mechanism. In the sarcomere at the level of the cross-bridges, the force production connects the thick filaments that contain the myosin contractile protein with the thin filaments that contain the actin protein [41]. Before the stimulation, the actin-myosin complex is in a resting state where no cross-bridge attachment and no force potential is present. When the stimulation begins, a calcium ion influx appears and the actin-myosin complex responds to it by altering its resting state to an activated state where force production can occur. This latter chain of events is the activation part of the stimulation-activation process. Researchers have defined the stimulation as the representation of the input

of the process and the activation as the response, or output of the process [41]. However, it is not easy to define the "amount" of activation produced given a specific input of stimulation since it is very difficult to quantify either stimulation or activation. The level of stimulation changes through the processes of motor unit recruitment and rate coding, but it is very hard to calculate the "amount" of stimulation that a muscle receives based on these two nonlinear mechanisms. The sarcoplasmic reticulum releases calcium ions, when stimulated neurally, which generates an activation (force potential) at the level of the cross-bridges. So activation is suggested to be measured as the number of attached cross-bridges that can produce force. In order to measure this amount and to avoid quantification difficulties it is suggested by Robertson [41] to place both stimulation and activation on relative scales that range from 0% to 100% for modelling purposes only. The actual relationship between stimulation and activation is difficult to determine, but is considered to be a direct linear relation [41].

When a motor unit is initially activated, a time delay between the onset or the neural action potential and the activation at the cross-bridge level appears. This time delay is caused by two factors. The first is the transit time for the MUAP to travel from the myoneural junction to the sarcoplasmic reticulum. The second is the length of time for the calcium ions to be released from the sarcoplasmic reticulum and become attached to the thin filaments. When this action is carried out, the inhibition for cross-bridge attachment imposed by the troponin-tropomyosin complex is removed. Then the alpha motor neuron ceases to send any more impulses and the force response from the motor unit is no longer required. Nevertheless, for a brief period of time, a supply of calcium ions still exists within the sarcomeres. This enables the cross-bridges to remain activated even in the absence of a stimulation. Usually the deactivation process lasts longer than the activation process. The duration of the deactivation is governed by the time the sarcoplasmic reticulum needs to reabsorb the free calcium ions within the sarcomeres. These time periods described above for both activation and deactivation are shown in Figure 2.14.

40
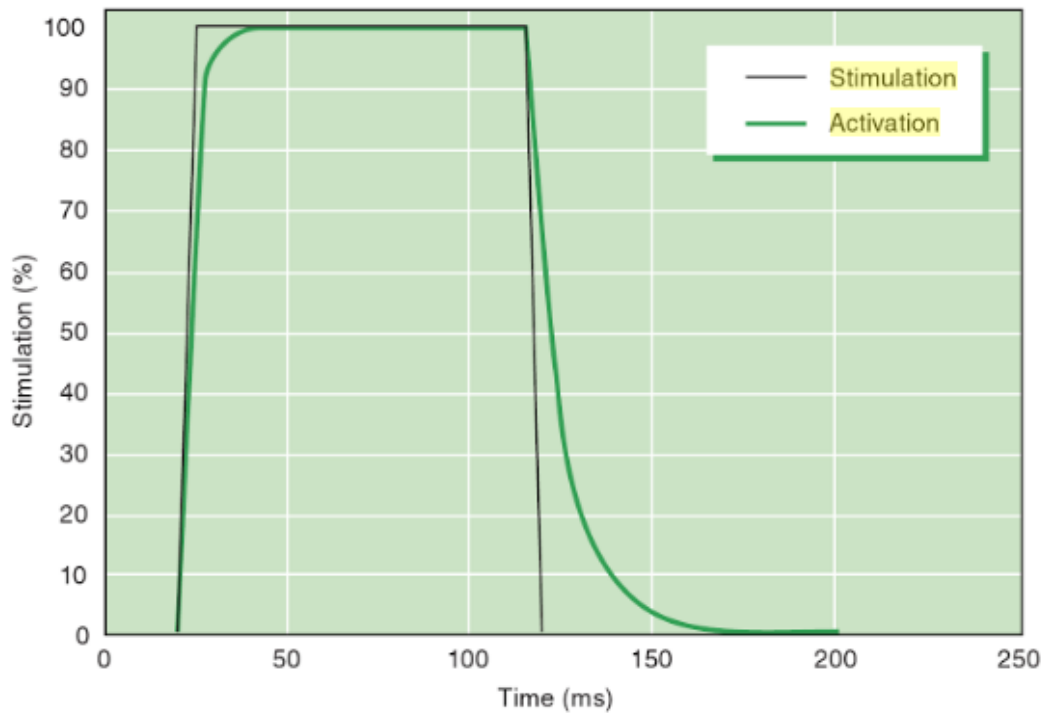
Figure 2.14. Representation of the relationship between the stimulation and the activation of the contractile element of a Hill-type model. The black line represents the stimulation and the green line represents the activation. Image taken from [41].

The force-activation mechanical property focuses on the force potential discussed previously. The term force potential, was introduced in order to explain that activation is not an actual force level, but rather a state where force can be generated [41]. The kinematic state the contractile element is in and its activation affect the actual force level that is measured in Newtons. Yet, the state of activation that is found in the form of a percentage of force potential, needs to be converted to an actual force expressed either in Newtons or as a percentage of a particular muscle's maximal force. Should this force be kept autonomous from any specific kinematic state, the force-activation relation would be conceptual only. However, it is not possible to measure the force produced in the contractile element without knowing its specific kinematic state. Consequently, the force-activation relation is direct and linear. For example, 10%, 30% or 60% of activation represents 10%, 30% or 60% of force [41].

41

The force-velocity relationship is a very important mechanical property of the contractile element. During any kind of human movement, shortening and lengthening of muscles occurs. So it is imperative to know the effect of muscle velocity on muscle tension. A mathematical relationship of the force-velocity components was famously introduced by Hill (1938)[40] with regard to the internal thermodynamics. The following equation describes Hill's force-velocity curve that takes the form of a rectangular hyperbola [1, 41]:

$$(P+a)(v+b) = (P_0 + a)b \qquad \text{(Eqn. 2.1)}$$

where P is the force of the contractile element at a specific instant in time, v is the velocity of the contractile element at the same instant in time, P_0 denotes the force level that the contractile element attains at that instant in time if the movement was isometric and a and b are muscular dynamic constants that were originally introduced by Hill in order to describe constants of energy release [41]. These dynamic constants depend on which muscle and which species they refer to and are responsible for the exact shape of the rectangular hyperbola and its intercepts on the force and velocity axes. For instance, muscles that are primarily characterised as slow-twitch muscles have different dynamic constants than those with a high proportion of fast-twitch fibres. It has been found that in fast-twitch fibres the maximal shortening velocity is about 2.5 times greater than in slow-twitch fibres regarding muscles that come from the same species [41]. It must be noted though that Hill's equation refers only to isometric or concentric contractile element velocities. Should a researcher want to include eccentric (lengthening) conditions of the contractile element, then they would have to modify the Hill equation.
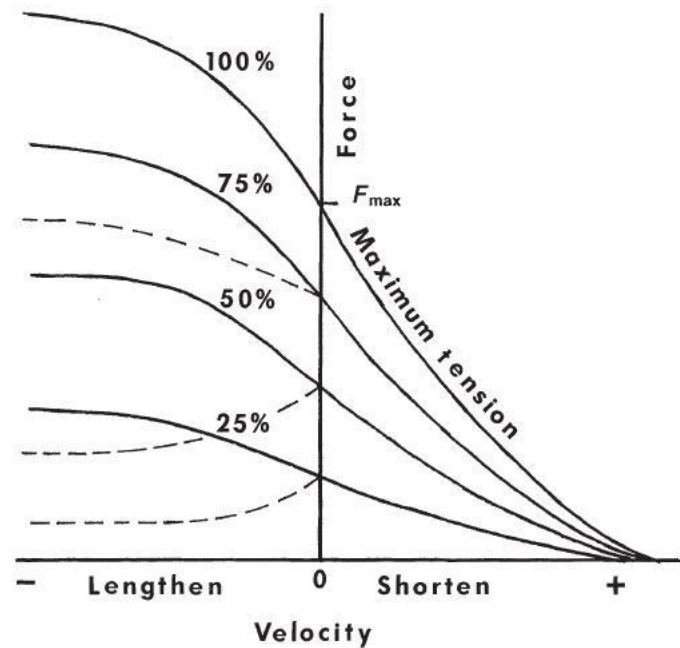
Figure 2.15. Representation of force–velocity characteristics of skeletal muscle for different levels of muscle activation. During shortening the curves follow the hyperbolic Hill model. However, during lengthening the curves depend on the experimental protocol; the solid lines are for isotonic activity, while the dashed lines are for isovelocity activity. Image taken from [1].

If a muscle shortens under load, its tension decreases. Figure 2.15 represents the force-velocity curve at a certain muscle length and for different levels of muscle activation; 25%, 50%, 75% and 100%. The usual curve is plotted for a maximum (100%) contraction. However, a case of 100% contraction can only be seen quite rarely, i.e. in athletic events and only for short periods of time. In the graph shown in Figure 2.15, the isometric contractions lie along the zero-velocity axis and should be regarded as a special case within the whole range of possible velocities.

Generally, a decrease in tension has been observed as the shortening velocity of a muscle increases. This has been associated with two main causes. The first cause seems to be the loss in tension as the cross-bridges in the contractile element break and then reform in a shortened condition. The second cause seems to be the fluid viscosity present in both the contractile element and the connective tissue [1]. Such viscosity causes friction and an internal force needs to appear in order to overcome the friction. Thus, a reduced tendon force is developed. The loss

of tension is associated with i) the number of cross-bridges breaking and deforming and ii) a passive viscosity. These two factors make the force-velocity curve rather complicated to describe. Regardless of the cause of the loss of tension, researchers agree that the total effect is similar to that of viscous friction in a mechanical system [1]. Hence, it can be modelled as some form of fluid damper. If all of the viscosity was related to the number of active cross-bridges, the slope of the force-velocity curve would be related to the activation. Similarly, if all the viscosity were passive, the slope would not depend on the activation at all.

The force-length relationship is the other important contractile element mechanical property. It describes the isometric force a muscle can produce depending on the different lengths of the contractile element. Gordon et al. (1966) [46] introduced the commonly accepted force-length relationship which was verified as the cornerstone of the well-known sliding filament theory of muscular contraction [1, 41]. This theory demonstrated that the shape of the force-length curve depends on the changes in the structure of the myofibril at the sarcomere level. The basic shape of the force-length relationship is shown in Figure 2.16 where the myosin and actin cross-bridge arrangement is also present. It can be seen that isometric force production is greatest at intermediate lengths of the contractile element. When the contractile element shortens or lengthens, the force declines. Anatomically these characteristics can be explained by the following sequence of events. At the resting length of the muscle, there is a maximum number of actin myosin bonding sites for the muscle fibre to generate contractile force. Due to this maximum number of cross-bridges between the filaments, a maximum tension is possible. As the muscle lengthens, the filaments are pulled apart, the number of cross-bridges reduces, there are fewer bonding sites to generate contractile force and consequently tension decreases. At full length there are no cross-bridges and the tension reduces to zero. When the muscle shortens to less than its resting length, the sarcomere shortens, the actin filaments begin to overlap and therefore the cross-bridges overlap reducing the available actin myosin bonding

sites. This causes tension to reduce which continues until a full overlap of the cross-bridges happens. The tension does not drop to zero, but is radically decreased by these interfering elements.
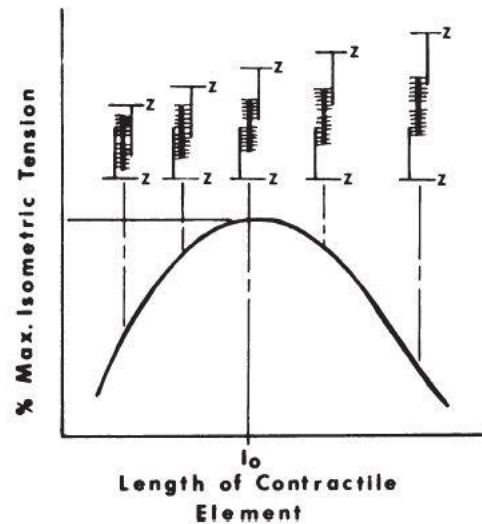
Figure 2.16. Representation of the force-length curve of a muscle as it changes length. The maximum tension/force appears at the resting length l_0 and a reduction in tension appears on both sides of the maximum due to interactions of the cross-bridge attachments in the contractile element. Image taken from [41].

In this study the relationship that has been used is the force-length relationship since we can obtain measurements of lengths and forces from our experiments. Even when the CE is not active and does not produce any force, the muscles present an elastic behaviour. The contractile element is enclosed by a connective tissue that behaves as an elastic band and is called the *parallel elastic component* (PEC) [1]. The elasticity of the parallel elastic component is treated as a passive response. When the muscle is at its natural resting length or less, the PEC is not stretched, it has no tension and the muscle force is caused entirely by the CE. When the muscle starts to lengthen, the PEC is stretched and as a result, tension starts to build up, at first slowly and then more quickly. Therefore, the force response from the PEC is added to that from the CE. The summation of the forces from both elements gives us the total muscle force-length characteristics [1, 45]. Since the early work by Hill, knowledge has grown on the *series elastic*

component (SEC) that represents all the connective tissue in series with the CE including the tendon which in our case is the Achilles tendon. It is believed that these SECs store large amounts of energy as muscles stretch before an explosive shortening that is usually seen in athletic movements. In order to determine the force-length characteristics of the SEC, experiments that require dynamic changes of force or length on an isolated muscle are needed [1]. That is why in our analysis we studied the isometric (constant muscle length) and isotonic (constant force) contractions of the gastrocnemius muscle-Achilles tendon complex. This is described in Section 4.2.4.

2.6 Musculoskeletal modelling

Transmitting muscle forces to bones, permitting locomotion and enhancing joint stability is the mechanical responsibility of the tendons since they are living tissues that respond to mechanical forces by changing their mechanical and structural properties in addition to their metabolism [13]. Musculoskeletal computer models are often created in order to understand and define the effect that pathological conditions and surgical procedures have on the movement and function of tendons. Such models are used to describe the actions of muscles by estimating muscle forces and muscle moment arms. Muscle forces are regularly calculated using mathematical models that engage force-velocity and force-length relations. The muscle moment arm, which is a quantitative measure of the ability of a muscle to produce movement about a joint, is determined by the path of the muscle and its tendon relative to the joint axis [47]. The next Section 2.6.1 gives a brief description of the musculoskeletal models created over the years and the state of art regarding foot modelling.

2.6.1 Foot modelling previously performed and models of the Achilles tendon

Over the years many researchers have taken interest in human locomotion, have studied it and analysed it. Due to the complexity of the movement a lot of assumptions and simplifications

46

were made when researchers created their models. Sometimes the simulations developed, were constrained to specific movements such as heel strike or toe off, or shorter periods of a movement such as the stance phase instead of the whole gait cycle [1]. Townsend and Seireg (1972) [48] introduced massless rigid lower limbs with 1 degree of freedom in order to model human movement. Hemami (1980) [49] suggested a three-segment, three-dimensional model with rigid legs and no feet. Pandy and Berme (1988) [50] used a five-segment planar model with no feet to simulate single support only. These models, with such serious simplifications, did not produce valid results of human locomotion problems, but were a good springboard step for further simulations and analyses of human motion.

Over the years more complete models were created where parts of the models were constrained kinematically (Townsend, 1981 [51]; Chao and Rim, 1973 [52]) by assuming sinusoidal trajectories of the trunk or pelvic segments [1]. Onyshko and Winter (1980) [53] introduced a seven-segment system in order to model the human body that consisted of two feet, two legs, two thighs, and Head-Arms-Trunk (HAT) segment. However, the model was not internally validated since it did not satisfy certain requirements, due to particular anatomical constraints. The model created, could 'walk', but only by altering the moment patterns [1]. As mentioned by Winter [1], such outcomes should make the researcher aware of the fact that even an incomplete model can result in a valid movement when faulty motor patterns are used. Thus, researchers should be very careful in the models they introduce and analyse.

More complex models with more degrees of freedom at each joint and more segments have been presented (Hemami et al., 1982b [54]; Chen et al., 1986 [55]), but no internal validity has been pursued. Simple motions though have been modelled quite effectively. Phillips et al. (1983) [56] used the accelerations of the hip swing together with the moments about the hip in order to model the swinging limbs of a human. Hemami et al. (1982a) [57] suggested locked knees in order to study and model the sway of the body in the coronal plane. In order to define

and validate the stability of the total system, adductor and abductor actuators at the hip and ankle were used as input [1].

There are currently relatively few mathematical models characterising the human Achilles tendon as part of a muscle-tendon unit. The Achilles tendon in the literature is modelled as a straight line that begins near the middle of the calf and is inserted on the posterior part of the heel, or just as a single point that is inserted into the middle part of the rear of the calcaneus bone [47]. As mentioned in Section 2.1, one can justifiably assume that the insertion point is the middle part of the calcaneus even though from the anatomy of the body we know that the Achilles tendon has two "slips" extending medially and laterally past its apex and inserting to the calcaneal tuberosity. In order to define stress and strain in the Achilles tendon and acquire information about its loading during motion, mathematical models have been developed and experiments using the methods of ultrasound and motion capture have been used so as to directly measure tendon length changes during dynamic movements [13, 47, 58-60]. Yet, there is vast agreement between all authors that it is a very challenging task to model the Achilles tendon correctly due to the difficulties bestowed when representing its structure, material properties, kinetics and mechanisms.

In order to overcome the above mentioned difficulties, to evaluate the internal bone and soft tissue movements and to estimate load distributions, 3D finite element models of the human foot and ankle have been developed [61]. The actual geometry of the soft tissues, the tendons and the foot skeleton were obtained through 3D reconstruction of Magnetic Resonance Images (MRI) and Ultrasound images [62]. What is more, strain is usually measured from the displacement of the clamps or by observing the motion of the markers attached to a surface of the tissue [63]. In Finite Element (FE) models stress and strain distributions are considered to be uniform throughout the cross-section of the specimen, while the modulus is measured from the slope of the stress-strain curve. Using MRI of human subjects, researchers have measured

the minimum and maximum cross-sectional area of the Achilles tendon and thus calculated its engineering stress and strain distribution. Numerical techniques and computer technology are continuously advancing, hence making the finite element method a versatile and successful tool for biomechanical research [61-64].

Numerous independent segments make up the structure of the foot and ankle complex. Therefore, single-segment foot models are inadequate in terms of revealing inter-segment foot kinematic changes during gait [65]. A solution to this problem is the development of multi-segment foot models such as the viscoelastic foot model developed by Gilchrist et al. (Figure 2.17)[66]. This is a three-dimensional, two-part model of the foot which has nine spring/damper systems as contact elements of the foot and the walking surface. The foot was modelled as two segments, the forefoot and the remaining part of the foot with a revolute joint between them [66, 67].
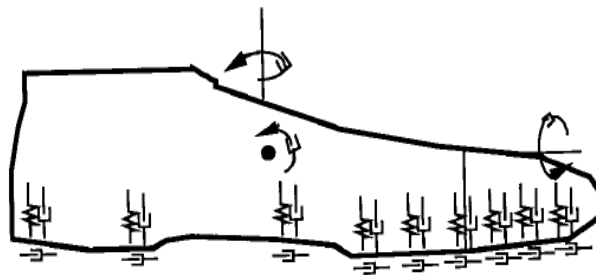
Figure 2.17. Diagrammatic representation of the Gilchrist foot model. Image taken from [66].

Even though a number of kinematic foot and ankle models have been developed only few seem to have external validity in literature such as the Milwaukee Foot Model and the Oxford Foot Model (OFM) [65, 68, 69]. Seo et al. [70] studied a 3D multi-segment model where they used 15 opto-reflective markers on the anatomical landmarks of each knee, tibial shank, ankle and foot. Their system consisted of 6 additional markers per foot in addition to the conventional Cleveland clinic lower extremity marker set. Five of them were placed around the knee and

tibial shank for calculation of the shank coordinate system. Four markers were placed on the ankle and hindfoot from which one on the medial and lateral malleolus and two on the calcaneus. Two markers on the midfoot at the navicular and cuboid and four on the forefoot where three were placed on the metatarsal area and one on the hallux (Figure 2.18). Through their study, they demonstrated that their model had high intra-session and inter-session repeatability when assessing foot motion. They also demonstrated acceptable reliability of marker placement even when though they used techniques without the wand marker that the Oxford Foot Model uses.
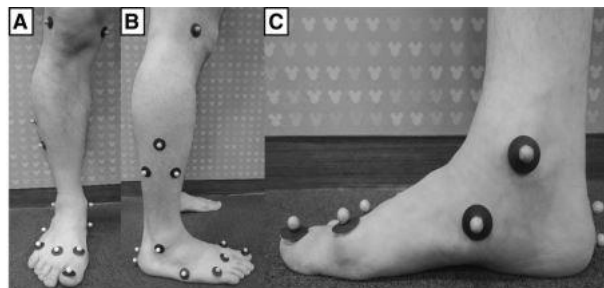
Figure 2.18. Diagrammatic representation of the Seo et al. 3D multi-segment foot model. Image taken from [70].

The Oxford Foot Model was developed by the Nuffield Orthopaedic Centre (NOC) and the University of Oxford using Vicon Nexus software. Vicon comes from the abbreviation of the words 'VIdeo' and 'CONverter'. The Oxford Foot Model designed by Carson et al.[29] is a multi-segment model that can calculate the hindfoot and forefoot and hallux motion. The original model consisted of a rigid tibial segment (tibia and fibula), a forefoot (five metatarsals), a rigid hindfoot (calcaneous and talus) and a hallux (proximal phalanx of the hallux). Based on the two main foot segments – hindfoot and forefoot – along with the separate hallux segment, the model outputs adjusted kinematics for the ankle as well as the added inter-segment angles. The NOC has used the Oxford Foot Model clinically for several years and has published many clinical papers on the validation of the model during this time [65, 69, 71-73].

In order to validate the Oxford Foot model, reliability and repeatability of the model was studied in adults. Carson et al. [71] found good repeatability between trials, between days and between testers where subtle patterns and ranges of motion between segments of the foot were consistently detected. Thus, they concluded that the Oxford Foot Model method permits objective foot measurement in gait analysis where quantitative and objective characterisation of the kinematics of the foot during a specific activity can be evaluated [71]. Dixon et al. [72] suggested that a multi-segment approach such as the Oxford Foot Model, can help quantify the important contribution of the midfoot ligaments and musculature to power generation. They recommended the use of multi-segment foot models, instead of the simple Plug-in Gait models, to estimate ankle and midfoot kinetics.

Stebbins et al. [65] adapted, studied and validated the Oxford Foot model using children as subjects. They recommended a few alterations to the original model in order to adapt it for children. The original foot model used physical markers on the tibia to calculate the knee joint centre, with the hypothesis that it would increase repeatability over the use of the conventional knee joint centre. The conventional knee joint centre calculates the middle of the distance between the femoral epicondyles by identifying the markers on the medial and lateral epicondyles placed in line with the flexion/extension axis [69]. Stebbins et al. [65] discovered that the markers on the tibia did not improve repeatability but produced a change to the amount of knee flexion. Therefore, to facilitate between study comparisons, Stebbins et al. recommended the use of the conventional knee joint centre. Furthermore, they recommended the elimination of the use of the heel wand marker during static calibration. In the original Oxford Foot Model, the heel wand marker and two posterior calcaneal markers define the plane of the anterior axis of the hindfoot. Stebbins et al. [65] observed and proved that the use of a virtual marker midway between the medial and lateral calcaneal markers as the third point to define the plane was more reliable for children than the wand marker.

Wright et al. [69] studied Stebbins modified Oxford Foot Model with respect to adults. They found that most of the variables regarding kinematics when calculated using the modified model, were very reliable for use in adult populations. This was studied and interpreted for initial contact and toe off of the foot. They also proved that when joint angles were reasonably referenced to a neutral standing position, error between marker set applications could be minimized. Generally, they found that hindfoot and forefoot motion showed high reliability and low error at initial contact and toe off of adult gait when calculated using the modified OFM. This information gained from the study of the repeatability and the errors of the modified OFM in adults, improves the ability to interpret both individual differences and group differences during kinematic investigations [69].

Recently, van Hoeve et al. [74] evaluated the repeatability of the Oxford Foot Model in healthy adults. The new approach of this study was that healthy adults were analysed by more than one observer and on separate days. Also, the number of trials needed for one single patient in order to get good results was assessed. The results presented, showed an intraclass correlation coefficient (ICC) that was moderate to excellent for inter-observer and intra-observer repeatability, a standard error of the measurements with 90% confidence bounds (SEM_{90}) and minimal differences (MD) with 95% confidence interval. The best results were found in the sagittal plane (flexion/extension) followed by the frontal plane (abduction/adduction) and the transverse plane (inversion/eversion). To conclude, the repeatability analysis provided by this study gave an excellent basis for objective measurement of the ankle and foot biomechanics [74]. Many models previously used were unable to replicate the experiments conducted under the exact same conditions and consequently could not be validated. The Oxford Foot Model is the most widely accepted model since it has been validated and it was able to evaluate the reliability of the protocol and the model.

2.7 Summary

As mentioned in Section 2.6.1, there are relatively few mathematical models that focus on the characterisation of the human Achilles tendon as part of a muscle-tendon unit. Mathematical models such as that of Zifchock et al. [47] represent the Achilles tendon as a straight line that begins near the middle of the calf and is inserted on the posterior part of the heel. Their findings are based on experiments performed on cadaveric specimens. Usually, stress and strain of the Achilles tendon have been measured through in vivo experiments that involve cadaveric specimens [75, 76]. This is not the most accurate way to measure stress and strain characteristics of a living tendon, since there is no blood flow in a cadaveric specimen and thus the mechanical properties of a living tissue differ from the cadaveric ones. However, this has been for years the way to obtain in vivo results for tendons.

Over the years more accurate methods to calculate the mechanical properties have been used, such as ultrasonography, motion capture experiments and muscle-tendon model analysis. The geometry of the Achilles tendon and the change in its length can be accurately captured through ultrasound imaging [58, 60, 77, 78]. Mechanical properties of the muscles connected to the Achilles tendon and the tendon itself can be calculated or predicted from muscle-tendon models such as the Hill-type muscle models [1, 41, 43, 79]. Also, human locomotion and specifically the motion of the foot, its muscles and its tendons can be investigated with motion capture systems [2, 36, 37, 65, 74]. Yet, the isolated use of ultrasound imaging or motion capture or muscle-tendon modelling does not give a complete analysis of a tendon or a muscle. Lichtwark et al. [58] used ultrasonography and motion capture in order to study the mechanical properties of the Achilles tendon during one-legged hopping. This approach yielded accurate results and provided a new technique for the measurement of the whole tendon length during dynamic activities. In the authors opinion, the combination of the above three mentioned methods is the

better way to fully describe and characterise the Achilles tendon and any other tendon during a specific movement. That is why this approach was used in this PhD study.

Specifically, in order to help describe the Achilles tendon and its properties, motion capture and ultrasound imaging were chosen as the experimental methods to assist in understanding the actual geometry of the tendon and the muscle as well as re-enacting the changes in length of the Achilles tendon and the gastrocnemius muscle when in movement. Both these methods are not invasive and can accurately describe human movement. A novel marker placement, described in Section 3.3.3.2, was created in order to provide valuable information for the Achilles tendon and the gastrocnemius muscle and enhance the already existing Plug-in Gait model used by our motion capture system. Clinically, models that reflect the anatomy and physiology as realistically as possible are preferred so that clinicians can understand the changes a parameter has in terms of anatomy and physiology.

Furthermore, the combination of already existing foot and muscle models such as the Hill-type muscle model (Section 4.2.2) were developed in order to better characterise the gastrocnemius muscle-Achilles tendon complex. A musculoskeletal model of the foot and the Achilles tendon was created so as to derive the Achilles tendon force of each individual that participated in our experiments. Hence, a validated model of the Achilles tendon that could provide specific parameters for a specific person studied, was a main goal of this thesis. When analysing the movement of a specific person, it is important for the researcher to be able to provide personalised results and not generic ones. The approach used in this thesis enabled the authors to successfully determine numerical values for the parameters studied that were specific to individual patients. All of these values presented in Chapter 5 were obtained experimentally through in vivo sessions.

Moreover, the Achilles tendon force that was derived from the system equations of the musculoskeletal model described in Chapter 4, was then implemented in the muscle-tendon model in order to derive the parameters of the model. Lastly, a non-linear approach of the behaviour of the Achilles tendon was studied and is portrayed in Section 5.3.2. The coupling of the Achilles tendon force from the musculoskeletal model to the muscle-tendon model and the non-linearity approach studied through a motion capture system, is to the best of the authors knowledge, novel in the field of muscle-tendon research.

Chapter 3. Instrumentation

In Chapter 3 the instrumentation necessary for the experiments of the thesis are described in detail. A general background introduction on accelerometers, goniometers, electro-goniometers, motion-capture systems, electromyograms and imaging techniques is given. A comparison of the instrumentation is presented and an explanation of which techniques were used is addressed. Lastly the author's own marker model is described on which the experiments are based.

3.1 Introduction and comparison of kinematic measurement techniques

Over the years the need for new information on the characteristics of normal and pathological human movement has inspired the evolution of methods for the capture of human movement. There are three main devices used to measure joint dynamics and human movement: accelerometers, goniometers and the use of images and video recordings that are then analysed. The most advanced and frequently used method is video motion capture (e.g. Vicon motion capture). Motion capture methods are divided into marker based systems and marker-less motion capture systems. The development of a non-invasive and marker-less systems is the next critical innovation in human motion capture. Thus far, marker-less methods are not widely available since the capture of human movement without markers is technically challenging and not very accurate. However, recent technical developments in computer vision provide the potential for marker-less human motion capture methods in the future. Marker based motion capture systems track distinctive markers attached to anatomical or geometrical locations of subjects or objects. Marker-less motion capture systems use image processing, multiple optical sensors and item recognition to locate different body segments [80]. Marker based motion capture offers higher accuracy than marker-less motion capture. The markers used in this thesis, from the Vicon Nexus hardware as described in Section 3.3.2, have 14 mm and 9.5 mm

56

diameters which is quite small compared to marker-less detection where there is a need to detect a cylindrical shape such as the lower part of the leg where the diameter could vary from 200 mm to 800 mm. For that reason, the derivation of the exact location of a certain point is more accurate for a marker based system than a marker-less system.

When comparing motion capture to goniometers and accelerometers, the former does not add mechanical components to the joint. Consequently, minimal effects on the mechanical dynamics of body movement appear. The system measures all markers in a global 3D space, thus there is no accumulation of errors when deriving the locations of multiple linked segments or body parts. That is why in this thesis marker based motion capture was preferred compared to the other mentioned methods so as to develop an accurate mathematical and mechanical model of the Achilles tendon. The assistance of a hand- held goniometer was used to calculate and validate angles between specific joints (such as ankle and heel joints) studied in the Gait Laboratory experiments. The hand-held goniometer does not interfere with marker placement and does not produce motion artefacts when a motion capture system is used, since it is not attached to the skin of the volunteer. Further details about the goniometers and the motion capture systems and how they were used are given in Sections 3.1.2 and 3.2 respectively.

3.1.1 Accelerometers

Accelerometers are devices that measure acceleration. Generally, these devices are force transducers capable of measuring the reaction forces associated with a given acceleration. If a limb segment has a mass m and an acceleration a, then the force exerted by the mass is $F = ma$. This force is measured by a force transducer which would normally be a strain gauge or piezoresistive type [1]. The force transducer generates a signal voltage V, which is proportional to the force. The mass m is known and constant and therefore V is proportional to the acceleration. With accelerometers the rate and intensity of body movement in up to three planes

(anterior-posterior, mediolateral and vertical) can be measured. They provide direct results of the acceleration from which the velocity and position can be calculated or computed through integration of the acceleration signal against time. However accelerometers are dependent on i) the position at which they are placed, ii) the orientation of this position, iii) the posture of the subject and iv) the activity performed by the subject [81]. Since the signal of the acceleration is dependent upon time, the errors when calculated can rapidly increase due to integration. That is why accelerometers are considered to be inferior compared to motion capture techniques.

3.1.2 Range of motion (ROM) and Goniometers

Copyright © 2012, 2008, 2004, 2000, 1996, 1992 by Saunders, an imprint of Elsevier Inc. All rights reserved.
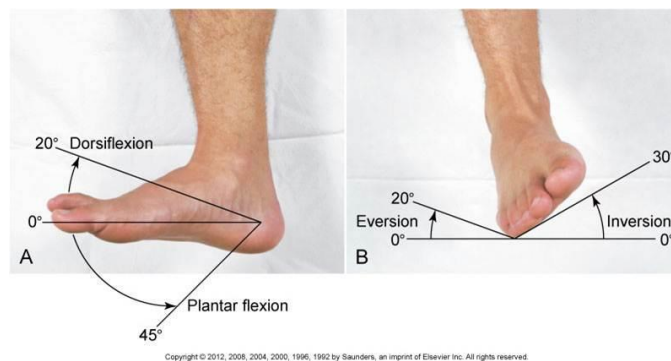
Figure 3.1. Examples of the range of motion (ROM) at the ankle joint when dorsiflexing, plantar flexing, everting and inverting the foot. Image taken from [82].

The flexibility of joints is defined as the range of motion (ROM) allowed at a joint and describes how much a joint can move. A joint usually rotates when it moves. Therefore, an angular movement is produced that is measured in degrees and thus the range of motion of a joint is usually measured in degrees. The range of motion of a joint is usually measured by the number of degrees from the starting position of a segment to its position at the end of its full range of movement (Figure 3.1). There are two types of ROM: i) *active* ROM, where a person voluntarily contracts their muscles around a joint and ii) *passive* ROM where an external force acts on a body around a joint and produces movement [83]. The most common way to measure ROM is by employing a double-armed goniometer (Figure 3.2). A double-armed goniometer is

constructed from a toughened clear plastic so that it does not break easily and is usually 12, 8 or 6 inches wide with 1 degree increments. There are centimetre and inch measurement readings along the proximal/fixed arm and the distal arm of the goniometer and 360-degree measurement readings around its circular disk. The stationary arm, which is the proximal/fixed arm of the goniometer, is placed parallel to the stationary body segment and holds a protractor. The circular disk, which is the protractor, has a pin in its centre which is the axis of the goniometer and is placed over the joint whose ROM is measured. The mobile arm, which is the distal arm, moves along the moving body segment. The angular degree between the endpoints of the goniometer denotes the range on motion of the joint for a specific movement.
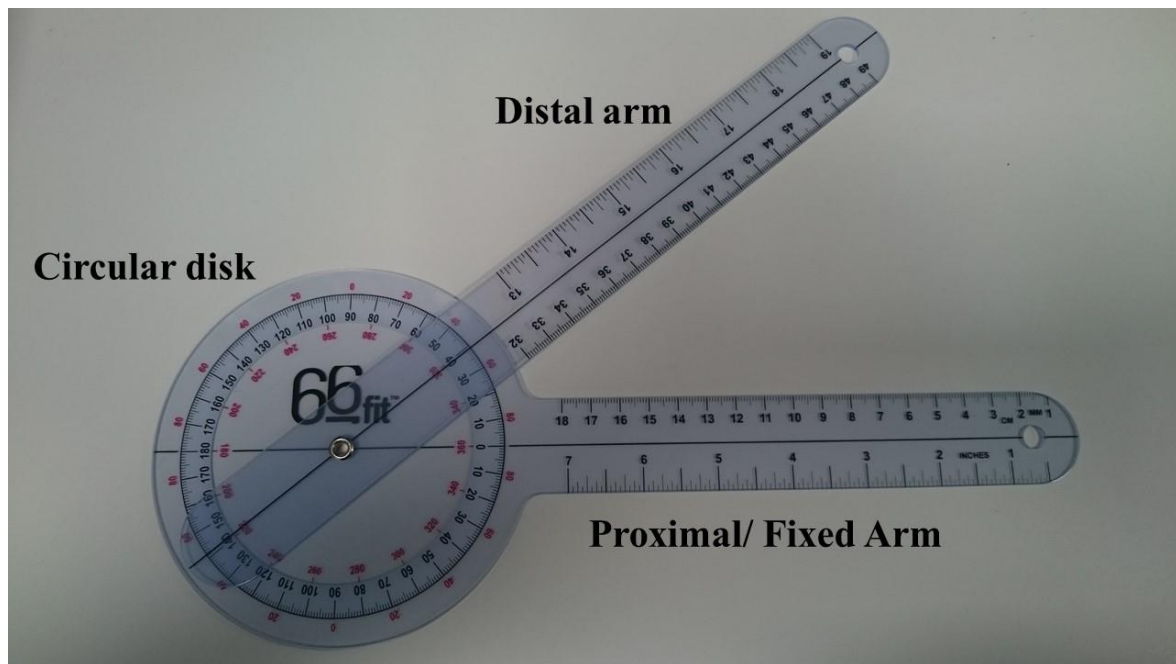
Figure 3.2. A double-armed goniometer. Demonstrating the circular disk, the distal arm and the proximal/fixed arm that are placed on joints and body segments in order to calculate the range of motion (ROM) at a joint.

In occupational and physical therapy, a goniometer is a very helpful instrument used to measure the range of motion of different joints of the body. It is a clinical tool that helps the doctor or the physician to obtain objective measurements and to accurately follow the progress of a patient before surgery or during a rehabilitation period [84, 85]. For example, when

measuring the knee joint, the pin of the circular disk (point of rotation) would be placed on the lateral epicondyle of the femur. The proximal arm is lined up with the greater trochanter of the femur and the distal arm of the goniometer is lined up with the lateral malleolus of the fibula. A measurement is then taken using the degree scale on the circular disk of the goniometer [86]. Goniometers are very useful tools that can be easily used by scientists when some knowledge of the anatomy, the joints and the muscles of a human body is attained. They are also relatively inexpensive, portable and can be accessed very easily. Reliability studies have shown that the goniometers present good overall intra-measure (i.e. between measures) and inter-tester (i.e. between testers) reliability when the measurements are repeated several times in an experiment. However, there are a few issues concerning the accuracy of the readings from a goniometer. Some studies suggest that these errors lie between 5 and 10 degrees when completing repeated measures [85, 86]. Whilst overall validity and reliability of the goniometer has been recounted as good they can be affected by incorrect application of the device; the reliability varies according to the joint and the range of movement that is measured. Concerns about the intra-measure and inter-tester reliability appear to increase when the scientist using the goniometer is not very experienced. Mistakes can be made when estimating the centre of rotation of the joint studied and the location of the bony landmarks when locating and maintaining the centre of the goniometer over the joint studied etc., thus all of these require consideration when using a goniometer in order to acquire the ROM of a joint [86].

The goniometer seen in Figure 3.2 is the one used in the experiments performed to determine angles between joints, bones and muscles. Angles θ_1, θ_2 and φ seen in Figures 4.6-4.9 in Sections 4.2 and 4.2.1 were calculated with the hand-held goniometer seen in Figure 3.2. In all sections in Chapters 4 and 5 when a goniometer is mentioned, it is referred to the one seen in Figure 2.3. For example, in order to calculate angle θ_1 which can be referred to as the heel angle, the pin of the circular disk was placed on the heel marker. The proximal arm of the goniometer

was lined with the surface of the foot and the distal arm was pointing at the ankle joint. Angle θ_2, that can be referred to as the ankle angle of the foot segment, was calculated by placing the pin of the circular disk on the ankle joint where the ankle marker was, the proximal arm of the goniometer was pointing at the heel marker and the distal arm was pointing at the toe marker. Lastly, angle φ that can be referred to as the Achilles tendon angle, was calculated by placing the pin of the circular disk on the heel where the heel marker was, the proximal arm of the goniometer was lined with the surface of the foot and the distal arm was aligned with the Achilles tendon and was pointing at the RAT marker (see Section 3.3.3.2 and especially Figure 3.16). These measurements were taken several times in order to find angles θ_1, θ_2 and φ for all the different movements studied, i.e. static movements (Figure 4.7) and dynamic movements (dorsiflexion and plantarflexion, Figures 4.8 and 4.9 respectively). Each angle was measured at least three times for each movement needed and the differences in the values found were 1 or 2 degrees. This showed a consistency in the calculation of the angles. Then the values of the angles were compared to the ones found from the reconstruction of the marker trajectories of the Vicon |Nexus system explained in Chapter 5. The values of the angles found with the goniometer and those found from the Vicon Nexus showed good agreement with a difference up to 5 degrees maximum. These results verified and validated that the values of the angles found were correct. Further analysis on why the hand-held goniometer was used is given in Chapters 5.

An electro-goniometer adds the capability of an instrumented measurement to the clinical goniometer by using a rotary displacement-measuring device such as a rotary potentiometer [87]. Electro-mechanical goniometers such as those provided by Biometrics Ltd (Figure 3.3) allow the time history of the angle between two body segments to be measured. They provide real-time measurements and instantaneous results of the measured angles without range limits. However, errors in the measurements appear since there is skin movement of the surface of the

human body against the skeletal segments (i.e. the bones). The gradient of the surface of the skin changes for different joint angles, during joint movement or interactions with other entities. These errors are difficult to quantify. Moreover, when analysing body segment locations that are connected in series, accumulated angle errors appear when multiple body segment locations are derived. A good example is the error accumulated from the ankle joint, knee joint and hip joint when the location of the foot relative to the trunk of the body is studied.

Figure 3.3. A Biometrics Ltd goniometer. Two green sections are attached to the upper and lower part of the knee with double sided tape. The flex of the metal braded connection measures the acute angle between the two green sections. Image taken from [88].

3.2 Gait Laboratory

Measurements of human movement dynamics compose the experiments necessary to support model development, model parameterisation, model validation and simulation of the Achilles tendon. The experiments necessary for this thesis were conducted in the University of Warwick's Gait Laboratory. Ethical approval complying with the research code of practice of the University of Warwick has been granted for all Gait Laboratory experiments and Ultrasound sessions at UHCW that will be mentioned in this thesis by the University's Biomedical and

Scientific Research Ethics Committee (BSREC full approval *Simulation of the Achilles tendon REGO-2013-578AM01*). All relevant documents are presented in Appendix A.

The Gait Laboratory comprises of two rooms, the actual lab (Figures 3.4 and 3.5), which is an 8m (length) x 3m (width) x 2m (height) room where the experiments take place and a control room (Figure 3.6) where the computer with the Vicon Nexus 1.8.5 software is located and from where the operator activates and controls the system. The Gait Laboratory contains a Vicon MX biomedical motion capture system which is a 3D motion capture system that uses a force plate to measure forces during different types of movement and a 16 channel electromyography (EMG) system to record the surface electrical activity of the skeletal muscles of subjects undergoing experiments in the laboratory. A more detailed description of the laboratory and its components will be given in the sections that follow.
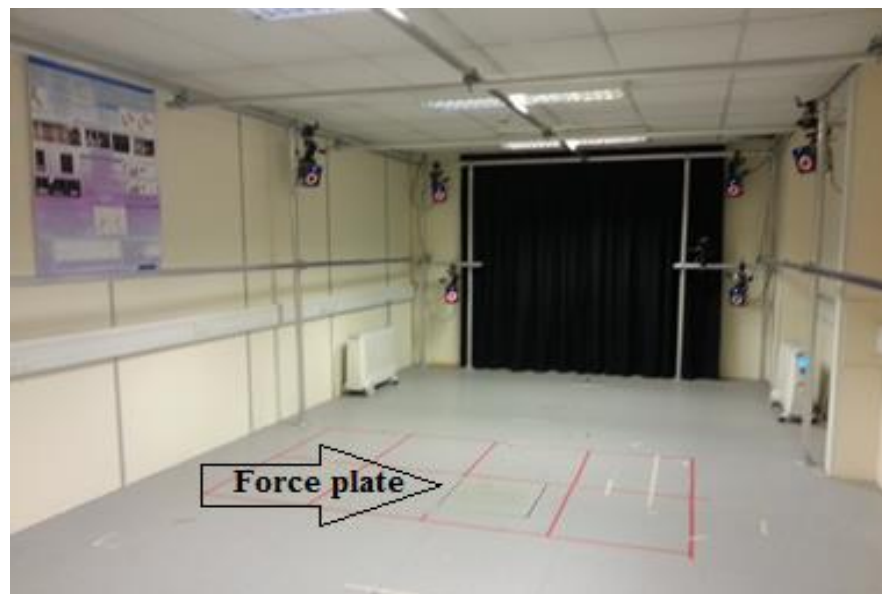
Figure 3.4. Gait Laboratory; front view of the actual lab where the motion capture area is located. It is displaying six infra-red motion capture cameras with blue indicator lights and red/infra-red ring lights mounted to a rigid metal frame. An AMTI force plate is installed into the raised floor at the centre of the motion capture area, as indicated by the arrow inn the figure.

Figure 3.5. Gait Laboratory; rear view of the actual lab where the motion capture area is located. It is displaying the other six infra-red motion capture cameras. The same AMTI force plate is indicated by the arrow in the figure to the left. The monitor next to the door shows a live reconstruction of the 3D space experiments conducted in the laboratory and is synchronised with the monitor in the control room in the figure to the right, where a 2D grid represents the floor and a grey square represents the force plate.

Figure 3.6. The control room with the computer containing the Vicon Nexus 1.8.5 software.

3.3 Three dimension (3D) motion capture - Vicon Nexus

In order to measure kinematic data, the Vicon MX biomedical 3D motion capture suite was used. It is a marker based motion capture system that tracks the positions of spherical reflective markers attached to a Velcro suit or directly to the skin of human subjects or objects being studied. For this PhD study, the markers were placed only onto the skin since errors due to relative movement of a suit can be avoided. The actual capture volume of the Gait Laboratory (Figures 3.4 and 3.5), where the experiments were conducted, comprises twelve infra-red (MX) cameras, one force plate and two digital video (DV) cameras (Figure 3.7).

Figure 3.7. Infra-red (MX) camera and Digital video (DV) Camera.

The 12 infra-red cameras are the heart of the system and are placed at different positions around the room as seen in Figures 3.4 and 3.5. The system uses infra-red (IR) and captures only the motion of the reflections of the specific markers used in the experiments. Normal room lighting does not interfere with the MX system and the MX cameras cannot capture the shape

and the form of the objects present in the laboratory unless they have markers on them. The IR source is provided by a ring of IR LEDs enclosing the lens for each MX camera. The ring of red light LEDs, as seen in Figure 3.7, is the strobe light for the camera and operates at 200 Hz. Thus each camera captures 200 frames per second according to the recommended settings for biomechanical studies by Vicon. This allows the recording of fast movement without aliasing and without introducing distortion or error to the signal. If the reflection of a marker appears in three or more of the camera shots, then the cameras "see" the marker and its position can be calculated. The system then tracks this specific marker in time and 3D space [89].

Apart from the 12 MX cameras, the Gait Laboratory has two colour digital video (DV) cameras. The DV cameras allow us to actually capture a video of any motion capture trials that are conducted in the Gait Laboratory in a way that is synchronised with the rest of the system and experiment. These videos help in assessing the trials so as to verify the computed 3D locations of the markers in the digitally reconstructed space. The DV cameras capture at 100 frames per second according to Vicon's recommended settings. Written consent by each subject involved is needed in order to videotape the trials and use them in any post-processing procedure.

The recorded files from the MX cameras are rather smaller than the DV camera files by one order of magnitude and require lower transfer and recording bandwidth, therefore the frame rate for the DV cameras is lower than that for the MX motion capture cameras. The MX and DV cameras are connected to two Vicon Giganet control boxes (Figure 3.8) and the video data are recorded within a computer in the control room. The recorded video footage is analysed and the 3D location of the markers reconstructed in a digital 3D space, using Vicon Nexus version 1.8.5. The software and analysis are described in the following sections.
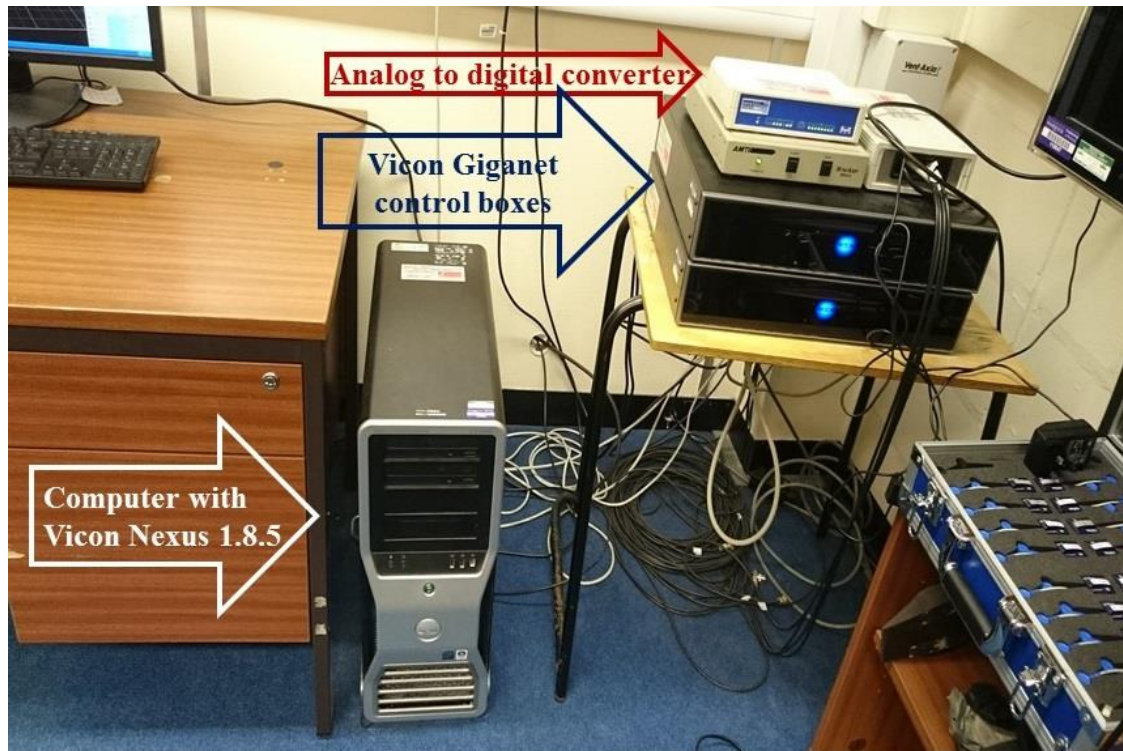
Figure 3.8. Vicon Giganet control boxes and computer installed with Vicon Nexus 1.8.5 software.

3.3.1 Force plate

The force plate installed in the floor at the centre of the capture volume in the Gait Laboratory

is an AMTI OR6-7 [90]. AMTI force plates can measure simultaneously the three force

components along the reference xyz axes and the three moment components about the xyz axes.

The forces and moments are measured by strain gauges attached to proprietary load cells near

the four corners of the platform. The gauges form six Wheatstone bridges having four active

arms each with eight or more gauges per bridge. Three of the output signals are proportional to

the forces parallel to the three axes and the other three outputs are proportional to the moments

about the three axes. Figure 3.9 shows the three force (F_x, F_y, F_z) and the three moment (M_x,

M_y, M_z) vector components that are measured as a subject makes contact with the force plate

[87, 91]. As seen in Figure 3.9, the arrows of the three forces F_x, F_y and F_z point in the direction

of positive force along each of the axes, following the right-hand rule and act along the axes of

an orthogonal x, y, z coordinate system. F_x and F_y, represent the horizontal or shear force components, and F_z is the vertical one. The M_x, M_y and M_z that illustrate the moment components, are rotations around the corresponding x, y and z axes. Positive moments have a clockwise rotation since they are determined according to the right hand rule. The origin for the measurements (x=0, y=0, z=0) lies at x, y and z offsets from the top surface geometric centre. The x and y axis origins are situated approximately in the centre of the top plate and the z axis origin lies at a significant distance (z_0) below the surface. The exact location of the measurement origin is provided with the force platform calibration certificate [91].
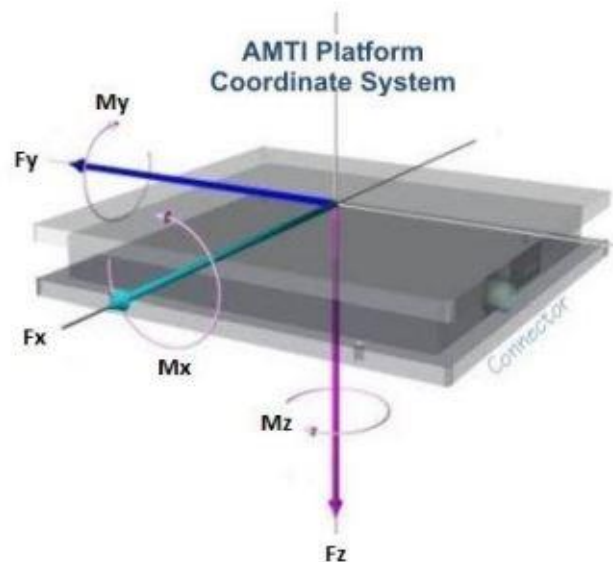
Figure 3.9. AMTI force plate illustrating the measured force and moment components. Image taken from [91].

The force and moment components are loaded into the Vicon Nexus software, more specifically into the Vicon Giganet control box, via an AMTI Miniamp amplifier [92] and an analogue to digital converter (ADC) (Figure 3.8). The force plate sampling rate is 1 kHz. Apart from the ground reaction force (GRF) and the moments in the x, y and z axes, the centre of pressure (CoP), the point where the GRF is assumed to originate can be calculated in the Vicon Nexus software in the x and y directions [87, 91, 93]. In static balance studies the CoP and the

GRF are studied and used to analyse forces [94]. If the Centre of Mass is not directly above the Centre of Pressure (CoP) then there is a torque on the body due to gravity and an unstable inverted pendulum type of scenario appears. The trajectories of the CoP are usually studied when analysing different gait patterns [95]. Equations 3.1 and 3.2 show how to calculate the CoP in the x and y directions respectively,

$$CoP_x = \frac{M_y}{F_z} \qquad \text{(Eqn. 3.1)}$$

$$CoP_y = \frac{M_x}{F_z} \qquad \text{(Eqn. 3.2).}$$

where z represents the direction of the origin coordinate of the force plate in relation to the vertical origin of the capture volume, y represents the direction of the origin coordinate of the force plate in relation to the right of the capture volume and x represents the direction of the origin coordinate of the force plate towards the control room.

In this thesis, the force plate was used to measure forces, moments and the CoP when a subject was dorsiflexing or plantar flexing their feet or walking around the Gait Laboratory. An extended description of these movements and their analyses are given in Chapters 4 and 5.

3.3.2 Markers

The reflective markers used in the experiments are plastic spheres covered in fluorescent tape that have a high visibility. They reflect the infra-red light from the MX cameras' ring lights to the MX camera's sensors. The sphere part of the marker is screwed to a black plastic base. This base has a flat surface at its foot and is attached to the subjects or objects studied by double sided tape which is medically approved and hypoallergenic. Markers of two different sizes were used in the experiments; 14 mm diameter spheres and 9.5 mm spheres, both with same sized

bases of 16 mm diameter and 2.5 mm thickness (Figure 3.10). Both 14 mm and 9.5 mm can be

detected by the system. For a Plug-in Gait model the markers needed are just the 14 mm ones.

However, for an Oxford Foot Model both 14 mm and 9.5 mm markers are required. Vicon

Nexus specifies in its guidelines, in the Plug-in Gait manual and the Oxford Foot Model manual,

which diameter markers need to be used in an experiment when the Vicon MX biomedical 3D

motion capture suite is used [96, 97]. The Oxford Foot Model has been described in Section

2.3.1 and the Plug-in Gait model is presented in Section 3.3.3.2.

Figure 3.10. Markers of 14 mm diameter (left hand side) and 9.5 mm diameter (right hand side).

3.3.3 Software and Data Processing

Data acquisition was undertaken using the Vicon Nexus system in the University of Warwick

Gait Laboratory and data post-processing that involved inverse dynamics was performed with

Vicon Nexus software version 1.8.5. Data post-processing usually involves i) computation and

reconstruction of the 3D location of each marker in each time-frame for the duration of an

experimental trial, using raw data acquired from the MX cameras, ii) labelling of each marker

according to marker template models provided by Vicon and iii) exporting the trajectories and

computed locations of the markers (kinematic data) and also exporting other data such as forces,

moments, powers, angles and EMG data for further analysis. Further analysis of kinematic data was performed using Excel 2013 and Matlab 2016a [98]. The reconstruction, labelling and exporting processes are described in the following sections.

3.3.3.1 Kinematic data reconstruction

Kinematics is the branch of biomechanics that studies movement with reference to the amount of time taken to carry out the activity. The bodies in motion are studied without concern as to what causes the motion but rather with describing and quantifying the linear and angular positions of the bodies and their time derivatives [41]. Whereas kinetics is concerned with what causes a body to move. It studies and records the forces and how they affect a specific movement studied [41]. In this thesis, kinematic data reconstruction is undertaken.

Reconstruction is the calculation of the three-dimensional position of each marker in each frame. The Vicon Nexus workstation does this using the two dimensional data from each camera, calibration parameters and a user-defined set of reconstruction parameters that depend on the volume and the type of capture [96]. As mentioned in Section 3.3, the 12 MX cameras that are placed in different angles around the Gait Laboratory detect the infra-red (IR) light reflected from the markers. In order to reconstruct the locations of the markers in 3D space, Vicon Nexus applies multiple view geometry computation to calculate and provide the 3D position of each marker from the 2D marker positions in the camera planes [99].
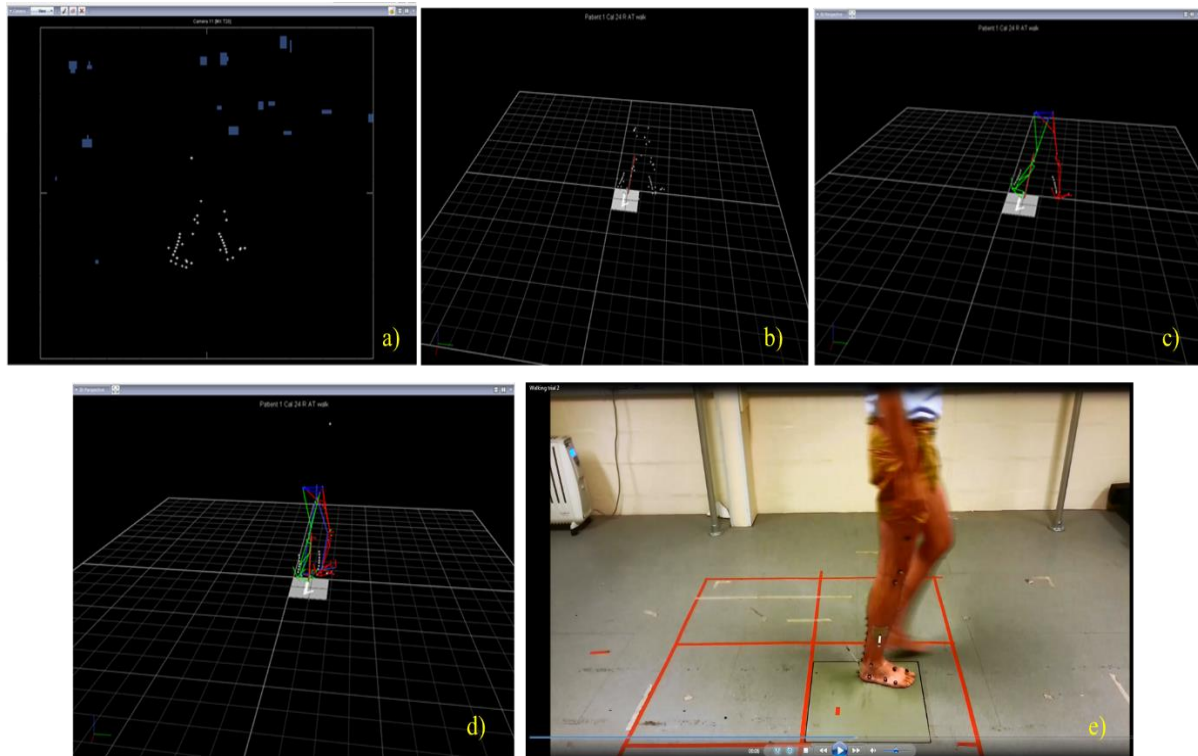
Figure 3.11. Images from one of the twelve MX cameras showing the different stages of marker reconstruction and labelling.

In Figure 3.11 we see images taken from one of the twelve MX cameras during the different stages of the reconstruction procedure. In figure a) white rectangles represent the frames of the camera sensors. The markers are represented by white dots and dark blue dots show masked areas where data are ignored, since they were created by reflections in the Gait Laboratory that are not related to the markers. In figure b) reconstructed markers are shown in 3D digital space, where the white grid illustrates the floor of the Gait Laboratory. The force plate is represented by a grey square labelled 1. The ground reaction force (GRF) at the force plate is illustrated by a red arrow. The arrow represents the GRF's origin (the centre of pressure; CoP) its magnitude and its direction. In figure c) each marker is labelled according to the Vicon Plug-in Gait marker system and all of them are linked to each other and create different body segments. In figure d) a 3D perspective view is shown. The ground reaction force is visible while the subject's right

foot is in contact with the ground during a walking trial. In figure e) data from a digital video (DV) are presented, allowing the marker labelling from figures a) to d) to be verified.

To calibrate the system, Vicon's recommended method was used. The Vicon MX system has a reported precision of 1 mm and accuracy of ±0.1 mm. The measured linear precision error is 0.4 mm and the measured gradient error of the x-y plane in the reconstructed space against the horizontal plane in the measured space is less than ±1° [42]. To obtain these errors, 8 markers were placed on the floor evenly distributed on the ring of a circle with 1 m radius as seen in Figure 3.12. Two markers were aligned along the x axis and two markers were aligned along the y axis. Reconstructed locations were compared against measured locations and the error between the measurements was found to be 0.2%. The markers aligned with the x and y axes were used to compute the angular error and the remaining four markers were used to ensure that the reconstructed marker locations were in the same plane [42].
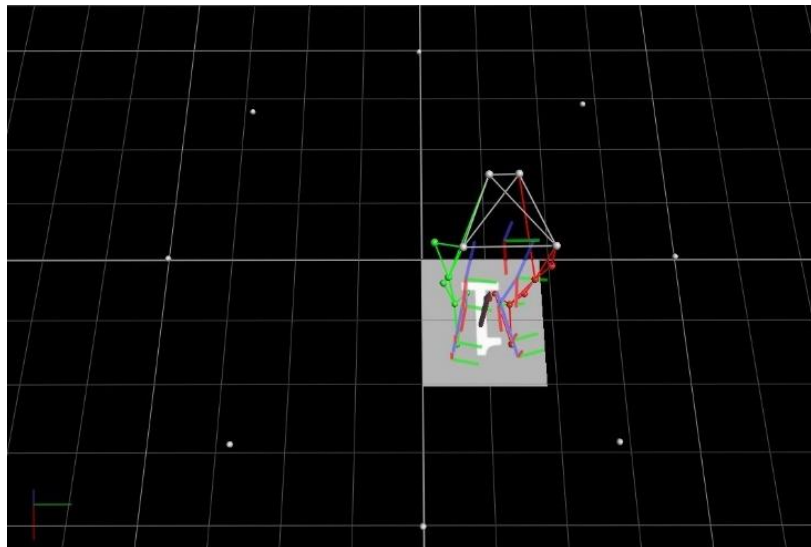
Figure 3.12. Representation of an eight marker placement on the floor of the Gait Laboratory; two markers are aligned along the x axis and two markers are aligned along the y axis.

3.3.3.2 Marker Placement and Labelling

During the experiments that were performed in the Gait Laboratory, three marker models were used. A marker model is the outline of markers used in motion capture in order to represent the different parts of the body. Generally, markers are placed in anatomical positions so that the location of body segments and joints can be located. All the distinct markers in the marker models have unique names. On most occasions, groups of markers are connected to each other so as to form a segment of the human body. An example can be seen in Figure 3.13 where four markers around the waist of the subject are associated together and form the segment of the model that represents the pelvis, the blue rectangle seen in the right figure that connects the two legs. However, markers can also be part of more than one segment. For example, a marker placed on the ankle can be linked with the segment representing the lower leg and the foot segment. The relative orientations between segments can be used to calculate joint angles, such as the knee and hip joint angles.
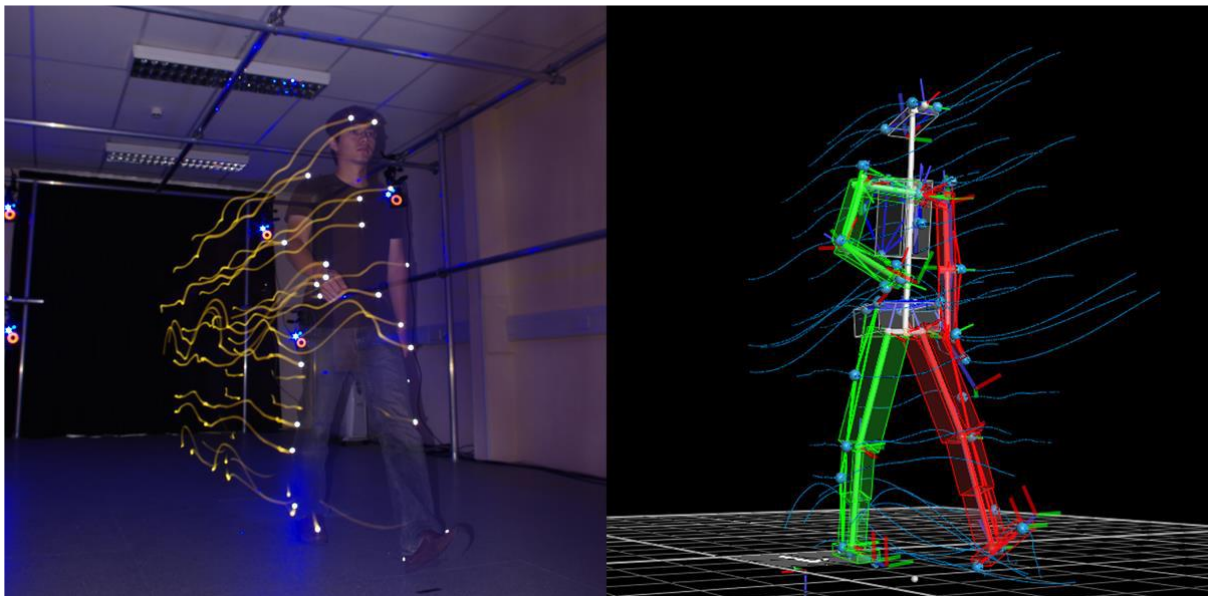
Figure 3.13. The human gait in digital form. Full body marker placement. Image taken from [42, 100].

Figure 3.13 shows a full body Plug-in Gait marker placement. This means that the markers are placed on the head, the torso, the hands, the pelvis, the legs and the feet of the volunteer. As seen in the left image, the markers are the white dots and their trajectories are represented by the yellow lines. The yellow lines are created from the reflection of the markers while the volunteer is walking. The left image is what happens in the actual lab and the right image is what the researcher can simultaneously see on the screen of the computer in the control room. In the right image, the markers are represented with blue dots and the trajectories of the markers are the blue lines. Green rigid body segments represent the right arm, upper and lower leg, foot etc while red body segments represent the left parts of the human body. Different marker placements create different body segments. The ones used in this study are explained below.

In this thesis the Oxford Foot Model, the Plug-in Gait model and a modification of that were used in order to illustrate the Achilles tendon. Plug-in Gait is a biomechanical model based on the Newington-Helen Hayes gait model that calculates joint kinematics and kinetics from the xyz marker positions and specific subject anthropometric measurements. Plug-in Gait modelling takes the real marker trajectories and generates virtual marker trajectories that represent kinematic and kinetic quantities (angles, moments, etc.) and representations of the modelled segments [101]. Figure 3.14 illustrates the front and back view of the lower body Plug-in Gait model placement that consists of 16 markers. This marker placement was tried and found not adequate enough for the Achilles tendon model, since it cannot give any information on the location of the tendon or the gastrocnemius muscle.
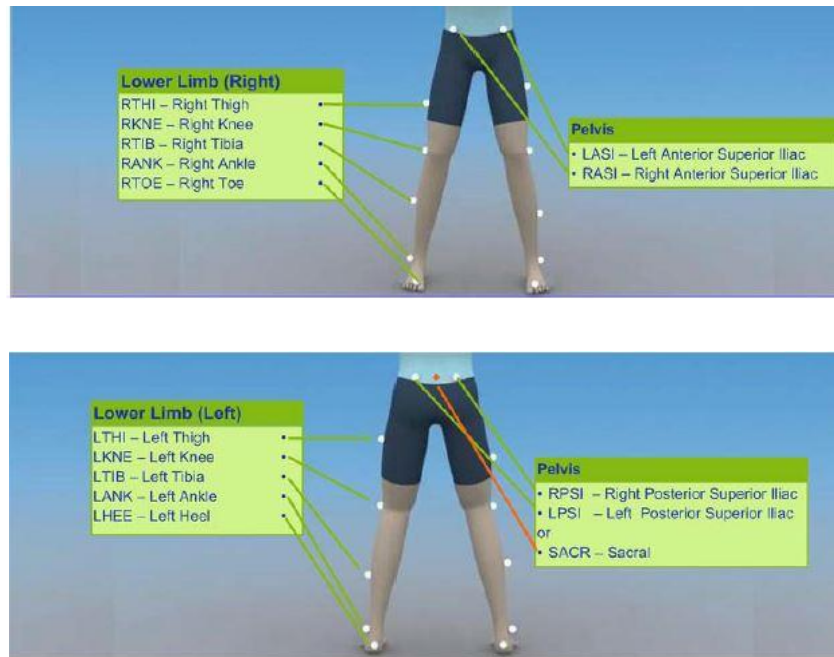
Figure 3.14. Front and back view of the Lower Body Plug-in Gait marker placement. Image taken from [101].

The Oxford Foot Model (OFM) was developed and validated by the Nuffield Orthopaedic Centre in collaboration with Oxford University. The Oxford Foot Model Plug-in for Vicon Nexus is an extension to the standard Plug-in Gait marker set. 43 markers are placed on the lower body in total instead of the 16 used in the Plug-in Gait one. However, all 16 markers of the Plug-in Gait are also used in the OFM as explained in the guidelines [97] and are placed in the same anatomical positions. Therefore, the toe, ankle, heel, knee, tibia, thigh and pelvis markers from the Plug-in Gait model are placed in the same anatomical positions in the OFM model as well. The marker placement of the OFM is illustrated in Figure 3.15. With the additional markers attached to both left and right lower limbs, the model can calculate a range of extra output variables (e.g. the hindfoot with respect to lab angles, foot progression angles) which can be used for later analysis [65, 97, 101]. Even though the OFM provides a researcher with a lot more information and variables regarding the foot, it does not give any extra information on the Achilles tendon.
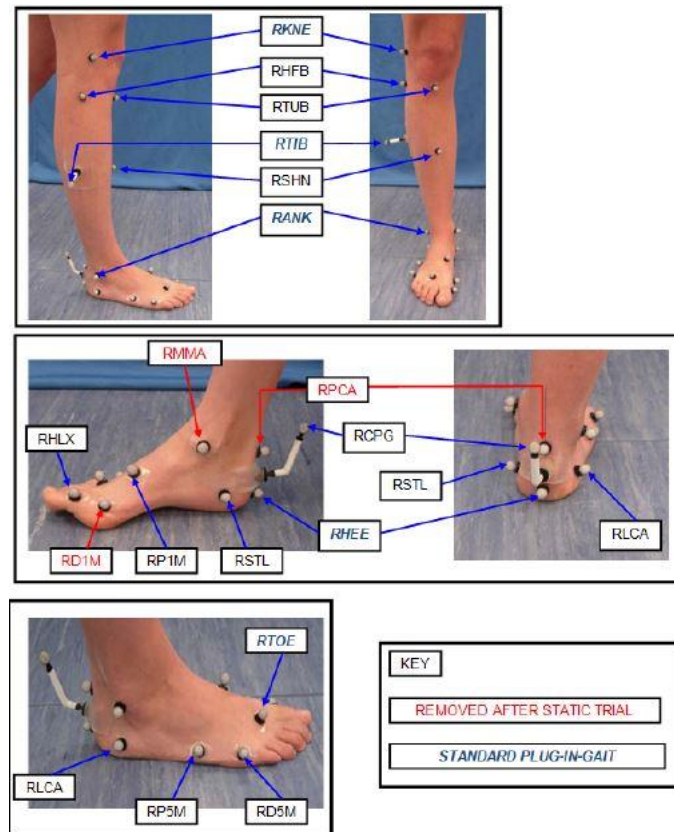
Figure 3.15. Representation of the Oxford Food Model marker placement. Image taken from [97].

A novel marker placement was created based on the Plug-in Gait model (Figure 3.16). After discussion and consultation with the Vicon Nexus team, a modification of the Plug-in Gait model was created in order to incorporate additional valuable information for the Achilles tendon and the gastrocnemius muscle. Six extra 14 mm markers were placed on both legs of the volunteers who performed the experiments. The point of insertion of the Achilles tendon is at the heel. Ultrasound sessions were performed at the University Hospitals of Coventry and Warwickshire (see Section 5.1.2) where the point of insertion of the Achilles tendon at the heel for each volunteer was found. The point was marked on each foot and the distance from the heel was measured. The heel marker of the Plug-in Gait model during the Gait Laboratory experiments, was placed at that exact position, as humanly possible, with the position measured at the ultrasound sessions. It was found that this position is usually the same position the heel marker of the Plug-in Gait model is placed when defined by the Vicon Nexus guidelines [101].

77
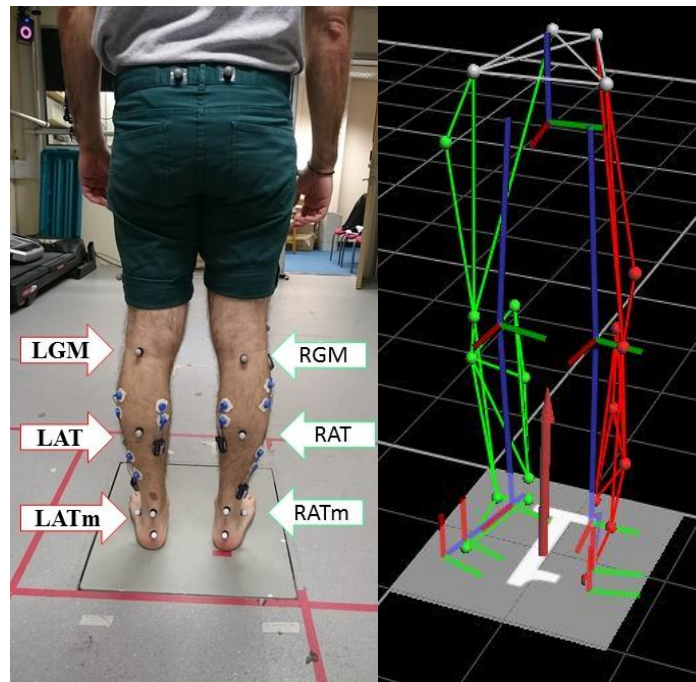
Figure 3.16. Novel Achilles tendon marker placement.

The firsts two extra markers, labeled RATm and LATm for the right and left foot respectively, were placed at the avascular zone of the Achilles tendon which as seen and felt by palpation was situated at approximately 5 cm above the point of insertion. As mentioned in literature, the avascular zone lies approximately 2 to 6 cm above the point of insertion [24]. It can be seen and felt my palpation since when the foot is dorsiflexed it sticks out in the deep back line of the feet. The second two extra markers, labeled RAT and LAT respectively, were placed at the origin of the Achilles tendon which is the lower margins of the heads of the gastrocnemius muscle. This position was again felt by palpation after the volunteers were asked to plantar flex their feet to activate their gastrocnemius muscles. In order to accurately find the gastrocnemius muscle, videos where physiotherapists and doctors were palpating the calves of patients to activate the gastrocnemius muscles were consulted. The third set of extra markers, labeled RGM and LGM respectively, were placed at the end of the gastrocnemius muscle before its insertion to the knee. The positions were again felt by palpation (Figure 3.16). The gastrocnemius muscle originates

from the femoral condyles that are situated at the back of the knee. Since it is quite hard to see where exactly the gastrocnemius muscle inserts in the knee, videos again where used to assist in finding the insertion of the gastrocnemius muscle with palpation.

Figure 3.16 represents the novel Achilles tendon marker placement where the figure to the left shows the back view of the Achilles tendon model marker placement based on the Plug-in Gait model. The extra markers along with their labels (LATm, RATm, LAT, RAT, LGM and RGM) are illustrated. The figure to the right shows the front view of the equivalent marker placement as produced by the Vicon Nexus system. This novel marker placement was tested with the Oxford Foot Model as well. However, the wand markers, the RCPG in Figure 3.15, of the Oxford Foot Model were creating errors, reflections and complications with reference to the RATm and LATm when the volunteers were asked to dorsiflex and plantarflex their feet. Also the markers placed at the tibial tuberosity, the RTUB in Figure 3.15, and the markers placed at the anterior aspect of the shin, RSHN in Figure 3.15, of the Oxford Foot Model caused discomfort and some pain to the volunteers when they were asked to lie of a medical bed with the prone position, i.e. facing down. For the above-mentioned reasons and since the OFM provides additional information about the foot and not the Achilles tendon, the OFM was not incorporated in out novel marker placement.

This new marker model illustrated in Figure 3.16, enabled the reconstruction of the lengths of the Achilles tendon and the gastrocnemius muscle during static and dynamic trials, lengths that were necessary for the dynamic analysis of the muscle-tendon model created. Data for the trajectories of the markers, of forces, of moments and EMG data were the same as those generated by the Plug-in Gait model and were exported and further analysed with Excel 2013 and Matlab 2016a. The data from all of the components of the system were collected in the system's software allowing a temporal and cross-sectional analysis of the sequences of events to be analysed.

3.4 Electromyogram (EMG)

Electromyography refers to the recording technique used to obtain an electromyogram. It is an experimental technique that focuses on how to develop, record and analyse myoelectric signals. An electromyogram (EMG) is a record of the external or internal electrical activity from a muscle associated with its contraction [1, 102, 103]. Electromyography is most commonly used as a clinical tool to identify when a muscle is activated, to determine whether a muscle is "on" or "off," and to a lesser extent, whether the activity is relatively "large" or "small". A kinesiological EMG focuses on the voluntary neuromuscular activation of muscles within functional movements, postural exercises, work conditions and treatment and training techniques [103]. There are many variables that affect an EMG signal at any time such as the velocity with which a muscle can elongate or shorten, the reflex activity, the magnitude and rate of the tension that builds up in a voluntary muscular activity and fatigue [1].
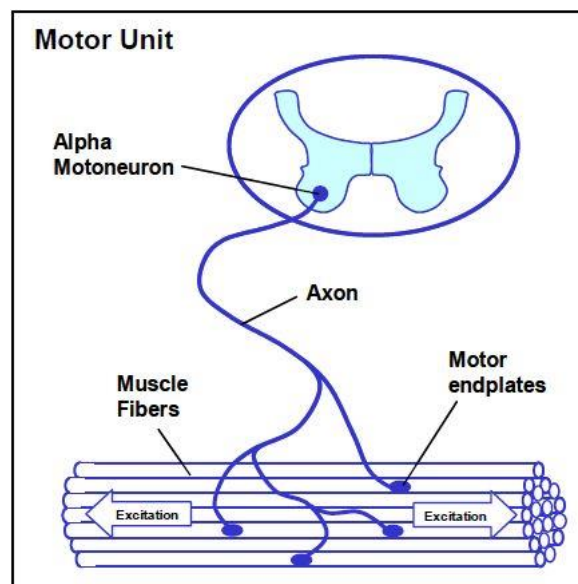
Figure 3.17. A schematic diagram of a motor unit, its axon and the motor endplates. Image taken from [103].

The EMG signal is based upon action potentials at the muscle fibre membrane resulting from depolarization and repolarization processes as described below. A *motor unit* is the smallest

functional unit able to represent the neural control of the contraction process of a muscle. It consists of the cell body and dendrites of a motor neuron, the multiple branches of its axon, and the muscle fibres that stimulate it (Figure 3.17). For a certain muscle, a motor neuron can control a number of motor units using special synaptic junctions called motor end plates. An action potential transmitted down the motor neuron reaches the motor end plate and activates a sequence of electrochemical events. This activation results in the excitation along the motor nerve. Transmitter substances are released at the motor endplates and an endplate potential is formed at the muscle fibre. The diffusion characteristics of the muscle fibre membrane are briefly modified and Na^+ ions that flow in and cause a membrane depolarization which results in a depolarization "wave" along the direction of the muscle fibres. Instant backward exchange of ions within an active ion pump mechanism restores the depolarization and this function is called repolarization. This depolarization and its subsequent repolarization wave is observed by the recording electrodes placed on the surface of a muscle [1, 103].

An EMG kit that records the surface electrical activity of the skeletal muscles via pads placed on the skin was used in the experiments. This assists in understanding how the Achilles tendon is interconnected with the nearest joints and the influence they have on the way different individuals walk. The EMG kit used in the Gait Laboratory inputs data from an Aurion Zero-Wire surface electromyography system to the Vicon Nexus software in order to record muscle activity. It uses silver/silver chloride (Ag/AgCl) hydrogel electrodes attached to the surface of the skin (Figure 3.18), and measures the EMG using small amplifiers. Sixteen (16) EMG channels are available. Each EMG channel samples at 1000 samples per second which is the accepted value in literature. Furthermore, each channel is located in a self-contained transducer unit which communicates wirelessly to a central receiver. The EMG central receiver then transmits analogue signals to the Vicon Giganet boxes. The EMG kit with the 16 channels can be seen in Figure 3.18. This picture was taken just to illustrate the EMG apparatus and how two

surface Ag/Cl hydrogel electrodes with adhesive pads can be attached to the surface of the skin. However, this figure does not show the correct placement of the EMG transducer on the gastrocnemius muscle since one pad is placed on the gastrocnemius lateralis and the other on the middle of the calf. The correct placement of the EMG transducers can be seen either in Figure 3.16 or in Figure 5.6 where the electrode separation distance is 10 mm and the electrodes are placed on the muscle belly of each muscle studied. Further information on the placement of the EMG electrodes on specific muscles of the legs of the volunteers is given in Section 5.1.3.2

The Zero-Wire surface EMG system was preferred over a wired EMG system, since there were no wired connections between the subject and the main system acquisition station present. Consequently, there were no constraints during any kind of movement that the subject needed to perform. Each wireless transducer is small and very light and has no actual effect on the subject's movement dynamics.
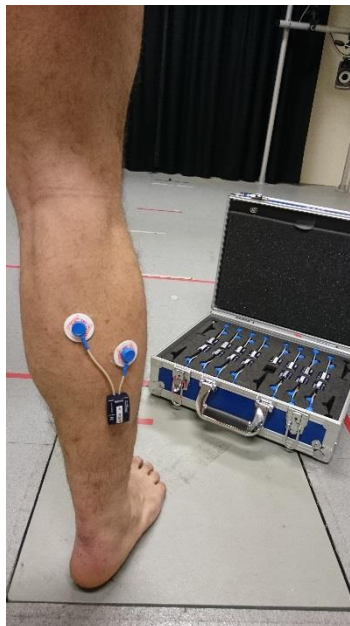
Figure 3.18. Two surface Ag/Cl hydrogel electrodes with adhesive pads are attached to the surface of the skin. The EMG kit with the 16 channels is illustrated.

3.5 Plantar Pressure – Tekscan

When in movement, the Achilles tendon tends to be affected mostly by the muscles in the medial section of the foot, these are the *tibialis posterior*, the *flexor digitorum longus* and the *flexor hallusis longus*, since as mentioned in Section 2.3 these muscles resist dorsiflexion and assist the gastrocnemius muscle and the Achilles tendon to create plantar flexion. That is why it is important to examine the internal forces of the tendon and its interconnection with joints, musculature and soft tissues. To do that, measurements of the plantar pressure, i.e. the distribution of force over the sole of the foot, is useful as it provides detailed information specific to each region of contact of the foot with the ground. The system used to measure the plantar pressure is a complete Tekscan system that includes Tekscan software along with the F-scan hardware [104].

The F-scan hardware contains a VersaTek Wireless/Datalogger, USB cables, CAT5E cables, a Li-Ion battery, two VC-1 VersaTek cuffs and two F-Scan sensors with Versatek edge connectors. The software is F-scan Research version 7.0 and was installed on the personal computer of the author of this thesis. The hardware collects plantar pressure data from the insole sensors and makes that information available to the software. Each sensor is sampled as the subject walks or performs any kind of movement studied. The software allows the user to view the collected sensor pressure data in real time, record this information as a "movie", and review it for further analysis [104].

The VersaTek Wireless/Datalogger (Figure 3.19) acts as a wireless gateway between the VersaTek cuffs (Figure 3.20) with the attached sensors (Figure 3.21) and the PC or laptop where the software is installed. A Li-Ion battery pack or a standard AC adapter powers the system. Two CAT5E cables are connected along the bottom of the Datalogger and lead to the VersaTek cuffs. On one side there is a USB port for microSD memory and a port for a USB cable that can

lead to the computer or laptop for a tethered configuration. There is also an integrated WiFi component that can wirelessly communicate with a host computer or laptop and that sends all of the data from the Datalogger to the computer or laptop for further analysis.

Figure 3.19. Versatek Wireless/Datalogger. Image taken from [104].

Figure 3.20. VC-1 VersaTek cuffs. Image taken from [104].

Figure 3.21. F-Scan insole sensor with Versatek edge connector. Image taken from [104].

The bottom of the VersaTek cuff connects to the insole's edge connector and its top part connects to the CAT5E. This cable then attaches to the VersaTek Wireless Datalogger as stated above. The VersaTek cuff gathers and processes the data from the insole sensors so that the information can be sent to the computer. The edge connector of the insole sensor connects to

the VersaTek cuff and snaps in place so that the insole sensor is prevented from dislodging. Each cuff has Velcro adhered to it so that it may be firmly attached to the Velcro ankle band, or any such surface (Figure 3.22) [104].

The F-Scan sensors are also called Tekscan plantar pressure insole sensors. They detect a subject's plantar pressure when they stand still or perform any type of movement that involves the feet. The Tekscan sensors (Figure 3.21) are Polyester sheets laminated with a substrate coating that is 0.076 mm thick. The presence of the protective substrate sheet makes the sensors stiffer, easier to handle and less able to conform to a curved surface. Each sensor is made up of 960 individual pressure sensing locations, which are referred to as 'sensing elements', 'sensels', or 'cells'. The sensels are arranged in rows and columns on the sensor. Each sensel can be seen as an individual square on the computer screen by selecting the 2D display mode. The output of each sensel is divided into 256 increments, and displayed as a value (raw sum) in the range of 0 to 255 by the software. The software uses a map to convert the pressure detected by the hardware into pressure data displayed in the real-time window on the host computer or laptop [104].
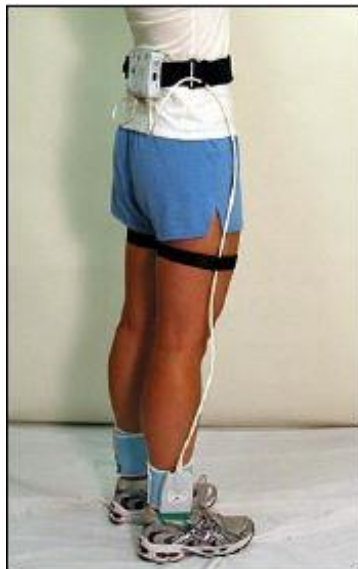
Figure 3.22. A subject set up with the whole F-scan system and ready for trials. Image taken from [104].

The Tekscan plantar pressure insole sensors are trimmed to different male and female shoe sizes. Then they are placed in shoes provided within the Gait Laboratory. In order to start any walking experiments, the subject needs to be set up with the F-scan hardware system. They are asked to put on the shoes with the insole sensors, taking care that the insole sensors remain as flat as possible inside the shoes. Then they are assisted to put on the waist belt that includes the VersaTek Wireless/Datalogger and battery. Ankle bands are wrapped around the subject's ankles and the VersaTek cuffs are attached to the bands by their Velcro backings. The VersaTek cuffs are connected to the sensors through the edge connectors and to the Datalogger through the CAT5E cables (Figure 3.22) [104]. Subsequently, the subject is ready to perform any movements or walking trials needed. For the purpose of this thesis, dorsiflexion and plantar flexion of the feet were studied as well as simple walking trials. Two dimensional and three dimensional distributions of forces, the centre of force and the trajectory of the centre of force, peak stances and average peak stances, graphs of forces versus time and of force versus distance are some examples of the outputs that the software can provide following the trials performed on subjects. The outputs needed for the model analysis and validation are further discussed in Chapter 5.

3.6 Imaging

Non-invasive medical imaging techniques such as Computed Tomography (CT), X-ray imaging, Magnetic Resonance Imaging (MRI) and Ultrasound (US) imaging have proven valuable for the study of the geometry of different parts of the body and evaluating pathologies. They can be used to improve the accuracy of the measured internal body component lengths, i.e. the gastrocnemius muscle and the Achilles tendon lengths that are needed for the parameterisation of the model.

Different imaging techniques can highlight different parts of the human body. While plain radiography can give a good outline of the bony alignment and can detect quite easily fractures, erosions, deformities and dislocations, it has very limited value in the assessment of chronic soft tissue disorders [105]. Computed tomography (CT) (Figure 3.23) is better since it can display bone fractures not seen by plain radiography and it performs a scan of the foot or ankle in a matter of seconds. However, it is of limited use in tendon, ligament and cartilage injuries because of its poor soft tissue definition [32]. Ultrasound (US) (Figure 3.24) is the best tool for assessing tendons and ligaments due to its fine resolution and ability to scan dynamically. It is used to evaluate chronic tendinopathy of the Achilles tendon, inflammation of its surrounding soft tissues (e.g. paratenon) and also to scan partial or complete tendon tears. A disadvantage of Ultrasound is its limited ability to assess the bones and their articular surfaces [32, 106]. Magnetic Resonance Imaging (MRI) (Figure 3.25) is an established and highly valuable imaging technique to assess major joints. This is because it can evaluate both the bony structures and the soft tissues of a patient. One minor disadvantage is its lengthy scanning times [31, 32, 107]. Nevertheless, MRI is very good for the assessment of musculoskeletal abnormalities because it permits direct depiction of tendons, ligaments, muscles, cartilage and bone without the requirement for intra-articular contrast and without exposing the patient to ionising radiation [107].
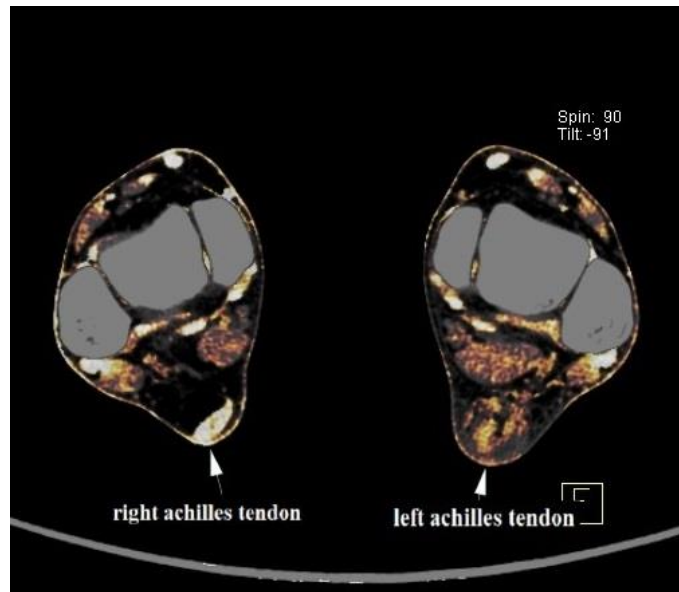
Figure 3.23. CT scan of an Achilles tendon. Image taken from [108].
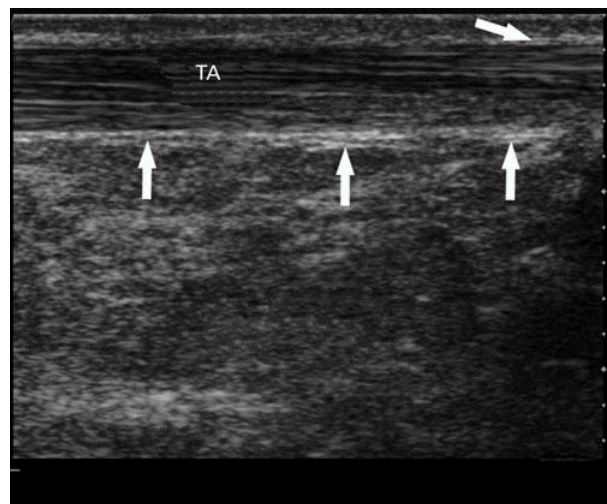
Figure 3.24. Ultrasound scan of an Achilles tendon. Image taken from [109].
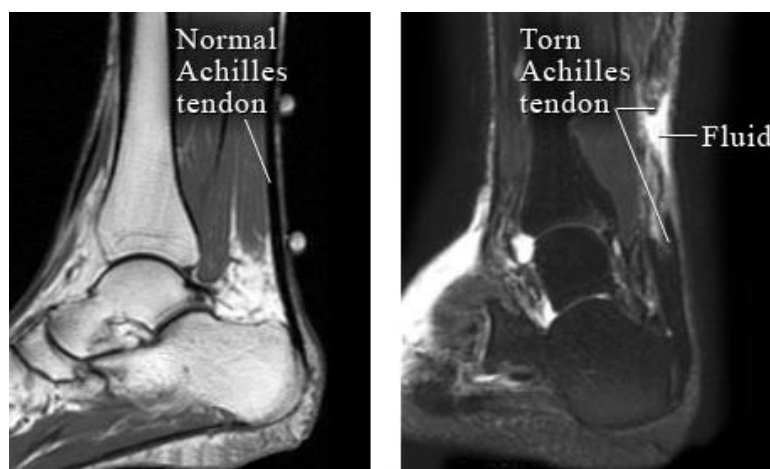
Figure 3.25. MRI scan of a normal and a torn Achilles tendon. Image taken from [12].

In this thesis, Ultrasound and Magnetic Resonance Images obtained through the University Hospitals Coventry and Warwickshire (UHCW) were used in order to define the geometry of the Achilles tendon, the gastrocnemius muscle, the tibia, the heel and the ankle. These images were also used to measure the changes in length of the Achilles tendon and the gastrocnemius muscle in dorsiflexion and plantar flexion of the foot segment. Both imaging techniques were used since they complement each other. MRI is less operator dependent than Ultrasound and provides us with a better overview of the surrounding tissues. It can assess not only the soft tissues, but also the bony structures. Ultrasonography is more cost effective, safe and generally more widely available than MRI. It can also evaluate a tendon in longitudinal as well as transverse projections, in both static and dynamic views [32, 106]. In order to obtain a complete view of the Achilles tendon, data taken from the previously mentioned images were combined. All images obtained from UHCW comply with NHS ethics approval for the collection and use of such images. Also as mentioned in section 3.2 ethical approval complying with the research code of practice of the University of Warwick had been granted for all Ultrasound sessions at UHCW by the University's Biomedical and Scientific Research Ethics Committee (Appendix A).

Chapter 4. Model Development

In this chapter the development of the mathematical, mechanical, musculoskeletal model of the Achilles tendon is described. Inverse dynamics is a widely known concept used in the field of mechanics connecting the aspect of kinematics and kinetics. It is a method of computing forces and moments of force indirectly from the kinematics and inertial properties of bodies in motion. In comparison, forward or direct dynamics use applied forces or torques to determine the resultant motion of bodies [41]. Inverse dynamics can be applied to stationary bodies as well as moving bodies. This approach is applied in conjunction with Newton's second and third laws, where the resultant force is divided into known and unknown forces. A single net force, that can be measured from experiments, is produced from the combination of the unknown forces in order for the unknown ones to be solved. A similar process is used to determine the unknown moments of force from a single net moment of force that can be computed. This method of determination of forces and moments is described in this chapter.

In Section 4.1 a description of the model derivation is given. In Section 4.2, a two segment model of the human foot and leg is presented that describes the development of the musculoskeletal model of the Achilles tendon. Newton's laws and the method of link-segment modelling are illustrated. They are used to derive the system equations necessary to mathematically model the skeletal system along with the Achilles tendon. In Section 4.3 the method used to model human skeletal muscle dynamics using Hill-type muscle models is portrayed. A gastrocnemius muscle-Achilles tendon model is presented and the derivation of the system equations that characterise the muscle-tendon model are provided.

4.1 Description of model derivation

In 'Research Methods in Biomechanics' [41] a detailed analysis on how to determine and quantify the patterns of forces produced by muscles, ligaments, bones etc., about a specific joint

is given. An outline of the analysis is presented in this section in order to introduce the reader to the method used for the creation of the Achilles tendon model. Figure 4.1 shows the anatomical forces of a free-body diagram (FBD) of the foot when it contacts the ground just before toe off. The anatomical forces crossing the ankle joint consist of many different types such as muscle forces, ligament forces and bone-on-bone forces. A few have not been considered by Robertson et al., i.e. forces from skin, bursa and joint capsule since they are very difficult to determine [41].
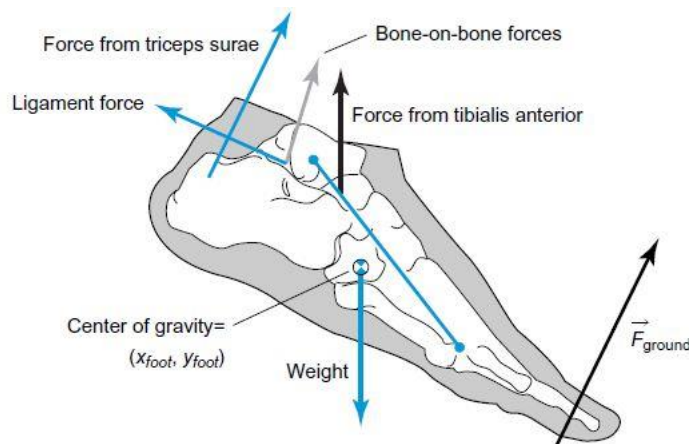
Figure 4.1. Schematic presentation of the anatomical forces of the free body diagram of the foot when it contacts the ground just before toe off. Image taken from [41].

The foot is considered to be a 'rigid body' so that its inertial properties have fixed values, since rigid bodies are objects that cannot be deformed and have no moving parts. Thus the centre of gravity of the foot, its mass and the mass distribution are constant. The next step in the analysis is to substitute a single muscle force with an equivalent force and moment of force about a common axis. This is done in order to enable the researcher to calculate the values of the unknown force from the measured known ones. The example presented in Figure 4.2 is taken from the text of 'Research Methods in Biomechanics' [41] and portrays how the muscle force exerted by the tibialis anterior muscle on the foot segment can be replaced by an

equivalent force and moment of force at the ankle centre of rotation. A force $\overrightarrow{F}^*$ equal in magnitude and direction to the force $\overrightarrow{F}$ of the tibialis anterior is placed at the ankle joint and a second force $-\overrightarrow{F}^*$ equal in magnitude, but opposite in direction to $\overrightarrow{F}^*$, is also placed at the ankle joint in order to maintain equilibrium and balance the free body system (Figure 4.2.b). Subsequently, the force couple $\overrightarrow{F}$ and $-\overrightarrow{F}^*$ is replaced by the moment of force $M_F \vec{k}$. Since the foot is considered to be a rigid body, the resulting force and moment of force seen in Figure 4.2.c have the same mechanical effects as the single muscle force seen in Figure 4.2.a.
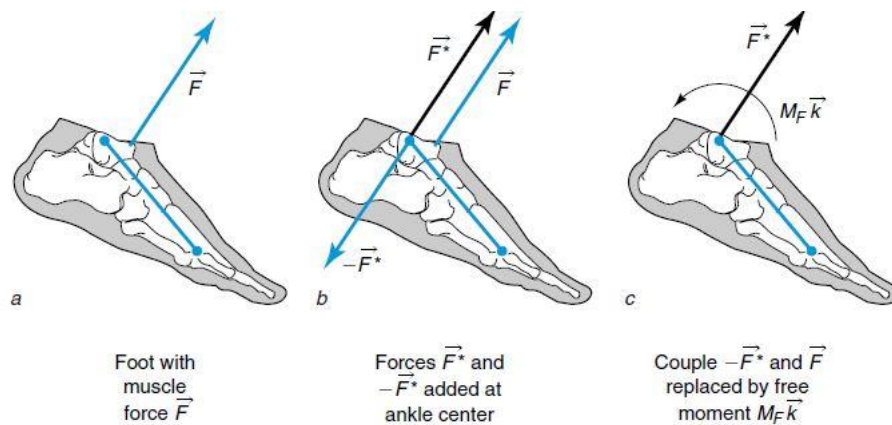
Figure 4.2. Representation of the analysis and replacement of a muscle force at the ankle axis of rotation by its equivalent force and moment of force. Image taken from [41].
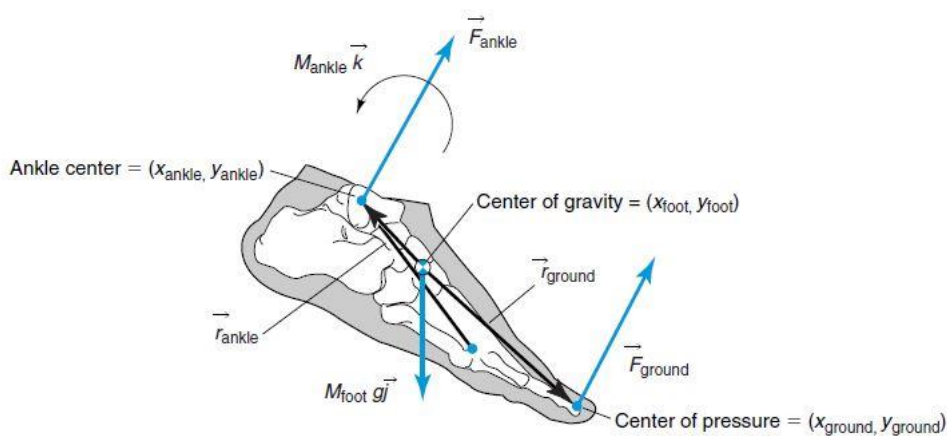
Figure 4.3. Representation of the free body diagram illustrating the net force and the net moment of force at the ankle axis of rotation. Image taken from [41].

In order to simplify a complex situation such as the existence of numerous forces acting across the ankle, the replacement of every force with its equivalent force and moment of force about a common axis has been suggested (Figure 4.3). The summation of the ankle forces and moments of force produces a single force and a single moment of force called the *net force* and the *net moment of force* respectively [41]. However, forces whose lines of action pass through the ankle joint centre do not produce any moment of force around the joint. Consequently, the structures that contribute to the net moments of force are the muscle forces. The ligament and bone-on-bone forces play a role mostly with respect to the net force of the ankle and only produce a moment of force when the ankle is at the ends of its range of motion.

The method used to numerically compute the internal kinetics of planar human movements is now presented. In order to calculate the forces and moments at specific joints, body kinematics and anthropometric data are applied. Three important principles are involved in this method; i) Newton's second law, ii) the principle of *superposition* and iii) a technique known as the *method of sections* [1, 41].

The principle of superposition states that when a system has multiple factors (i.e., forces and moments) under certain conditions we can either sum the effects of those factors or handle them independently [41]. For example, a body rotates when a moment (or torque) is applied to it. By using the principle of superposition, when one or more of these actions occur they can be analysed separately. Thus, all forces and moments that create movement to a specific joint can be separated into x, y, z coordinates and solved independently.

The main concept behind the method of sections is to divide a mechanical system into specific components and determine the relations between them. For example, the lower extremities of a human are segmented into thighs, legs, and feet. Then applying Newton's second law, using measured values of ground reaction forces (GRF), the acceleration and mass

of each segment, the forces acting at the joints can be determined. This process is called the

link-segment or *iterative Newton-Euler method,* and is schematically presented in Figure 4.4.

As can be seen in Figure 4.4, the body is 'cut' at the joints of interest, i.e. the ankle, the knee

and the hip. Free body diagrams of the segments of the body are created. At the most distal

segment, i.e. the foot segment, the unknown horizontal and vertical forces and the

corresponding moments are generated according to the positive directions of the global

coordinate system (GCS). At the next segment, i.e. the foot segment, following Newton's third

law, the unknown forces and moments are generated according to the negative directions of the

GCS. Lastly, the equations of motion for one of the segments are solved [1, 41].
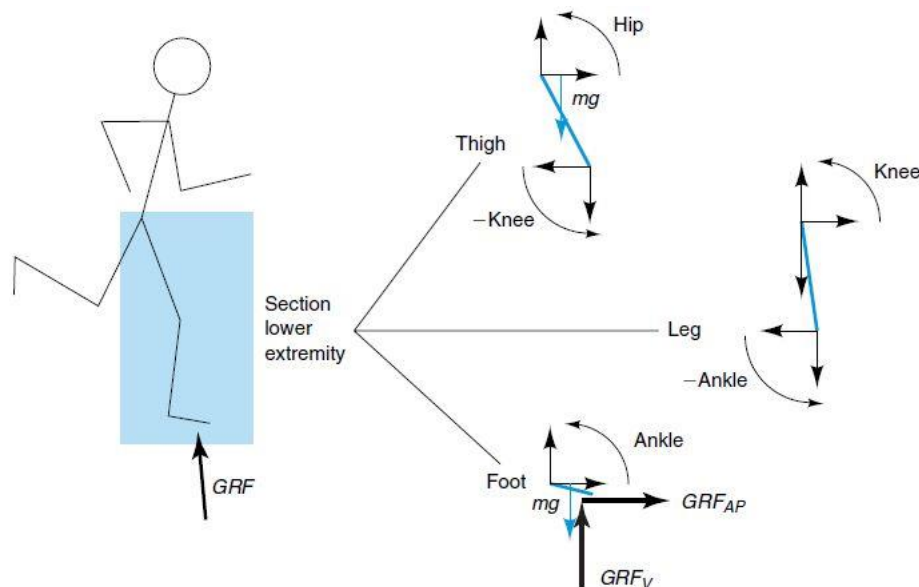
Figure 4.4. Schematic representation of the method of sections where the human lower extremity is divided into three different segments: the thigh, the leg and the foot. Image taken from [41].

The process described follows a specific order. The most distal segment is the first to be

analysed, then followed by the analysis of its proximal segment until all unknowns are found.

The reason behind this procedure is that only three equations can be applied to each segment,

since only three unknowns for each segment can be assigned; a horizontal force, a vertical force

and a moment. As seen in Figure 4.4, the thigh or leg segments have six unknowns, two forces

and one moment at each joint whereas the foot segment, which is the most distal segment, has only three. Therefore, the analysis begins at the segment that has only one joint and then moves to the adjacent segment. Newton's third law is then employed which states that every action has an equal but opposite reaction. Thus, at the joints present, the forces on the distal end of one segment must be equal and opposite to those on the proximal end of the adjacent segment [1, 41]. When examining the foot, leg and thigh segments, only the foot has the necessary three unknowns (horizontal and vertical force and a moment). This is why in the analysis the foot segment is the first to be solved. The forces and actions at the ankle joint of the foot segment have equal and opposite reactions at the ankle joint of the leg segment. Then the unknown reactions at the knee joint can be calculated etc. This analysis is schematically represented in Figure 4.5.
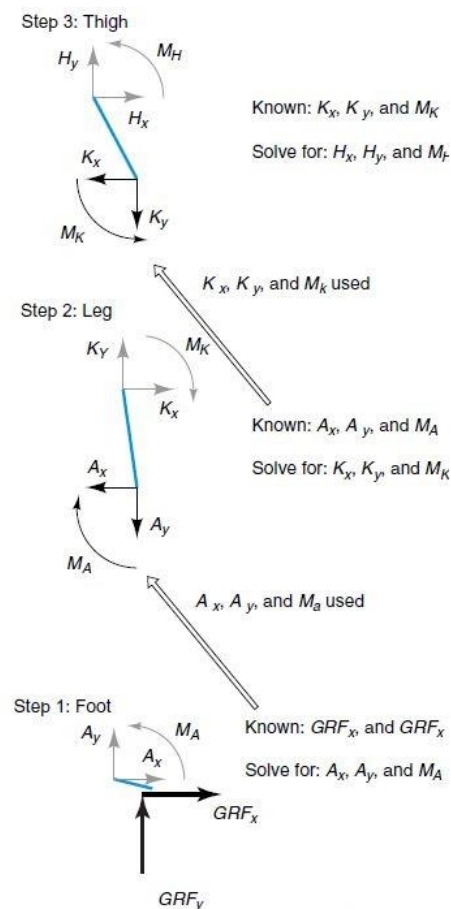
Figure 4.5. Representation of the link-segment analysis of the foot, leg and thigh segments of the human lower extremities. Image taken from [41].

4.2 Achilles tendon model

Even though bones form the framework of the body and provide stabilisation, they cannot move body parts by themselves. Motion and movement come from the alternation of the contraction and relaxation of muscles. Most skeletal muscles attach to the bones and they produce movement during contraction. Tendons connect muscle to bone and are located all over the human body. Tendons are considered more elastic because they mainly consist of collagen matrices that have elastic properties [58]. As mentioned in Section 2.1 the Achilles tendon is a fibrous tissue that connects the gastrocnemius muscle to the calcaneus bone. When the calf muscles contract, they apply a force to the Achilles tendon and therefore push the foot downwards which results in walking, jumping, running, standing on toes, etc. [18]. Like other tendons, the Achilles tendon transmits tensile forces from the leg to the foot according to the amount of stretch it undergoes. Inversion of the heel, as well as plantar flexion, are produced by these forces when they pass through the ankle and the subtalar joints. Thus, movement in the subtalar joints and the ankle is created [13]. The mechanical properties of the Achilles tendon allow it to store and transmit elastic strain energy during fast locomotion and other movements [58]. That is why it is described as an energy-saving mechanism and a spring and shock absorber during gait [28]. It has been demonstrated, through measurements of the mechanical properties of the Achilles tendon, that there is a variation in the elastic properties and the stiffness of the tendon between individuals [110, 111].

A two segment model of the human foot and leg was created in order to develop a musculoskeletal model of the Achilles tendon [112]. Only these two specific segments of the foot and the leg were chosen since the Achilles tendon connects them. As shown in Figure 4.6, the model is comprised of i) the Achilles tendon connecting the heel and the gastrocnemius muscle, ii) the gastrocnemius muscle connecting to the Achilles tendon and the tibia, iii) the

tibia originating from the ankle joint and ending at the knee and iv) the foot, that is represented by a triangle whose vertices are the heel, the ankle joint and the toe [112]. In the literature the foot is represented either as a rigid body or as two segments when the toe joint is included. Since in both Winter's book [1] and Robertson's book [41], the foot is assumed to be a rigid body when analysing movements, the foot segment for the purpose of the experiments in this thesis is represented as rigid.
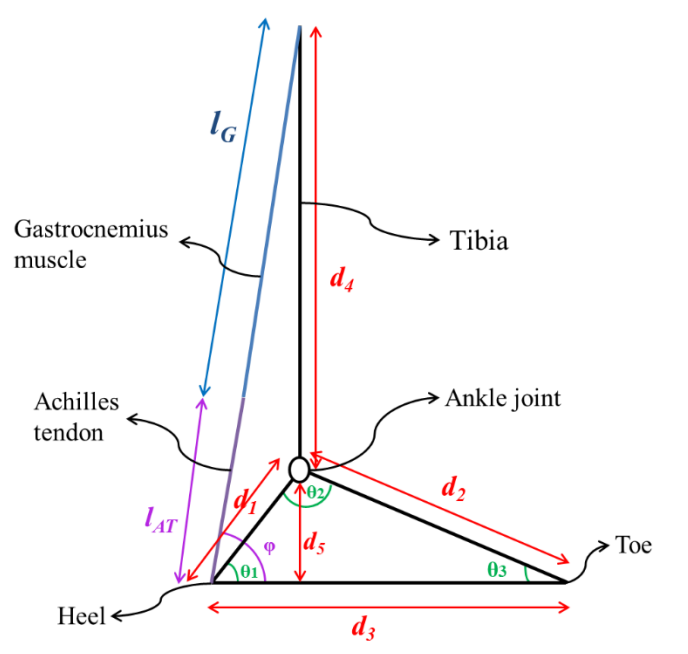
Figure 4.6. Two segment model of the foot-leg illustrating the connection between the Achilles tendon, the gastrocnemius muscle, the heel and the tibia [112].

The ankle consists of three joints: the ankle joint, the subtalar joint, and the inferior tibiofibular joint. The ankle joint connecting the tibia (leg bone) to the talus (foot joint) has one degree of freedom and the movements produced at this joint are dorsiflexion and plantar flexion of the foot. That is why these movements were chosen to be studied in the Gait Laboratory experiments. The subtalar joint, which occurs at the meeting of the talus and the calcaneus, allows the inversion and eversion of the foot, but plays no role in dorsiflexing or plantar flexing the foot and it also has one degree of freedom. The subtalar joint can also allow pronation and supination to occur which provides the third degree of freedom. Since the ankle joint is the

dominant one in the foot segment, the subtalar joint was not incorporated in the model developed.

The lengths (in mm) seen in Figure 4.6 define the distances given in Table 4.1. The explanation of how they were determined is given in Section 5.1.3.

Table 4.1. Definition of distances

d_1 (mm)	the distance between the heel and the ankle joint
d_2 (mm)	the distance between the ankle joint and the toe
d_3 (mm)	the distance between the heel and the toe
d_4 (mm)	the length of the tibia
d_5 (mm)	the distance of the ankle from the floor
l_G (mm)	anatomical length of the gastrocnemius muscle
l_{AT} (mm)	anatomical length of the Achilles tendon

4.2.1 System equations

Knowledge of the patterns of the forces exerted by the gastrocnemius muscle on the Achilles tendon and vice versa is necessary in order to study the forces that the Achilles tendon transmits from the leg to the foot. Hence, it is crucial to calculate these forces indirectly using anthropometric and readily available kinematic data. The process by which the reaction forces and muscle moments are computed has been described in Section 4.1 and is called link-segment modelling [1, 113]. In order to calculate joint reaction forces and muscle moments we need to have full knowledge of the external forces applied to the joints, a kinematic description of the movement and accurate anthropometric measurements for each of the volunteers participating

in the experiments. Using this two segment model and inverse dynamics it should then be possible to predict any joint and tendon reactions needed [114].

Newton's second and third laws were used to derive the system equations for the musculoskeletal model of the Achilles tendon shown in Figures 4.6, 4.7, 4.8 and 4.9. Figures 4.6 and 4.7 portray the ankle joint dynamics when a volunteer is standing still in an upright position, Figure 4.8 when dorsiflexing their foot and Figure 4.9 when plantar flexing their foot. As seen in Figure 4.7 the foot is represented by a triangle whose vertices are the heel (H), the ankle joint (A) and the toe (T). All other references to this triangle in this thesis will be referred to as the triangle HTA.
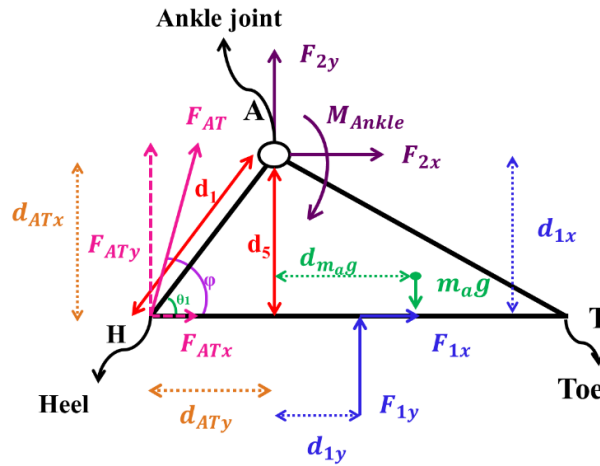
Figure 4.7. Free body diagram of the foot segment during weight bearing in a static position [112].

The equations describing a static situation, when a volunteer is standing still on the force plate, (Figure 4.7) are given by:

$$\sum F_x = ma_x \Rightarrow \sum F_x = 0 \Rightarrow F_{1x} + F_{2x} + F_{ATx} = 0 \qquad \text{(Eqn. 4.1)}$$

$$\sum F_y = ma_y \Rightarrow \sum F_y = 0 \Rightarrow F_{1y} + F_{2y} + F_{ATy} - m_a g = 0 \qquad \text{(Eqn. 4.2)}$$

$$M_{ankle} = F_{1x} d_{1x} + F_{1y} d_{1y} - m_a g d_{m_a g} + F_{ATx} d_{ATx} - F_{ATy} d_{ATy} \qquad \text{(Eqn. 4.3)}$$

where the definition of the variables included in these equations are given in Table 4.2. The accelerations along both the x and y axes of the segment is 0 m/s^2 since during a static trial the subject does not move.

Table 4.2. Definition of variables for the static trial

x	Subscript that represents the horizontal plane of action
y	Subscript that represents the vertical plane of action
F (N)	Force applied to the ankle joint or the heel depending on the subscripts
1	Subscript that signifies the external ground reaction force
2	Subscript that denotes the force acting on the foot at the ankle joint because of the tibia
AT	Subscript that symbolises the Achilles tendon force acting on the foot at the heel
α	Subscript that represents the centre of the mass of the foot
$m_a g$ (N)	Force due to the mass of the foot under gravity
M_{ankle} (N mm)	Moment at the ankle joint
d (mm)	Distance of the ankle joint from the heel, the Achilles tendon and the centre of mass of the foot depending on the subscript
m (kg)	Mass of the foot segment
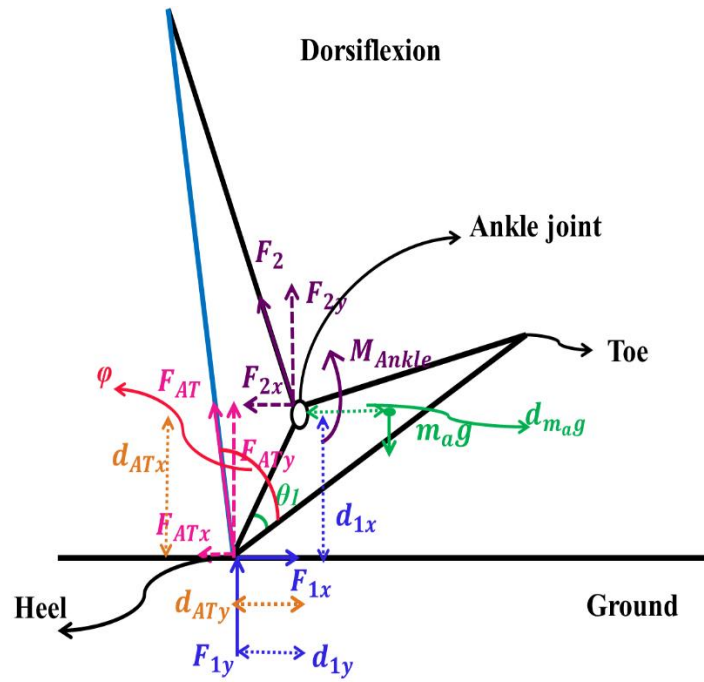
Figure 4.8. Dorsiflexion of the foot [112].
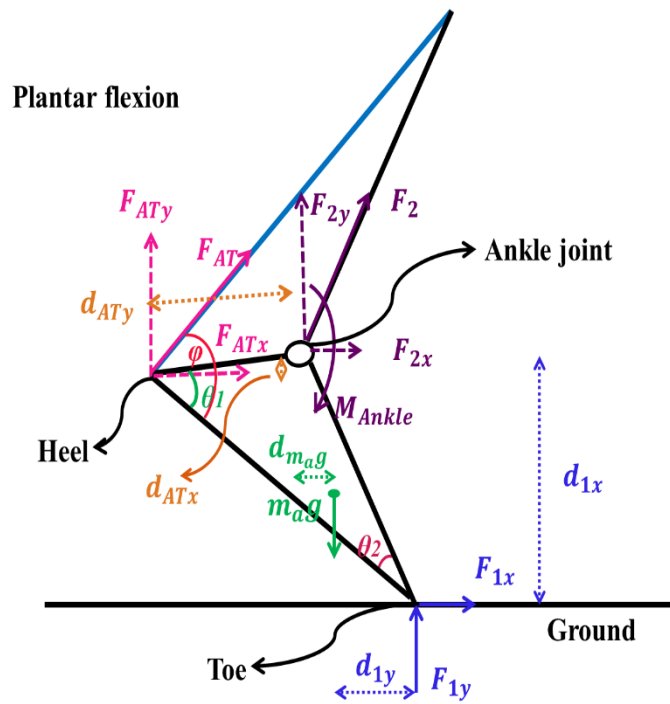
Figure 4.9. Plantar flexion of the foot [112].

101

Table 4.3. Definition of variables for a dynamic trial

x	Subscript that represents the horizontal plane of action
y	Subscript that represents the vertical plane of action
F (N)	Force applied to the ankle joint or the heel depending on the subscripts
1	Subscript that signifies the distance between the level that F_{1x} and F_{1y} is applied and the ankle joint
2	Subscript that denotes the distance between the level that F_{2x} and F_{2y} is applied and the ankle joint
AT	Subscript that symbolises either the Achilles tendon force acting on the foot at the heel or the distance between the level that F_{ATx} and F_{ATy} is applied and the ankle joint depending on the superscript
$m_a g$ (N)	Force due to the mass of the foot under gravity
α_x, α_y (mm/s^2)	Acceleration of the foot segment in the horizontal and vertical plane of action respectively
α (rad/s^2)	Angular acceleration of the foot segment
M_{ankle} (N mm)	Moment at the ankle joint
d (mm)	Distance of the ankle joint from the heel and the Achilles tendon depending on the subscript
$d_{m_a g}$ (mm)	Distance calculated from the coordinates of the markers and table 4.1 from Winter [1]
I (kg mm^2)	Moment of inertia about the ankle joint calculated from the coordinates of the markers and table 4.1 from Winter [1]
m (kg)	Mass of the foot segment

The equations describing the dynamics of dorsiflexion and plantar flexion as seen in Figures 4.8 and 4.9 respectively are listed below.

$$\sum F_x = ma_x \Rightarrow F_{1x} + F_{2x} + F_{ATX} = ma_x \qquad \text{(Eqn. 4.4)}$$

$$\sum F_y = ma_y \Rightarrow F_{1y} + F_{2y} + F_{ATy} - m_a g = ma_y \qquad \text{(Eqn. 4.5)}$$

$$M_{ankle} = F_{1x}d_{1x} + F_{1y}d_{1y} + m_a g d_{m_a g} + F_{ATx}d_{ATx} + F_{ATy}d_{ATy} - I\alpha \qquad \text{(Eqn. 4.6)}$$

where the definitions of the variables included in these equations are given in Table 4.3. The accelerations along the x and y axes of the segment are no longer 0 m/s^2 since the subject is in motion. In Figures 4.8 and 4.9, θ_1 is the angle between the sides HT and HA of the triangle HTA and φ is the angle between the Achilles tendon and the sole of the foot. The force $m_a g$ and its distance $d_{m_a g}$ from the ankle joint found in Equations 4.2, 4.3, 4.5 and 4.6 are calculated using the anthropometric data taken from Table 4.1 in Winter's book 'Biomechanics and Motor Control of Human Movement' [1]. This table is provided in Section 5.1.3 were the experimental methodology is described. The moment of inertia about the ankle joint I (kg mm^2) found in Equation 4.6 is calculated from the anthropometric data in Table 4.1 from Winter and from the following Equation:

$$I = m\rho_0^2 + mx^2 = I_0 + mx^2 \qquad \text{(Eqn. 4.7)}$$

where I_0 (kg mm^2) is the moment of inertia about the centre of mass of the segment, m (kg) is the mass of the segment, ρ_0 (mm) is the radius of gyration of the segment and x (mm) is the distance between the centre of mass and centre of rotation of the segment. This equation is based on the parallel-axis theorem [1]. All calculations are based on the examples given in Winter on how to evaluate all the unknowns in Equations 4.1-4.7 from experimental data taken from a motion capture system, such as Nexus as used in the experiments [1].

4.2.2 Gastrocnemius muscle – Achilles tendon complex analysis and system equations

A range of mechanical models Crowe (1970)[115], Gottlieb and Agarwal (1971)[116], Winter (1995)[1], Haeufle (2014)[43] – exist, that describe and calculate the tension of a muscle depending on different inputs. All of them use a modified Hill-type muscle model with different connections between the contractile element (CE), the parallel elastic component (PEC) and the series elastic component (SEC) elements. Generally, Hill-type muscle models have as an input, muscle-tendon lengths, muscle-tendon contraction velocities or neural muscle stimulations and as an output a force that is usually applied between the insertion points and the origins of the muscle or tendon analysed. By simulating different movements of the muscles with these models, one can predict the passive and active muscle forces.
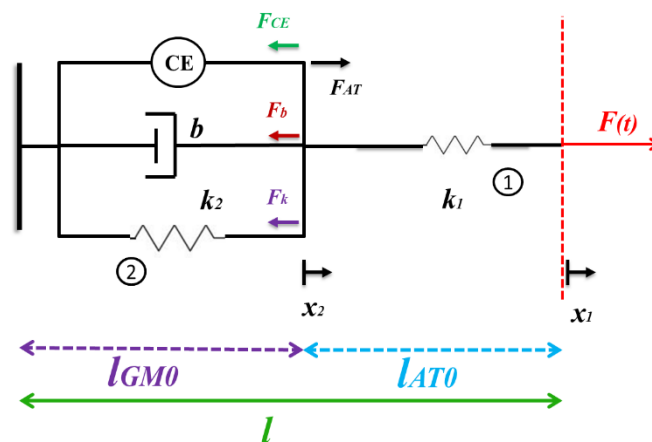
Figure 4.10. Analysis of movement of the Modified Hill-type muscle model representing the gastrocnemius muscle-Achilles tendon complex [112].

As depicted in Figure 4.10, a modified Hill-type muscle model has been used to investigate the mechanical characteristics of the Achilles tendon and the gastrocnemius muscle. The gastrocnemius muscle is represented by: i) the contractile element (CE) that represents the force source when the muscle is activated, ii) the parallel damping element that is described by a

damper where b (Ns/m) is the damping coefficient and denotes the ability of the muscle to resist its shortening or lengthening depending on the movement studied, and iii) the parallel elastic component (PEC) that is defined by the spring numbered as 2 in Figure 4.10 with stiffness k_2 (N/m) that characterises the ability of the gastrocnemius muscle to return to its natural resting length. A series elastic element k_1 shows the series elastic component (SEC) of the model and represents the behaviour of the Achilles tendon in the complex [1, 40, 43, 45, 58, 117, 118]. All other connective tissue was ignored since the Achilles tendon is the dominant tendon connecting the heel to the gastrocnemius muscle and the one that can be studied more accurately with the methods used in the associated experiments. The damping characteristic of the SEC is considered to be relatively small and does not influence the general behaviour of the model; that is why it is ignored in this study.

4.2.3 Response of the Active Muscle

The transfer function of the Hill-type muscle model seen in Figure 4.10 can be generated and used to find the active muscle response. A similar approach has been investigated for the muscles of the upper limb [45]. As seen in Figure 4.10 the externally measured force F can be defined by the force of the contractile element F_{CE} that is changed by the force of the damping element F_b and that of the parallel elastic element F_k. The total force F is transferred through the series elastic element that represents the Achilles tendon whose force is denoted by F_{AT}, resulting in the following two equilibrium equations:

$$\vec{F} = \vec{F}_{CE} + \vec{F}_b + \vec{F}_k \qquad \text{(Eqn. 4.8)}$$

and $\vec{F} = \vec{F}_{AT}$. $\qquad$ (Eqn. 4.9)

Analysing the movement of the muscle-tendon complex in Figure 4.10 gives the following equations where (Eqn. 4.10) and (Eqn. 4.11) are the system specific forms of (Eqn. 4.8) and (Eqn. 4.9) respectively:

$$F = F_{CE} - b\frac{dx_2}{dt} - k_2 x_2 \qquad \text{(Eqn. 4.10)}$$

$$F = k_1 (x_2 - x_1)^{\alpha} \qquad \text{(Eqn. 4.11)}$$

where α is a positive integer (α =1,2 or 3). If the spring element describing the Achilles tendon is considered to be linear then α equals 1 and if it is considered non-linear then α equals 2 or 3. For values greater than 3, the simulations created in order to solve Equations (4.10) and (4.11) produce results that cannot represent the muscle-tendon complex. Since the Achilles tendon is the dominant tendon that transmits the force from the heel (and the foot eventually) to the gastrocnemius muscle and vice versa and since no other external forces are applied to the muscle-tendon model, F is assumed to be equal to F_{AT} in Equations (4.10) and (4.11). Initially we assume that the spring is linear (α=1). Nonlinearity of the spring element will be discussed in Chapter 5. The displacement of the gastrocnemius muscle is denoted by x_2 and the displacement of the muscle-tendon complex is x_1 and is measured from the insertion point of the Achilles tendon to the heel which is at the right end of spring 1 in Figure 4.10. As mentioned previously, muscles and tendons have natural resting lengths when no force or stimulation is acting upon them. The natural lengths of the muscle and the Achilles tendon are denoted by l_{GM0} and l_{AT0} respectively. When in movement the length of the muscle and the tendon change and become $l_{GM}=l_{GM0}+x_2$ and $l_{AT}=l_{AT0}+x_1-x_2$ respectively.

Assuming zero initial conditions:

$$x_1(0) = x_2(0) = 0. \qquad \text{(Eqn. 4.12)}$$

Using Equation (4.11) to replace x_2 in Equation (4.10) and taking Laplace transforms gives:

$$F_{CE}(s) = \frac{k_1 + k_2 + bs}{k_1} F_{AT}(s) + (k_2 + bs) X_1(s) \,. \qquad \text{(Eqn. 4.13)}$$

Equation 4.13 can be rearranged into two different forms.

One is the equation that describes the external muscle force/tension F_{AT} as a function of the force produced by the active contractile element. Solving (4.13) for F_{AT} gives:

$$F_{AT}(s) \frac{k_1 + k_2 + bs}{k_1} = F_{CE}(s) - (k_2 + bs) X_1(s) \Rightarrow$$

$$F_{AT}(s) = F_{CE}(s) \frac{k_1}{k_1 + k_2 + bs} - \frac{k_1(k_2 + bs)}{k_1 + k_2 + bs} X_1(s) \,. \qquad \text{(Eqn. 4.14)}$$

The other is the expression of displacement X_1 in terms of the external force and the force from the contractile element of the active muscle. Solving (4.13) for X_1 gives:

$$X_1(s)(k_2 + bs) = F_{CE}(s) - \frac{k_1 + k_2 + bs}{k_1} F_{AT}(s) \Rightarrow$$

$$X_1(s) = \frac{F_{CE}(s)}{(k_2 + bs)} - \frac{k_1 + k_2 + bs}{k_1(k_2 + bs)} F_{AT}(s) \,. \qquad \text{(Eqn. 4.15)}$$

In order to test the model against known system responses, the following scenarios were investigated. In an isometric contraction, the muscle contracts without shortening considerably since both of its ends are strictly fixed so that it cannot shorten or lengthen. Even though the length of the entire muscle does not change, the individual muscle fibres will shorten. Examples of isometric exercises comprise of holding a weight in place above the ground or pushing against a stationary object. When the muscle is stimulated it contracts isometrically and the resulting external force can be measured experimentally [119, 120]. This scenario can be investigated using Equation (4.14) where the second term is excluded, since no change in

length, at least externally, is present. This means that x_1 equals zero, but x_2 can be nonzero. Thus, (4.14) becomes:

$$F_{AT}(s) = F_{CE}(s)\frac{k_1}{k_1 + k_2 + bs} \ . \tag{Eqn. 4.16}$$

Assuming a maximum tetanic stimulation, where the muscle has been maximally stimulated and remains that way for some time, the input can be represented by a step function with magnitude F_{CE}. The Laplace transform of the step function, Equation (4.16) becomes:

$$F_{AT}(s) = F_{CE}\frac{k_1}{k_1 + k_2 + bs}\frac{1}{s} \ . \tag{Eqn. 4.17}$$

Rearranging the variables in Equation (4.17) gives:

$$F_{AT}(s) = \frac{F_{CE}k_1}{b}\left(\frac{1}{(\frac{k_1 + k_2}{b}) + s}\cdot\frac{1}{s}\right) \Rightarrow F_{AT}(s) = \frac{F_{CE}k_1}{b}\left(\frac{1}{s(\frac{k_1 + k_2}{b} + s)}\right). \tag{Eqn. 4.18}$$

A partial fraction expansion of (4.18) gives:

$$\frac{1}{s(\frac{k_1 + k_2}{b} + s)} = \frac{A}{s} + \frac{B}{\frac{k_1 + k_2}{b} + s} \Rightarrow 1 = \frac{A}{s}s(\frac{k_1 + k_2}{b} + s) + \frac{B}{\frac{k_1 + k_2}{b} + s}s(\frac{k_1 + k_2}{b} + s)$$

$$\Rightarrow 1 = A(\frac{k_1 + k_2}{b} + s) + Bs \Rightarrow 1 = A\frac{k_1 + k_2}{b} + As + Bs \Rightarrow 1 = A\frac{k_1 + k_2}{b} + (A + B)s \ . \tag{Eqn. 4.19}$$

Comparing the coefficients of s in Equation (4.19) yields:

$$A + B = 0 \Rightarrow B = -A \ . \tag{Eqn. 4.20}$$

Comparing the constant terms in Equation (4.19) gives:

$$1 = A\frac{k_1 + k_2}{b} \Rightarrow A = \frac{b}{k_1 + k_2} \Rightarrow B = -\frac{b}{k_1 + k_2} \ . \tag{Eqn. 4.21}$$

Substituting the coefficients of *A* and *B* into Equation (4.18) and taking the inverse Laplace transforms yields:

$$F_{AT}(t) = \frac{F_{CE}k_1}{b} L^{-1}\{\frac{1}{s(\frac{k_1+k_2}{b}+s)}\} \Rightarrow F_{AT}(t) = \frac{F_{CE}k_1}{b} L^{-1}\{\frac{\frac{b}{k_1+k_2}}{s} - \frac{\frac{b}{k_1+k_2}}{s+\frac{b}{k_1+k_2}}\}$$

$$\Rightarrow F_{AT}(t) = \frac{F_{CE}k_1}{b} L^{-1}\{\frac{b}{k_1+k_2}\frac{1}{s} - \frac{b}{k_1+k_2}\frac{1}{s+\frac{b}{k_1+k_2}}\}$$

$$\Rightarrow F_{AT}(t) = \frac{F_{CE}k_1}{b}(\frac{b}{k_1+k_2}1 - \frac{b}{k_1+k_2}e^{-\frac{k_1+k_2}{b}t}) \Rightarrow F_{AT}(t) = \frac{F_{CE}k_1}{b}\frac{b}{k_1+k_2}(1-e^{-\frac{k_1+k_2}{b}t})$$

$$\Rightarrow F_{AT}(t) = \frac{F_{CE}k_1}{k_1+k_2}(1-e^{-\frac{k_1+k_2}{b}t}) \hspace{2cm} \text{(Eqn. 4.22)}$$

Equation (4.22) takes the form of a step response of a first order linear system where the time constant is $b/(k_1+k_2)$ and the gain of the system is $k_1/(k_1+k_2)$.
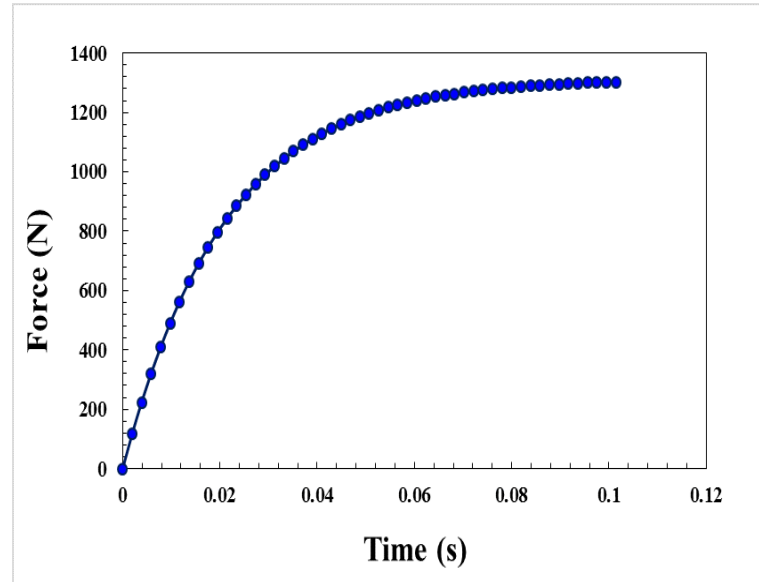
Figure 4.11. Representation of the calculated force/tension over time that builds up when using the modified Hill-type muscle model.

Nominal random values were used in Matlab 2016a to create a plot for Equation (4.22) shown in Figure 4.11. It resembles the build-up of tension measured in the isometric experiment of a tetanic stimulation of a muscle (Figure 4.12) in Freivalds [45]. Note that the force/tension (F_{CE}) of the contractile element when the muscle is activated, is affected by the combination of the parallel and series elastic elements that reduce its value. If the values of k_1 and k_2 are relatively equal, the force reduces to almost 50%. However, the values are not that close in the actual muscle, so the reduction is relatively small.

Considering an isotonic contraction, tension develops to a maximum value and then remains constant while the muscle changes its length. There are two types of isotonic contractions. A concentric contraction is where the muscle shortens when its tension is greater than the force opposing it and an eccentric contraction, where the muscle elongates and lengthens when the force is greater than the muscle tension [44, 119, 120]. In the muscle-tendon complex studied, during isotonic contractions, the force exerted on the tendon is assumed to be constant.

During isotonic contraction, the contractile element shortens, stretching the series elastic element before it develops tension so, for this case, its force F_{CE} is considered to be constant. For a purely passive movement F_{CE} is zero, hence the first term of Equation (4.15) can be excluded yielding:

$$X_1(s) = -\frac{k_1 + k_2 + bs}{k_1(k_2 + bs)} F_{AT}(s).$$ (Eqn. 4.23)

Using a unit step input to describe the muscle-tendon tension, Equation (4.23) transforms to:

$$X_1(s) = -\frac{k_1 + k_2 + bs}{k_1(k_2 + bs)} \frac{1}{s}.$$ (Eqn. 4.24)

Rearranging Equation (4.24):

$$X_1(s) = -\frac{\frac{k_1+k_2}{b}+s}{k_1(\frac{k_2}{b}+s)}\frac{1}{s} \Rightarrow X_1(s) = -\frac{1}{k_1}(\frac{\frac{k_1+k_2}{b}+s}{(\frac{k_2}{b}+s)}\frac{1}{s}).$$ (Eqn. 4.25)

A partial fraction expansion of (4.25) gives:

$$\frac{\frac{k_1+k_2}{b}+s}{\frac{k_2}{b}+s}\frac{1}{s} = \frac{A}{s}+\frac{B}{\frac{k_2}{b}+s} \Rightarrow \frac{k_1+k_2}{b}+s = \frac{As(\frac{k_2}{b}+s)}{s}+\frac{Bs(\frac{k_2}{b}+s)}{\frac{k_2}{b}+s}$$

$$\Rightarrow \frac{k_1+k_2}{b}+s = A(\frac{k_2}{b}+s)+Bs = A\frac{k_2}{b}+As+Bs \Rightarrow \frac{k_1+k_2}{b}+s = A\frac{k_2}{b}+(A+B)s.$$ (Eqn. 4.26)

Comparing the coefficients of *s* in Equation (4.26):

$$A+B=1 \Rightarrow B=1-A.$$ (Eqn. 4.27)

Comparing the constant terms in Equation (4.26) gives:

$$A\frac{k_2}{b}=\frac{k_1+k_2}{b} \Rightarrow A=\frac{k_1+k_2}{b}\frac{b}{k_2} \Rightarrow A=\frac{k_1+k_2}{k_2} \Rightarrow B=\frac{k_2}{k_2}-\frac{k_1+k_2}{k_2} \Rightarrow B=-\frac{k_1}{k_2}.$$ (Eqn. 4.28)

Substituting the coefficients of *A* and *B* into Equation (4.25) and taking the inverse Laplace transforms yields:

$$x_1(t) = -\frac{1}{k_1}L^{-1}\{\frac{\frac{k_1+k_2}{b}+s}{(\frac{k_2}{b}+s)}\frac{1}{s}\} \Rightarrow x_1(t) = -\frac{1}{k_1}[L^{-1}\{\frac{\frac{k_1+k_2}{k_2}}{s}\}+L^{-1}\{\frac{-\frac{k_1}{k_2}}{\frac{k_2}{b}+s}\}]$$

$$\Rightarrow x_1(t) = -\frac{1}{k_1}(\frac{k_1+k_2}{k_2}-\frac{k_1}{k_2}e^{-\frac{k_2}{b}t}) \Rightarrow x_1(t) = -\frac{k_1+k_2}{k_1k_2}+\frac{e^{-\frac{k_2}{b}t}}{k_2}$$ (Eqn. 4.29)

Nominal values were used in Matlab 2016a to simulate Equation (4.29) as shown in Figure 4.12. In this scenario a unit step input of force is applied and the contractile element stretches the series elastic element before it develops tension of its own. The damping element does not react initially. Nevertheless, the series elastic spring stretches and a step jump of movement is observed where the displacement of the muscle-tendon complex does not start from zero. Subsequently, the muscle continues to load and the damping element begins to yield until the two elastic springs balance out the CE force and the movement stabilises. The plot in Figure 4.12 resembles the figure of the measured creep (the change in the displacement over time) in the isotonic experiment of the upper limb model (Figure 4.15) in Freivalds [45].
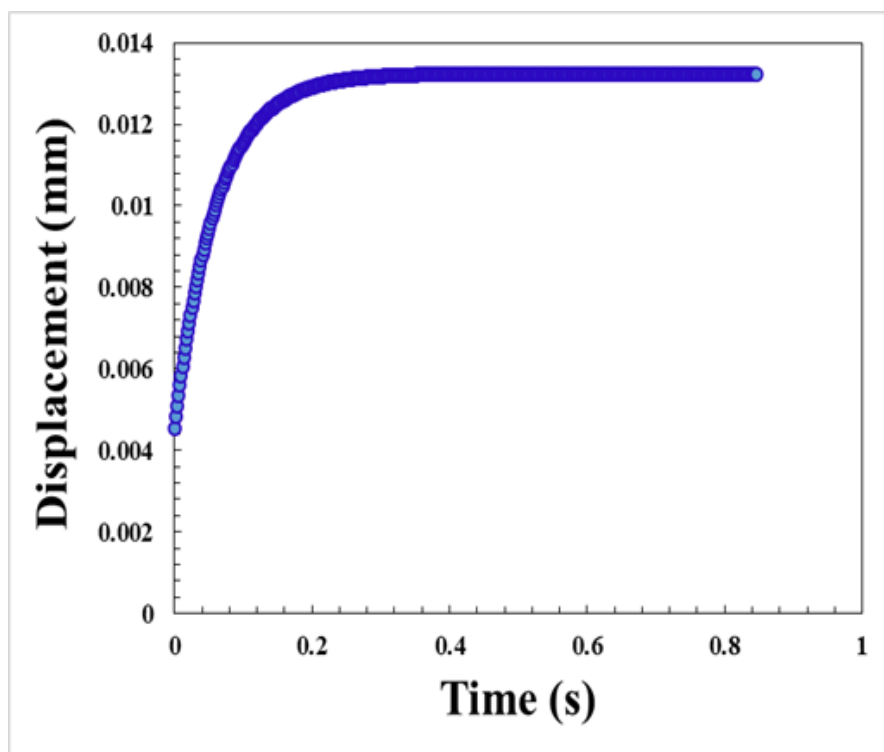
Figure 4.12. Calculated displacement of Hill-type muscle model versus time.

4.3 Summary of the chapter

In this chapter, the derivation of the system equations has been described. The full set of the model equations is given by Equations (4.1)-(4.3) and (4.4)-(4.6) with coupling of (4.10)-(4.11). Using kinetic and kinematic Gait Laboratory data and the method described in Section 4.1, Equations (4.1)-(4.3) for the static trials and Equations (4.4)-(4.6) for the dynamic trials, i.e. dorsiflexion and plantar flexion, are solved numerically and yield the Achilles tendon force F_{AT} that is then substituted into the muscle-tendon model, described in Section 4.2.2, in order to estimate the parameters of the model. Parameter estimation was performed in the time domain and is described in Section 5.3.1. In order to validate the model qualitatively Laplace transforms of the model equations were used as described above. Further details on this analysis are given in Chapter 5.

Chapter 5. Model Validation and Simulation

In Chapter 4, a model of the Achilles tendon-gastrocnemius muscle was developed. Model parameters must be anatomically meaningful. They can be obtained from direct measurements resulting from experiments, calculations based upon collected data or a method called parameter estimation where all parameter values must be unique. Generally, when biomechanical models of a muscle-tendon complex are created, not all the model parameters can be directly measured in vivo. Thus, parameter estimation techniques are required.

In this chapter, the experimental methodology to support the modelling of the Achilles tendon is described. The participants that took place in the experiments are introduced. Experimental analysis of the data obtained from the experiments is presented. A mathematical technique called structural identifiability analysis is defined in order to assure that the parameter values in the muscle-tendon model can be uniquely determined from measured data, assuming perfect noise-free data is available. Ultrasound images of the volunteers, direct measurements and additional mathematical calculations were used to parameterise the model. Comparisons between the measured movements obtained from the Gait Laboratory and Ultrasound sessions and the simulated movements of the muscle-tendon model are given. Ground reaction forces, forces on specific joints and moments and angles for the ankle that were obtained from the Vicon Nexus system are analysed. Model validation was performed from the experimental data captured for each volunteer and from reconstruction of the movements of specific trajectories of the joints, muscles and tendons involved in those movements. This was done in order to investigate if the methods described in this study can give parameter values obtained from in vivo experiments that in turn can help in the development of models that can predict specific movements.

5.1 Experimental design to support the modelling of the Achilles tendon

5.1.1 Participants

Five healthy volunteers from the University of Warwick took part in the experiments, after giving written informed consent. Two were male and three female, between the ages of 25 to 35 years, with body mass 79±10kg and body height 1.70±0.10m. None of them had experienced any Achilles tendon injuries or ruptures in the past or had any Achilles tendon pathologies. There were no other requirements of the participants apart from their ability to walk around a room for up to 10 minutes unaided. As mentioned in Section 3.2, ethical approval complying with the research code of practice of the University of Warwick had been granted for all the Gait Laboratory sessions and Ultrasound sessions at UHCW by the University's Biomedical and Scientific Research Ethics Committee (BSREC full approval *Simulation of the Achilles tendon* REGO-2013-548AM01) (Appendix A).

5.1.2 Ultrasonography

In this study ultrasound scans were provided by the University Hospitals of Coventry and Warwickshire (UHCW) in order to measure the changes in length of the Achilles tendon in dorsiflexion and plantar flexion of the foot segment so as to design and validate the gastrocnemius muscle-Achilles tendon complex [32, 106]. Ultrasound sessions were performed at the UHCW with five volunteers from the University of Warwick. A sonographer scanned the Achilles tendons on both feet of the volunteers. The model used was a Logiq 9 ultrasound scanner (GE Medical Systems, Slough, UK) employing 12/9 MHz linear transducer (GE LOGIQ E9). A lubricating gel was placed onto the skin of the volunteers by the sonographer. A small handheld device called a transducer was placed onto the skin, and moved over the Achilles tendon. The lubricating gel allowed the transducer to move smoothly and ensured that there was continuous contact between the sensor and the skin. The transducer was connected to

a computer and a monitor. Pulses of ultrasound were sent from a probe in the transducer, through the skin and into the body. They then bounced back from the structures of the body and were displayed as an image on the monitor. The transducer was held in a longitudinal orientation. Thus, the images of the volunteer's Achilles tendon anatomy appeared in the sagittal plane.

Figure 5.1. Example of a patient lying on a medical bed in the prone position during an ultrasound session. Image taken from [121].

The volunteers were asked to lie still on a medical bed in the prone position and their feet rested freely beyond the end of the bed. This position is named as neutral or resting position. The sonographer scanned the volunteers in that position to measure the natural resting length, also named as anatomical length, of the Achilles tendon. An example of a patient lying still on a bed in the prone position is given in Figure 5.1. However, this figure does not illustrate any of the actual volunteers that participated in the ultrasound sessions, it is just given as an example. Then the volunteers were asked to dorsiflex and plantar flex their feet to the maximum of their abilities in order to acquire the elongation and shortening of the Achilles tendon respectively. First, dorsiflexion was studied. The volunteers were still lying on the medical bed in the prone position and were asked to dorsiflex their feet to the maximum of their abilities,

starting from the resting position but without lifting their feet or placing the ankles at 90 degrees. The total length of the Achilles tendon was scanned by the sonographer and the elongation of the Achilles tendon of each foot was measured. Then, plantar flexion was studied. Again, the volunteers were lying on the medical bed in the prone position and were asked to plantar flex their feet to the maximum of their abilities, starting from the resting position but without lifting their feet or placing the ankles at 90 degrees. The total length of the Achilles tendon was scanned by the sonographer and the shortening of the Achilles tendon of each foot was measured. The natural resting lengths and the total lengths of the Achilles tendons scanned during the ultrasound sessions are presented in Table 5.1 bellow.

Table 5.1. Natural resting length and total lengths of the Achilles tendons of five volunteers measured during Ultrasound sessions

Subject	Length of the Achilles tendon Right foot			Length of the Achilles tendon Left foot		
	Natural resting length (mm)	Total length Dorsiflexion (mm)	Total length Plantar flexion (mm)	Natural resting length (mm)	Total length Dorsiflexion (mm)	Total length Plantar flexion (mm)
Subject 1	171.7	198.1	158.2	174.9	189.2	134.2
Subject 2	154.3	160.2	144.7	150.2	165.0	135.0
Subject 3	169.0	181.2	116.4	170.0	180.7	115.1
Subject 4	151.8	174.9	142.5	144.1	154.1	135.6
Subject 5	170.9	205.2	143.5	167.6	182.0	132.9

Ultrasonography is a very safe procedure since it does not use a high magnetic field to produce an image, it is cost effective and can also evaluate a tendon in longitudinal as well as transverse projections, in both static and dynamic views. All images obtained from UHCW and used for this study comply with NHS ethics approval for the collection and use of such images. An example of the images taken is presented below (Figures 5.2, 5.3 and 5.4).

Figure 5.2. Ultrasound of the Achilles tendon in the neutral position. Its origin is at the gastrocnemius muscle at the level of the lower margins of the heads of the calf muscle which is indicated by the yellow cross to the left of the figure. Its insertion point is the middle part of the back of the heel which is indicated by the yellow cross with the yellow '1' to the right of the figure.

118

Figure 5.3. Ultrasound of the Achilles tendon while the volunteer is dorsiflexing the foot. Its origin is at the gastrocnemius muscle at the level of the lower margins of the heads of the calf muscle which is indicated by the yellow cross to the left of the figure. Its insertion point is the middle part of the back of the heel which is indicated by the yellow cross with the yellow '1' to the right of the figure.

Figure 5.4. Ultrasound of the Achilles tendon while the volunteer is plantar flexing the foot. Its origin is at the gastrocnemius muscle at the level of the lower margins of the heads of the calf muscle which is indicated by the yellow cross to the left of the figure. Its insertion point is the middle part of the back of the heel which is indicated by the yellow cross with the yellow '1' to the right of the figure.

5.1.3 Experimental methodology and analysis

In this section a description of the methodology used to obtain the results of this study is given. In order to acquire measurements for the parameters describing our muscle-tendon model described in Section 4.2.2 and to validate our results, plantar flexion, dorsiflexion and human gait were studied. Gait analysis is considered very reliable since it uses computers and videography to capture, observe and interpret the different kinds of movements [36, 39]. Vicon's three-dimensional (3D) biomechanical motion capture system was used to determine kinetics and kinematics of the foot in order to solve Equations (4.1)-(4.6) for the Achilles tendon force.

Commencing with the lengths presented in Table 4.1 in Section 4.2, they were determined by palpation and surface measurement of the legs of the volunteers before placement of the markers during the Gait Laboratory sessions. They were then compared with the lengths calculated from the coordinates of the markers placed on the feet of the volunteers and especially at the origins of the Achilles tendon and the gastrocnemius muscle (Vicon Nexus analysis [122]). All lengths were measured in mm, while the volunteers were standing still in an upright position so that the orientation of each segment was exactly the same as the representation of the coordinate system, i.e. the normalised directions of the three axes in global space with reference to the force plate [65]. The angles shown in Figure 4.6 were measured with a goniometer. A description of how the measurements were performed has been given in Section 3.1.2.

As mentioned in Section 4.2.3, F_{AT} is calculated from experimental data and is substituted into the muscle-tendon model. For the static trial Equations (4.1)-(4.3), and for the dynamic trial Equations (4.4)-(4.6), F_{1x} and F_{1y} compute the ground reaction force, F_{2x} and F_{2y} represent the force on the ankle joint, a_x and a_y give the acceleration of the foot segment and M_{ankle} gives

the moment at the ankle joint. The Vicon Nexus system gives directly the net force and the net moment of force at the ankle joint. The methodology explained in Section 4.1 was applied in order to calculate the forces and the moments in Equations (4.1)-(4.6) and to determine the Achilles tendon force. In order to validate the values of the ground reaction forces, Tekscan plantar pressure insole sensors were used. The volunteers were asked to perform the same dorsiflexion, plantar flexion and walking trials while being markered up according to the Achilles tendon Plug-in Gait model and while wearing specific shoes with the insoles provided by the Gait Laboratory. The F-scan software calculates and displays Force versus time graphs among other outputs. The data for the ground reaction forces from the F-scan software were compared to the data from the Vicon Nexus system. The values of the forces over time were found to differ only at the first or second decimal place with a percentage between 3% to 5%. Thus, there was good agreement between the two measuring devices.

All distances d_{1x}, d_{1y}, d_{2x}, d_{2y}, d_{ATx}, and d_{ATy} that are explained in Tables 4.2 and 4.3 were calculated from the coordinates of the markers placed on the feet of the volunteer provided by the Vicon Nexus system. As mentioned in Section 4.2.1 $m_a g$ and $d_{m_a g}$ are calculated from Winter's Table 4.1 [1]. This table provides the segment mass as a fraction of the body mass and the centres of mass as fractions of the lengths of the segments and can be seen in Figure 5.5 below. The angles in the triangle HTA and that of the Achilles tendon seen in Figures 4.7, 4.8 and 4.9 in Section 4.2.1 are estimated from the coordinates of the markers placed on the ankle joint, the heel, the toe and the Achilles tendon during the experiments conducted in the University of Warwick Gait Laboratory. They were also measured with a goniometer during the experiments in order to cross check the values.

TABLE 4.1 Anthropometric Data

Segment	Definition	Segment Weight/Total Body Weight	Center of Mass/ Segment Length		Radius of Gyration/ Segment Length			Density
			Proximal	Distal	C of G	Proximal	Distal	
Hand	Wrist axis/knuckle II middle finger	0.006 M	0.506	0.494 P	0.297	0.587	0.577 M	1.16
Forearm	Elbow axis/ulnar styloid	0.016 M	0.430	0.570 P	0.303	0.526	0.647 M	1.13
Upper arm	Glenohumeral axis/elbow axis	0.028 M	0.436	0.564 P	0.322	0.542	0.645 M	1.07
Forearm and hand	Elbow axis/ulnar styloid	0.022 M	0.682	0.318 P	0.468	0.827	0.565 P	1.14
Total arm	Glenohumeral joint/ulnar styloid	0.050 M	0.530	0.470 P	0.368	0.645	0.596 P	1.11
Foot	Lateral malleolus/head metatarsal II	0.0145 M	0.50	0.50 P	0.475	0.690	0.690 P	1.10
Leg	Femoral condyles/medial malleolus	0.0465 M	0.433	0.567 P	0.302	0.528	0.643 M	1.09
Thigh	Greater trochanter/femoral condyles	0.100 M	0.433	0.567 P	0.323	0.540	0.653 M	1.05
Foot and leg	Femoral condyles/medial malleolus	0.061 M	0.606	0.394 P	0.416	0.735	0.572 P	1.09
Total leg	Greater trochanter/medial malleolus	0.161 M	0.447	0.553 P	0.326	0.560	0.650 P	1.06
Head and neck	C7–T1 and 1st rib/ear canal	0.081 M	1.000	— PC	0.495	0.116	— PC	1.11
Shoulder mass	Sternoclavicular joint/glenohumeral axis	—	0.712	0.288	—	—	—	1.04
Thorax	C7–T1/T12–L1 and diaphragm*	0.216 PC	0.82	0.18	—	—	—	0.92
Abdomen	T12–L1/L4–L5*	0.139 LC	0.44	0.56	—	—	—	—
Pelvis	L4–L5/greater trochanter*	0.142 LC	0.105	0.895	—	—	—	—
Thorax and abdomen	C7–T1/L4–L5*	0.355 LC	0.63	0.37	—	—	—	—
Abdomen and pelvis	T12–L1/greater trochanter*	0.281 PC	0.27	0.73	—	—	—	1.01
Trunk	Greater trochanter/glenohumeral joint*	0.497 M	0.50	0.50	—	—	—	1.03
Trunk head neck	Greater trochanter/glenohumeral joint*	0.578 MC	0.66	0.34 P	0.503	0.830	0.607 M	—
Head, arms, and trunk (HAT)	Greater trochanter/glenohumeral joint*	0.678 MC	0.626	0.374 PC	0.496	0.798	0.621 PC	—
HAT	Greater trochanter/mid rib	0.678	1.142	—	0.903	1.456	—	—

*NOTE: These segments are presented relative to the length between the greater trochanter and the glenohumeral joint.
Source Codes: M, Dempster via Miller and Nelson; *Biomechanics of Sport*, Lea and Febiger, Philadelphia, 1973. P, Dempster via Plagenhoef; *Patterns of Human Motion*, Prentice-Hall, Inc. Englewood Cliffs, NJ, 1971. L, Dempster via Plagenhoef from living subjects; *Patterns of Human Motion*, Prentice-Hall, Inc., Englewood Cliffs, NJ, 1971. C, Calculated.

Figure 5.5. Table 4.1 with anthropometric data taken from Winter [1].

Then the Achilles tendon force was substituted into the muscle-tendon model, described in Section 4.2.2, in order to estimate the parameters b, k_1, and k_2 of the model and to solve Equations (4.10) and (4.11). Displacements x_1 and x_2 (in mm) were calculated from the displacements measured from Gait Laboratory experiments. In more detail, l_{GM}, l_{GM0}, l_{AT} and l_{AT0} (in mm) were found from the displacements captured in the experiments and computed from $l_{GM}=l_{GM0}+x_2$ and $l_{AT}=l_{AT0}+x_1-x_2$. The volunteers that participated in the Gait Laboratory sessions, the same as those that participated in the ultrasound sessions, were asked to stand still on a force plate, to dorsiflex and plantar flex their feet which means to flex and extend their feet at the ankle respectively. For the Gait Laboratory experiments, the origin and insertion of the gastrocnemius muscle and the Achilles tendon were determined by palpation of the legs of the

122

volunteers before marker placement commenced. The natural resting length and the maximum lengths after elongation and shortening of the tendon obtained from the Gait Laboratory experiments of dorsiflexion and plantar flexion respectively. Those were the ones used to solve Equations (4.10) and (4.11) since they are captured in the time domain. The natural resting length of the Achilles tendon l_{AT0} as well as the change in its length during plantar flexion and dorsiflexion were also measured directly from the ultrasound images as seen in Table 5.1. However, those represent only the maximum values of the movements and are not captured over time. A comparison of the lengths obtained from the ultrasounds and those from the Gait Laboratory experiments is given in Section 5.1.3.1.

The natural resting length of the gastrocnemius muscle l_{G0} was determined by surface measurement and palpation of the legs of the subjects before placement of the markers. These lengths were then compared with those calculated from the coordinates of the markers placed at the origins of the Achilles tendon and the gastrocnemius muscle respectively (Vicon Nexus analysis). All lengths were measured in mm with measuring tape before the marker placement and compared with the calculated ones from the system after the marker placement. Since the gastrocnemius muscle is a curved surface, measuring its length with a measuring tape gives just an approximation that can be checked through ultrasound tests. The lengths of the gastrocnemius muscle for the muscle-tendon model in Section 4.2.2 were calculated using the experimental data measured along with data in Table 4.3 from Winter [1]. This table gives the mass, fibre length, physiologic cross-sectional area and pennation angle of some muscles of the human body including the gastrocnemius.

5.1.3.1 Comparison of Achilles tendon lengths obtained from Ultrasound and Gait Laboratory sessions

As mentioned in Section 5.1.2, the natural resting length and total lengths of the Achilles tendons of five volunteers were measured during Ultrasound sessions. Before the static and dynamic experiments commenced, each volunteer was markered and was asked to lie down on a medical bed similar to the one from the UHCW. Then the volunteer was asked to lie still for a few seconds in order to capture the natural resting length of the Achilles tendon and the gastrocnemius muscle. After that the volunteer was asked to perform the same, as humanly possible, dorsiflexion and plantar flexion movements as the ones performed at the UHCW (see Section 5.1.2). The changes in length were also captured and reconstructed via the Vicon Nexus system. The values are represented in Table 5.2. This was done in order to see the difference between the actual length of the Achilles tendon and the one measured in the Gait Laboratory.

As expected differences in the measured values from the Ultrasound experiments and the Gait laboratory experiments were found. The mean difference between the natural resting length of the Achilles tendon was found to be 65.42 mm with a standard deviation of 17.51 mm for the right foot and a mean of 68.52 mm with a standard deviation of 19.11 mm for the left foot. The elongation of the Achilles tendon during dorsiflexion of the right foot displayed a mean difference of 60.62 mm with a standard deviation of 27.86 mm and a mean difference of 75.32 mm with a standard deviation of 20.03 mm for the left foot. The shortening of the Achilles tendon during plantar flexion of the right foot displayed a mean difference of 55.14 mm with a standard deviation of 17.32 mm and a mean difference of 66.29 mm with a standard deviation of 21.23 mm for the left foot. Even though differences in length from the Ultrasound and the Gait Laboratory data appear, the order of magnitude of the values of the lengths and that of the changes of length is the same in both sets of experiments. Consequently, the differences in

length and change of length that occurred are not worrying since palpation of the feet always introduces an error in calculations. Vicon Nexus also takes into consideration these errors of palpation [101].

Table 5.2. Natural resting length and maximum total lengths of the Achilles tendons of five volunteers measured during Vicon Nexus motion capture experiments

Subject	Averaged Length of the Achilles tendon Right foot			Averaged Length of the Achilles tendon Left foot		
	Natural resting length (mm)	Maximum length Dorsiflexion (mm)	Maximum length Plantar flexion (mm)	Natural resting length (mm)	Maximum length Dorsiflexion (mm)	Maximum length Plantar flexion (mm)
Subject 1	247.2	260.49	202.9	254.06	268	215.24
Subject 2	219.0	236.2	198.2	216.2	245.0	189.1
Subject 3	232.09	242.3	178.9	245.45	258.6	195.9
Subject 4	237.09	263.5	222.62	229.39	251.5	216.6
Subject 5	209.4	220.2	178.4	204.3	224.5	167.4

As mentioned in Section 2.1, the Achilles tendon consists of distinct fascicles arising from the gastrocnemius muscle and the soleus muscle. This may cause the development of non-uniform behaviour during functional tasks such as dorsiflexion, plantar flexion and walking. It has been observed that inter-fascicle sliding within the human Achilles tendon, creates non-uniform deformations [77]. J.R. Franz et al. [77] found that the deep Achilles tendon underwent significantly greater distal displacements when the ankle was dorsiflexed and consequently smaller peak elongation than the superficial Achilles tendon. More specifically they found that

the deep Achilles tendon underwent 16–29% smaller elongation than the superficial. This suggests that the fibres of the soleus muscle tend to lengthen more during stance than the fibres of the medial gastrocnemius muscle. This also represents a valid reason in the differences observed between the measured natural lengths and elongation of the Achilles tendon during the Ultrasound sessions compared to the lengths measured during the Gait Laboratory sessions.

Evidence for unique gastrocnemius and soleus muscle-tendon behaviour during movement has been illustrated by researchers. Ishikawa et al. [123] demonstrated that the fibres of the medial gastrocnemius muscle remain isometric or shorten during the late stance phase of walking while those of the soleus muscle lengthen. These differences in the length of a muscle-tendon complex affect the way that muscles operate when producing forces and generating powers [77, 123]. Biomechanically, non-uniform displacements of the Achilles tendon may be generated from different loading of the triceps surae muscles. Even though a tendon has the same elastic modulus, its absolute stiffness may vary considerably between bundles due to the relatively longer and smaller cross-section of tendon fascicles arising from the gastrocnemius and soleus muscles [11]. Also, differences in the elongation of tendon fascicles arising from each muscle of the triceps surae may occur at different ankle angles. Finally, differences in muscle-tendon loading for a given external load can produce depth differences between the superficial and deep regions of the Achilles tendon [77].

5.1.3.2 Muscle Activation Analysis

Surface EMG data for the gastrocnemius lateralis, gastrocnemius medialis, soleus and tibialis anterior were collected for all five volunteers while they were dorsiflexing and plantar flexing their feet and while walking. The muscles were identified by palpation of the feet of the volunteers. In order to correctly identify the muscles studied, tutorials and online videos demonstrating physiotherapists and orthopaedics palpating and locating the gastrocnemius

lateralis, gastrocnemius medialis, soleus and tibialis anterior muscles on patients were used. The electrodes of the EMGs were applied to the muscle belly of each muscle where the electrode separation distance was approximately 10 mm as stated in literature. Prior to any electrode attachment, 'Nuprep skin prep gel' was applied to the skin of the volunteers in order to remove any dead cells from the surface of the lower limbs of the volunteers that could affect the electrode-skin interface impedance [1]. An example of the electrode placement is shown in Figure 5.6. The application of the electrodes was verified by having the volunteers perform a series of tests that would activate each muscle group and by simultaneously observing the EMG signal on the Vicon Nexus monitor. The EMGs of these specific muscles were recorded as an objective measure of muscle activation for the movements studied.

Figure 5.6. Side view of surface EMG electrode application on the gastrocnemius lateralis, gastrocnemius medialis, soleus and tibialis anterior muscles of a volunteer during Gait Laboratory experiments.

As mentioned in the literature, the spectrum of the EMG has been reported with a range from 5 Hz at the low end to 2000 Hz at the upper end. For surface electrodes, the motor unit action potentials (m.u.a.p.) have negligible power beyond 1000 Hz since they are longer in duration

[1]. The upper cutoff frequencies are usually 5Hz for surface EMGs when computer pattern recognition of individual m.u.a.p.'s is being done.

The EMG data were processed in Matlab 2016a. Initially the raw signal was plotted for all muscles studied. Then, an analog filtering was applied to the raw signal before it was digitised in order to remove any DC offset. The DC offset is an offsetting of a signal from zero, a baseline drift of the signal that could be associated with movement of skin, perspiration, etc. These filters abstract low frequency components of a signal and force the mean value to be zero or nearly zero [124]. A rectification of the EMG signal followed. The full-wave rectifier gives the absolute value of the EMG, typically with a positive polarity. The original raw EMG signal has a mean value of zero as mentioned above. Yet, the full-wave rectified signal does not cross through zero and has an average or bias level that oscillates with the strength of the muscle contraction. When examining the amplitude changes of the full-wave rectified signal visually, a good indication of the changing contraction level of the muscle is observed. Lastly, a linear envelope of the EMG signal was created. Once the full-wave rectified signal is filtered with a low-pass filter, a linear envelope is generated. This envelope resembles a moving average since it follows the trend of the EMG and looks like the shape of the tension curve. In this study, the EMG signals were low pass filtered at 5Hz using a zero-phase, fifth order Butterworth filter [1, 79, 124]. As mentioned in Section 3.4 each EMG channel used in the experiments samples at 1000 Hz which is the accepted value in literature.

As mentioned in the literature, EMGs can be used to determine the extent of a force produced by a muscle based on the amplitude of the EMG signal. It is believed that generally the EMG-muscular force relationship is linear, especially under isometric contractions [1, 41]. Small incremental changes in the force produced by a muscle, cause linearly related incremental changes in the EMG amplitude [41]. As seen in Figures 5.7, 5.8 and 5.9 the muscle that is mostly activated during dorsiflexion is tibialis anterior and the muscle that is mostly activated

in plantar flexion is gastrocnemius. Tibialis anterior is illustrated by a blue line, soleus by a red line, gastrocnemius medialis by a purple line and gastrocnemius lateralis by a green line. The zero values that appear in the graphs represent the time periods when the volunteer was in a static position, not moving their foot. This occurred just before lifting their foot for dorsiflexion (0-1 s) and for plantar flexion (0-1 s) and when putting their foot down on the ground, (5-6 s) for dorsiflexion and (6-8 s) for plantar flexion. In Figure 5.9, a clearer view of the plantar flexion of the right foot of a volunteer is represented. The values of the tibialis anterior are very close to zero. That is why the blue line looks like a straight line over the x axis.
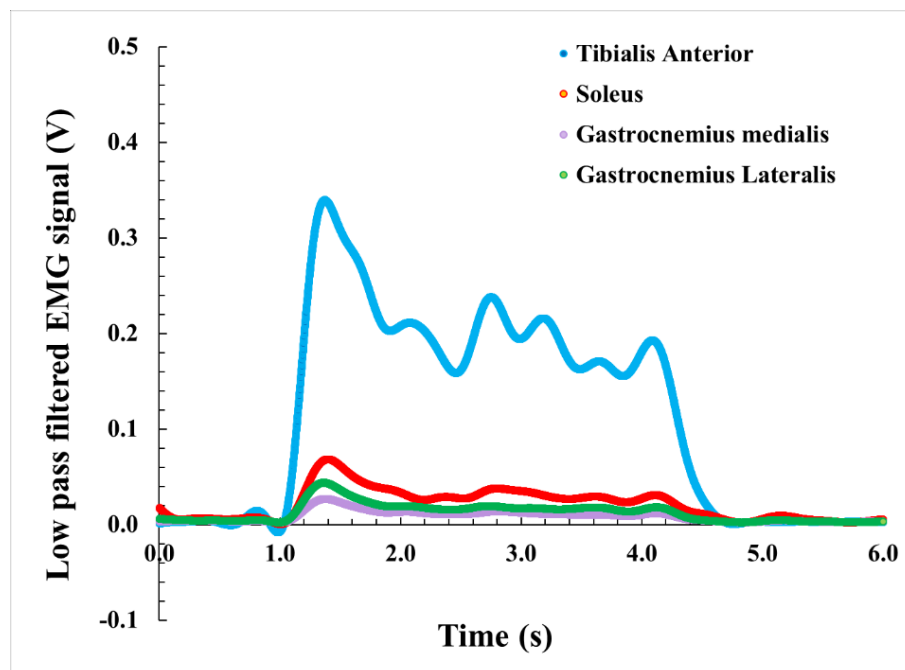
Figure 5.7. Low pass filtered EMG signals of the Tibialis Anterior (blue line), Soleus (red line), Gastrocnemius medialis (purple line) and Gastrocnemius lateralis (green line) while the volunteer dorsiflexes the foot.
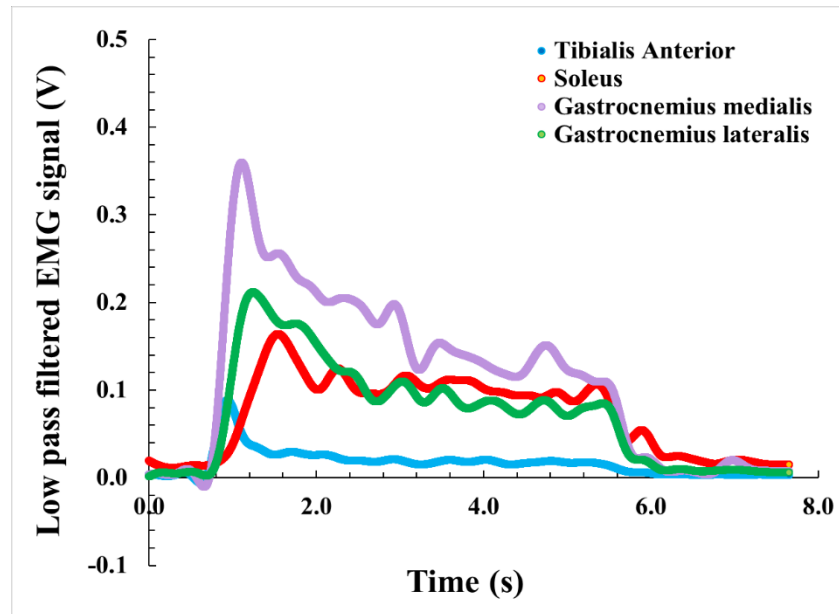
Figure 5.8. Low pass filtered EMG signals of the Tibialis Anterior (blue line), Soleus (red line), Gastrocnemius medialis (purple line) and Gastrocnemius lateralis (green line) while the volunteer plantar flexes the foot.
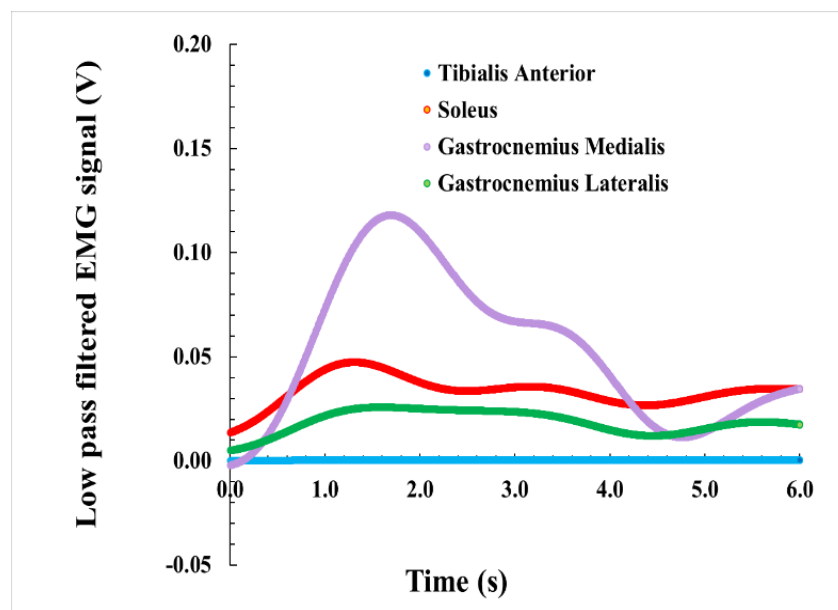
Figure 5.9. Low pass filtered EMG signals of the Tibialis Anterior (blue line), Soleus (red line), Gastrocnemius medialis (purple line) and Gastrocnemius lateralis (green line) while the volunteer plantar flexes the foot.

130

5.1.3.3 Repeatability and reproducibility analysis

Repeatability and reproducibility are ways of measuring precision in the field of biomedical engineering. The variation between measurements that are repeated for the same subject under identical conditions is cited as the repeatability of measurements [125]. This means that the same observer performs the experiments or the measurements, the same instrument or method is used to capture the measurements and the measurements are made over a short period of time, over which the underlying value can be considered to be constant. A variability in measurements for the same subject in a repeatability study can appear due to errors made from measurement process itself [125].

Reproducibility has to do with the variation in measurements of a subject observed when the conditions governing the experiments change[125]. Thus, reproducibility assesses whether a whole study or experiment can be reproduced entirely. The changing conditions may be because of different measurement methods or instruments being used, measurements being taken by different individuals, at different locations, or measurements being made over a long period of time, within which the 'error free' level of the variable could undergo non-negligible change. Reproducibility, if put simply determines whether the findings of an experiment can be replicated [125].
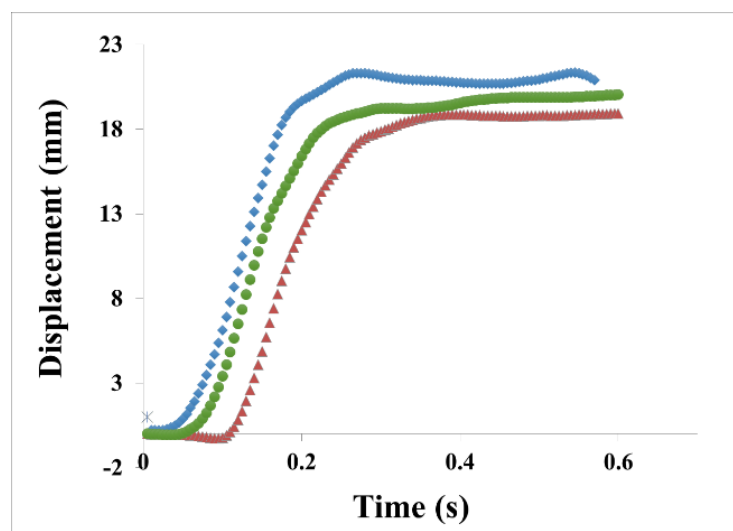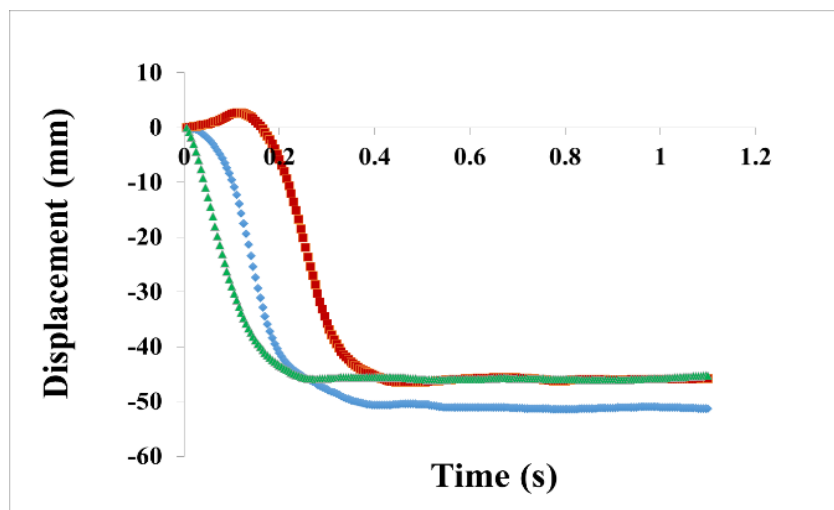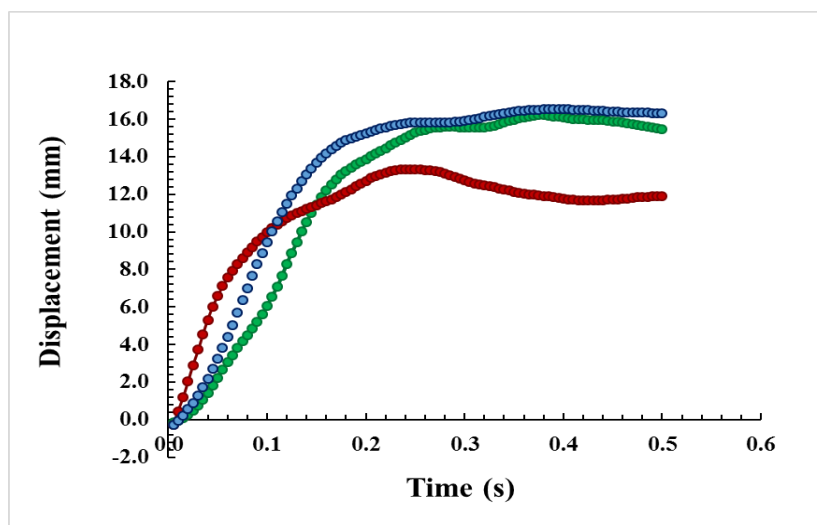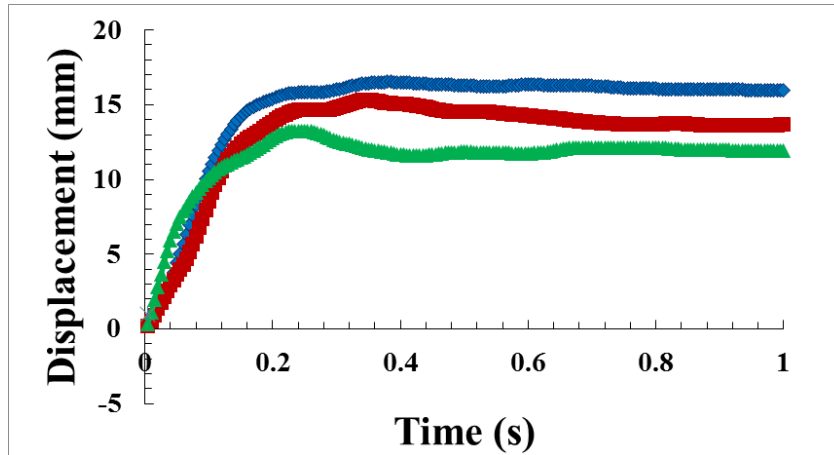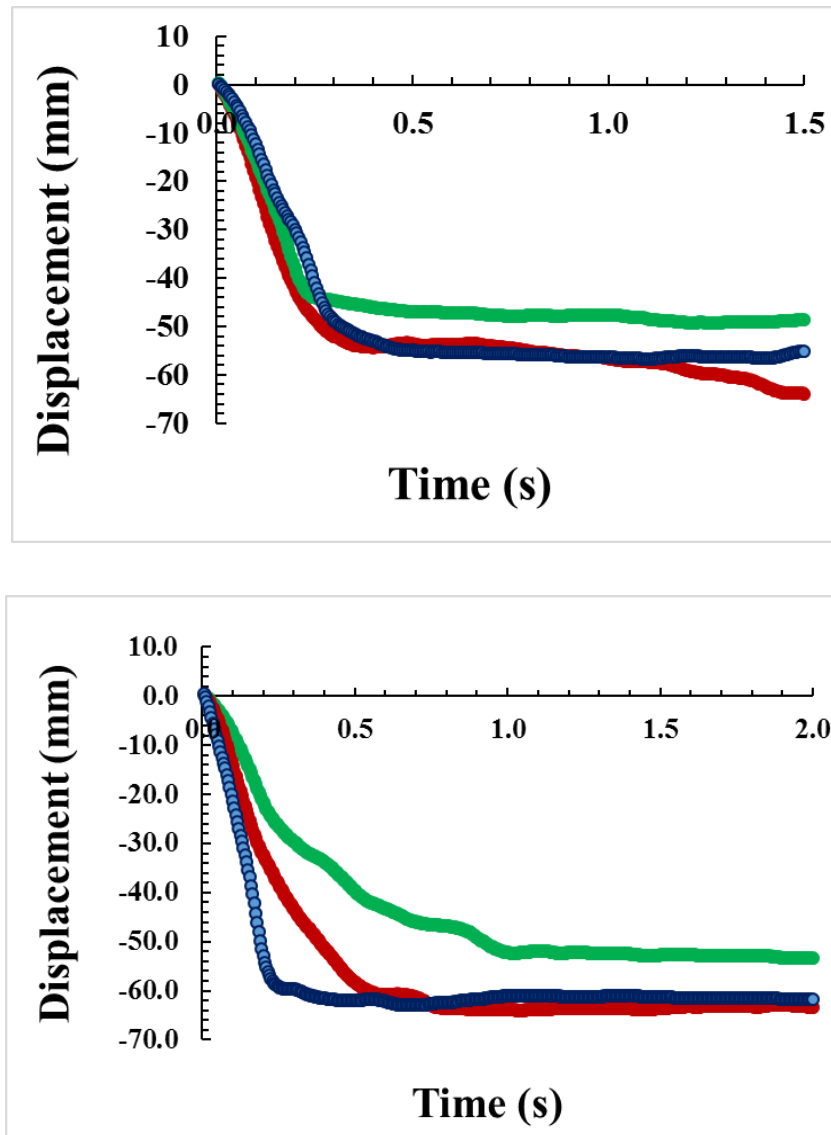
Figure 5.10. Displacement of the Achilles tendon vs time while two volunteers dorsiflex their foot (top three figures). Displacement of the Achilles tendon vs time while three volunteers plantar flex their foot (bottom three figures).

A repeatability and reproducibility analysis was performed throughout the experiments in order to confirm the findings of this thesis. Regarding the repeatability analysis, all of the subjects performed in one day three consecutive trials of dorsiflexing the right foot, three trials of plantar flexing the right foot, three trials of dorsiflexing the left foot, three trials of plantar flexing the left foot, three walking trials while stepping on the force plate with the right foot and three trials while stepping on the force plate with the left foot. All results showed good

133

repeatability. Figure 5.10 demonstrates the displacement of the Achilles tendon over time of three volunteers for the three repeated trials while they were dorsiflexing their foot (first three figures) and the displacement of the Achilles tendon over time of three volunteers for the three repeated trials while they were plantar flexing their foot (next three figures). Regarding the reproducibility analysis, one subject performed the same trials over two consecutive days. The markers were removed and reapplied at the same positions as the previous day. The error of the measured marker trajectory data for the two days lies between the range of 3-7% which is considered an acceptable error [125].

5.2 Identifiability analysis

Structural identifiability analysis should be performed when developing mathematical models, since it assists in determining whether parameters in a mathematical model can be uniquely identified or otherwise from the available observations. Parameters can be either globally identifiable, locally identifiable, or unidentifiable. Globally identifiable parameters are those that can be uniquely identified, locally identifiable are those that have a finite number of solutions and unidentifiable are those that have an infinite number of solutions.

Structural identifiability is defined as follows. Let the generic parameter vector p belong to a feasible parameter space P such that $p \in P$. Let $y(t, p)$ be the output function from the state-space model. Further, consider a parameter vector $\overline{p}$ where $y(t, p) = y(t, \overline{p})$ for all t. If this equality, in a neighbourhood $N \subset P$ of p, implies that $p = \overline{p}$ then the model is structurally locally identifiable. If $N = P$ then the model is globally structurally identifiable. For a structurally unidentifiable parameter, p_i in p, every neighbourhood N around P has a parameter vector $\overline{p}$ where $p_i \neq \overline{p}_i$ that gives rise to identical input-output relations [126, 127].

Before commencing the parameter estimation, structural identifiability analysis of the model should be taken into account as part of the experimental design process. The gastrocnemius

muscle model and its respective model equations have been derived from the mechanical properties of the muscle and its anatomical structure, so it is important to determine if unique values of the model parameters can be obtained. Parameters such as body weight, body segment weight, tendon length, muscle length and leg length can be directly measured or calculated from the experiments. However, other parameters such as the damping constants of the muscle and the spring constants of the muscle and the tendon are embedded in the muscle-tendon complex and cannot be directly measured in vivo. Performing in vivo experiments and obtaining in vivo measurements is the most accurate procedure to parameterise the models for living subjects. Therefore, parameter values that cannot be directly measured must be obtained through model fitting and parameter estimation techniques. In order to obtain unique parameter estimates when real data are available from experiments, a globally or at least locally identifiable model has to be defined. If the model is proven to be unidentifiable, then re-parameterisation techniques can be used to possibly give a locally identifiable model [126, 127]. The data used in the analysis are assumed to be perfect, i.e. continuous and noise free.

Equations 4.11 and 4.12 were studied in order to determine the structural identifiability of the parameters of the muscle-tendon model. For observations of x_1, x_2 and F_{CE} and for the linear case where $a=1$, the model parameters b, k_1, and k_2 are clearly structurally identifiable by comparison of $y(t, \boldsymbol{p}) = y(t, \overline{\boldsymbol{p}})$.

5.3 Results

5.3.1 Parameter Estimation

Parameter estimation was performed in the time domain for each volunteer in order to acquire a set of fitted values for the parameters b, k_1, and k_2. Measured data of ankle and heel angle trajectories and Achilles tendon trajectories as well as gastrocnemius muscle trajectories were obtained from the experiments and were used to investigate the best fit for the parameters

of the model, while simulated data were obtained from inverse dynamics created from Equations (4.10)-(4.11) to determine model validation. As mentioned in Section 5.1.3 the values of x_2, (x_2-x_1) and dx_2/dt were calculated from the experimental data for each volunteer. The derivative term, dx_2/dt, was determined using the central difference formula:

$$\frac{dx_2(t_i)}{dt} = \frac{x_2(t_{i+1}) - x_2(t_{i-1})}{2\Delta t}$$
(Eqn. 5.1)

where t_i $(i=1,2,\ldots,N)$ are the sample times for a fixed time step $\Delta t = t_{i+1} - t_i$ [1].

The curve fitting toolbox in Matlab 2016a was used in order to fit our experimental and simulated data [128]. Equation (4.10) was used in order to find values for the parameters b and k_2 and Equation (4.11) (for $a=1$) was used in order to find values for the parameter k_1. Custom equations were created to see which was the best fit for the dorsiflexion and plantar flexion experiments. The parameters b, k_1, and k_2 were constrained to be positive numbers and their confidence intervals are represented by the numbers in brackets under their values in Tables 5.3, 5.4, 5.5 and 5.6. Tables 5.3 and 5.4 indicate the b, k_1, and k_2 parameter values for dorsiflexion of the right and left foot respectively, whereas Tables 5.5 and 5.6 indicate the b, k_1, and k_2 parameter values for plantar flexion of the right and left foot respectively. A step input was found to appropriately describe the form of the force of the contractile element when the volunteers were dorsiflexing their feet. The residuals appeared random with no apparent pattern and the Root Mean Square Error (RMSE) for the best fit for each volunteer is presented in both Tables 5.3 and 5.4. Plantar flexion was found to be better defined by an impulsive input. The residuals appeared random with no apparent pattern and the RMSE for the best fit for each volunteer is presented in Table 5.5 and 5.6. All parameter values have a 95% confidence bound.

Table 5.3. Values for the parameters b, k_1, and k_2 and their confidence intervals for each volunteer for dorsiflexion (Right foot)

Volunteer	b (Ns/mm)	k_2 (N/mm)	RMSE
1	11.3 (10.16, 12.41)	284 (267, 302)	0.127
2	2 (1.00, 3.00)	186 (168, 203)	0.477
3	2.2 (2.00, 4.00)	89.9 (62.3, 117.6)	0.231
4	1.1 (0.0, 2.3)	102.5 (95.7, 109.3)	0.087
5	16 (7.00, 24.6)	320.6 (313, 328)	0.725

Volunteer	k_1 (N/mm)	RMSE
1	51 (49.0, 52.0)	0.504
2	101.9 (101.3, 102.5)	0.536
3	38.4 (37.7, 39.1)	0.323
4	83 (79.0, 86.0)	0.902
5	100.7 (98.1, 103.3)	1.402

Table 5.4. Values for the parameters b, k_1, and k_2 and their confidence intervals for each volunteer for dorsiflexion (Left foot)

Volunteer	b (Ns/mm)	k_2 (N/mm)	RMSE
1	11.57 (10.15, 12.7)	139 (133- 147)	0.153
2	7.0 (6.0, 8.0)	63.37 (60.73, 66.01)	0.1458
3	7 (5.24, 8.9)	14.19 (13.25, 15.13)	0.125
4	6.58 (4.0, 9.1)	68.96 (49.06, 88.8)	0.142
5	13.23 (11.83, 14.64)	316.3 (241.2, 591.1)	0.523

Volunteer	k_1 (N/mm)	RMSE	
1	37.1 (35, 39.2)	0.748	
2	42.55 (41.73, 43.37)	0.279	
3	54.6 (53.7, 55.5)	0.466	
4	71 (67.9, 72.9)	0.745	
5	145.5 (133.6, 157.4)	0.23	

Table 5.5. Values for the parameters b, k_1, and k_2 and their confidence intervals for each volunteer for plantar flexion (Right foot)

Volunteer	b (Ns/mm)	k_2 (N/mm)	RMSE
1	13.5 (11.03, 15.02)	90.0 (50.16, 110.6)	0.667
2	5.13 (4.14, 6.75)	58.59 (56.15, 61.04)	2.21
3	3.247 (1.771, 4.722)	12.99 (10.71, 15.28)	1.191
4	1.42 (0.538, 3.378)	32.26 (28.82, 35.7)	1.092
5	11.78 (10.79, 12.7)	175.1 (170.1, 180.1)	0.5235

Volunteer	k_1 (N/mm)	RMSE
1	36.0 (32.0, 41.0)	0.7594
2	46.34 (45.11, 47.57)	1.554
3	47.25 (45.74, 48.76)	0.5284
4	67.3 (65.2, 69.3)	0.4622
5	94.3 (92.33, 96.26)	0.852

Table 5.6. Values for the parameters b, k_1, and k_2 and their confidence intervals for each volunteer for plantar flexion (Left foot)

Volunteer	b (Ns/mm)	k_2 (N/mm)	RMSE
1	10.2 (9.0, 11.5)	100.0 (90.0, 150.0)	0.767
2	1.44 (1.04, 2.221)	66.48 (63.05, 69.91)	0.736
3	0.712 (0.632, 0.857)	18.39 (15.43, 21.35)	1.204
4	0.754 (0.650, 0.0917)	62.5 (57.83, 67.18)	1.249
5	5.04 (2.85, 7.22)	70.55 (68.73, 72.45)	1.789

Volunteer	k_1 (N/mm)	RMSE
1	31.0 (27.0, 34.3)	0.709
2	60.43 (58.29, 62.56)	1.093
3	38.96 (36.09, 41.80)	0.959
4	79.39 (70.81, 87.92)	1.471
5	84.62 (83.5, 85.72)	0.9594

As seen in Tables 5.3 to 5.6 the values of the parameters b, k_1, and k_2 are different for each subject for dorsiflexion and plantar flexion of the foot. They have similar orders of magnitude, but their values have differences that lie in the ranges of i) (1.1-16) (Ns/mm) for the damper element b for dorsiflexion and (0.7-11.78) (Ns/mm) for plantar flexion, ii) (37.1-145.5) (N/mm) for the spring element of the Achilles tendon k_1 for dorsiflexion and (31-94.3) (N/mm) for plantar flexion and iii) (14.19-320) (N/mm) for the spring element of the gastrocnemius muscle k_2 for dorsiflexion and (12.99- 175.1) (N/mm) for plantarflexion. In plantar flexion, the primary muscles acting are the gastrocnemius, the soleus and plantaris muscles where the gastrocnemius is the most dominant and the only one that crosses both the ankle and the knee joint. In dorsiflexion, the most dominant muscle responsible for lifting the foot is the tibialis anterior that is located in the anterior part of the foot and is not connected with the Achilles tendon or the gastrocnemius or soleus muscle. This could be a reason for the differences in the values of the parameters b, k_1, and k_2 in dorsiflexion and plantar flexion.

In addition, a difference in the values of the parameters across the volunteers and across the feet of each volunteer is observed. This is expected since the volunteers have different heights, body masses and different backgrounds e.g. in sports training. However, across the right and left foot of each volunteer the orders of magnitude of the values for b, k_1, and k_2 are similar. Volunteer 3 with the lowest values of the spring element k_1 and the lowest values of the damper element b in both dorsiflexion and plantar flexion had previously attended years of dance classes. Volunteer 5 that had the greatest body mass, appears to have the highest values of b in both dorsiflexion and plantar flexion for both feet which means that the gastrocnemius muscles have an ability to resist more when shortening or lengthening. However, since the sample of the volunteers is small, it is not possible to draw more generic conclusions for a general population. Volunteer 5 also appears to have the highest values of k_1, and k_2 for dorsiflexion

and plantar flexion for both feet. This means that there is a need of a greater force in order to stretch the volunteers Achilles tendon and muscle.
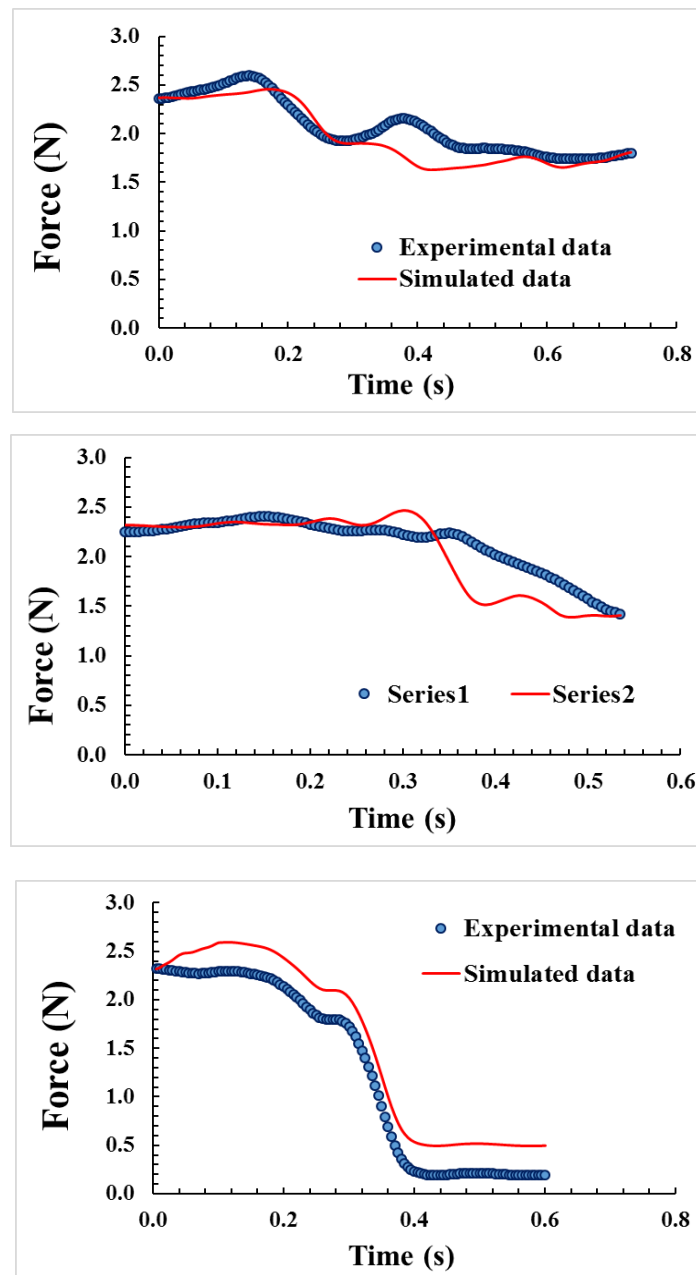
Figure 5.11. Simulated and experimental data of the force of the Achilles tendon for volunteer 1 plotted over time.

Following the parameter estimation, the values of the parameters b, k_1, and k_2 were used to plot the simulated data of the force for the Achilles tendon over time along with the experimental data of the Achilles tendon within the model (4.6)-(4.11) over time for each

142

volunteer. An example plot of the simulated and experimental responses for volunteer 1 are given in Figure 5.11 where the first figure represents the dorsiflexion of the right foot, the second figure represents the dorsiflexion of the left foot and the third figure represents the plantar flexion of the right foot.
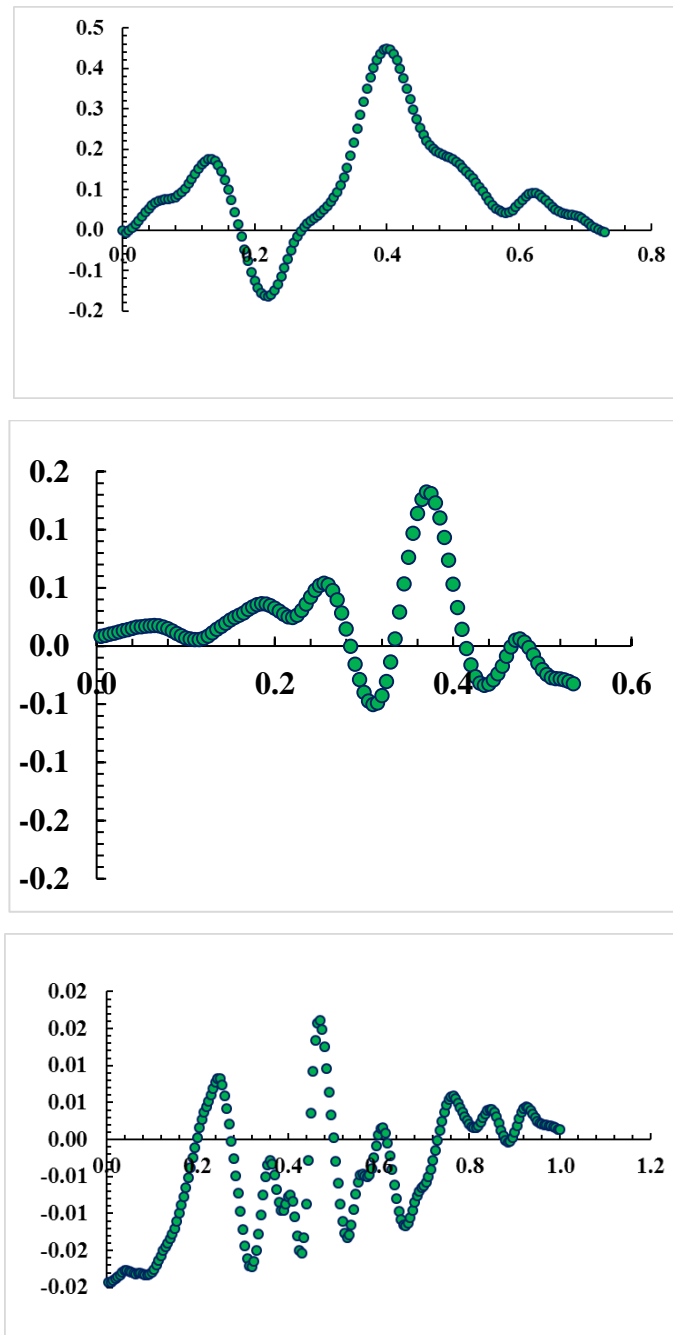
Figure 5.12. Plotted residuals of the Achilles tendon force data for dorsiflexion (first two figures) and for plantarflexion (last figure) for volunteer 1. The discrete points show the duration of the whole movement.

The residuals for the simulated and measured Achilles tendon force data were also calculated and plotted for each volunteer. These appeared random in all cases with no apparent pattern. An example is shown in Figure 5.12 where the residuals of the force data for the dorsiflexion and plantarflexion respectively, of volunteer 1 are plotted for the whole movement.

(a)

(b)

(c)

144
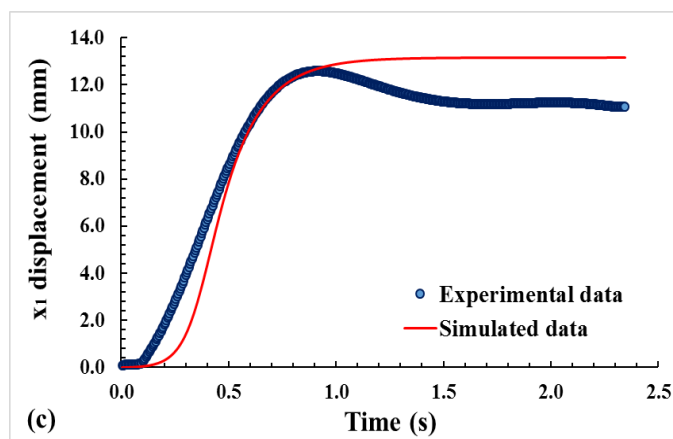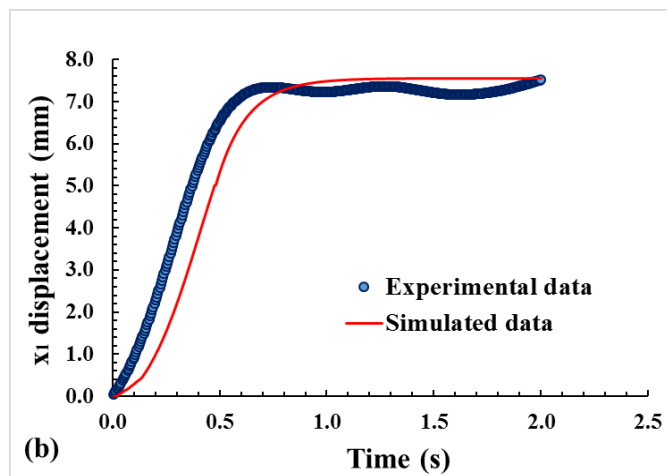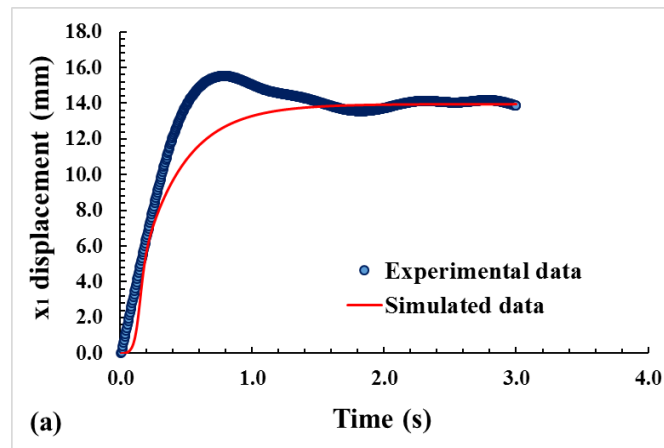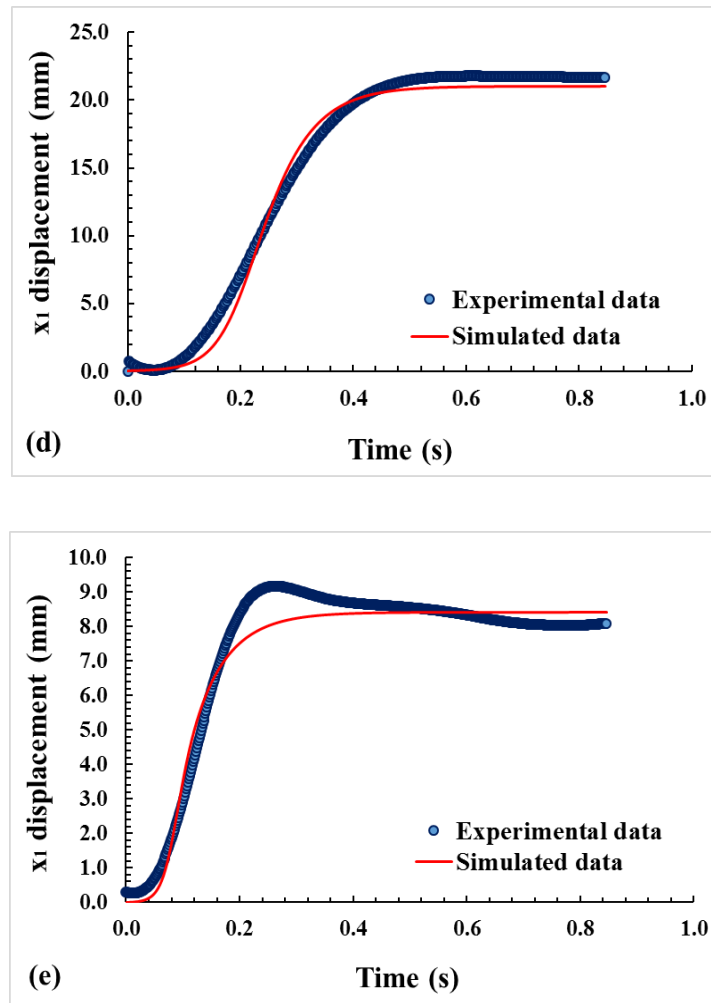
Figure 5.13. (a), (b), (c), (d), (e). Experimental and simulated data of the displacement of the Achilles tendon over time fitting the measured trajectories of the displacement over time of the Achilles tendon when dorsiflexion of the right foot occurs for different volunteers.

145

(b)

(c)

(d)

146

(e)
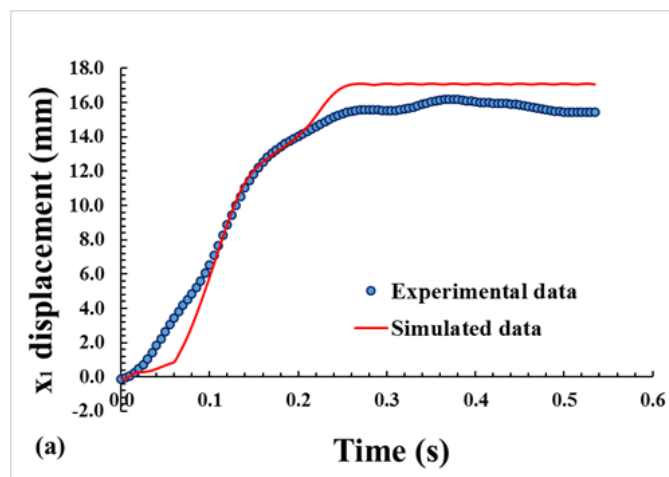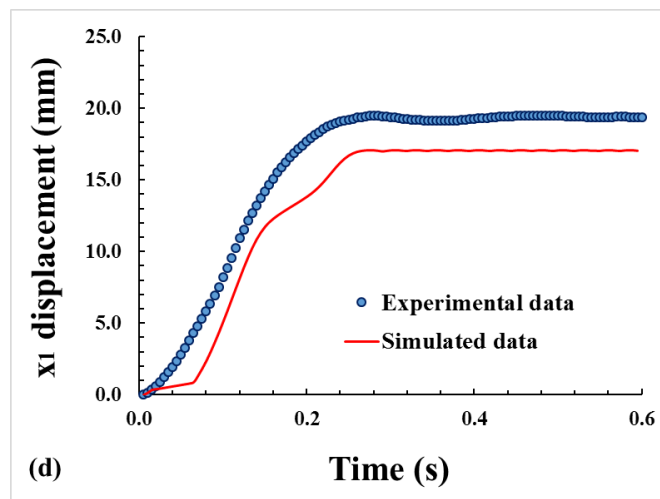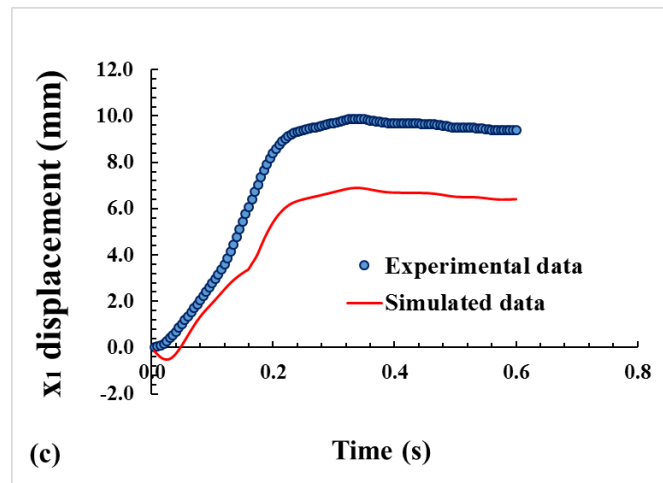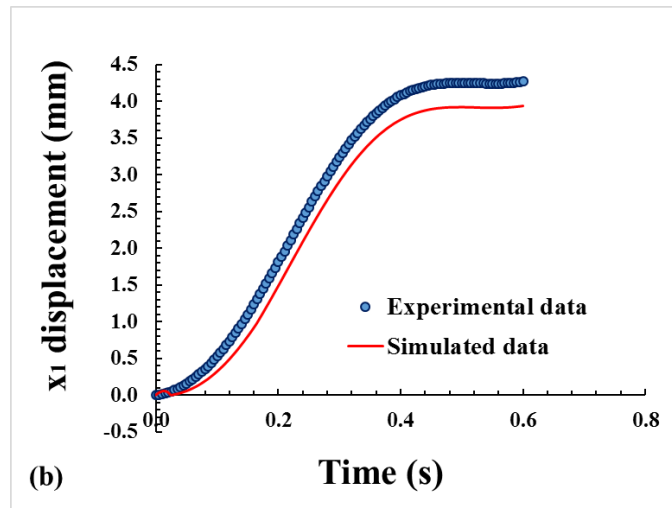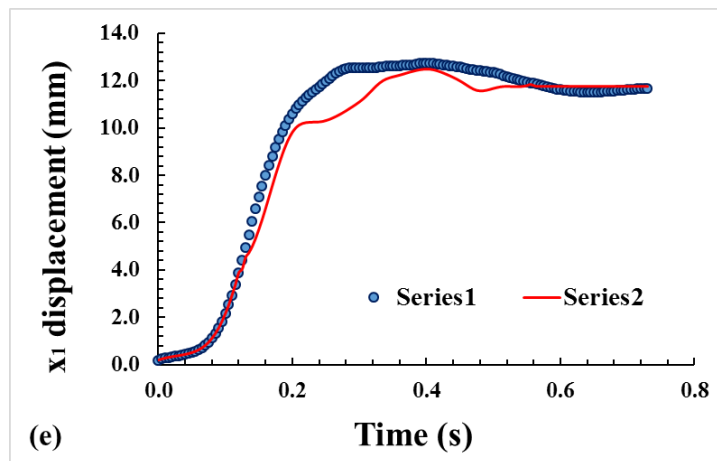
Figure 5.14. (a), (b), (c), (d), (e). Experimental and simulated data of the displacement of the Achilles tendon over time fitting the measured trajectories of the displacement over time of the Achilles tendon when dorsiflexion of the left foot occurs for different volunteers.

(a)

(b)

147
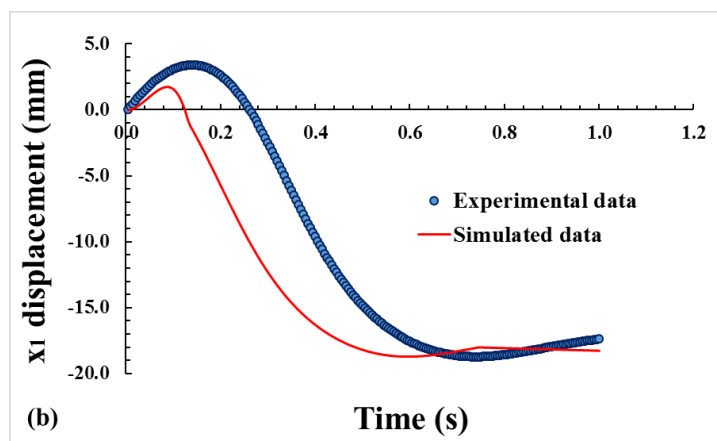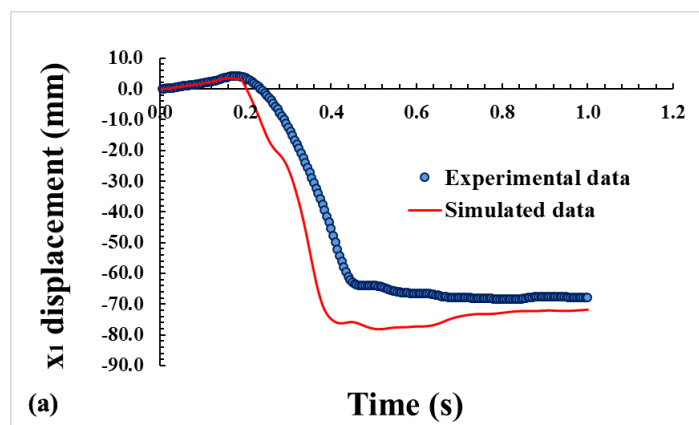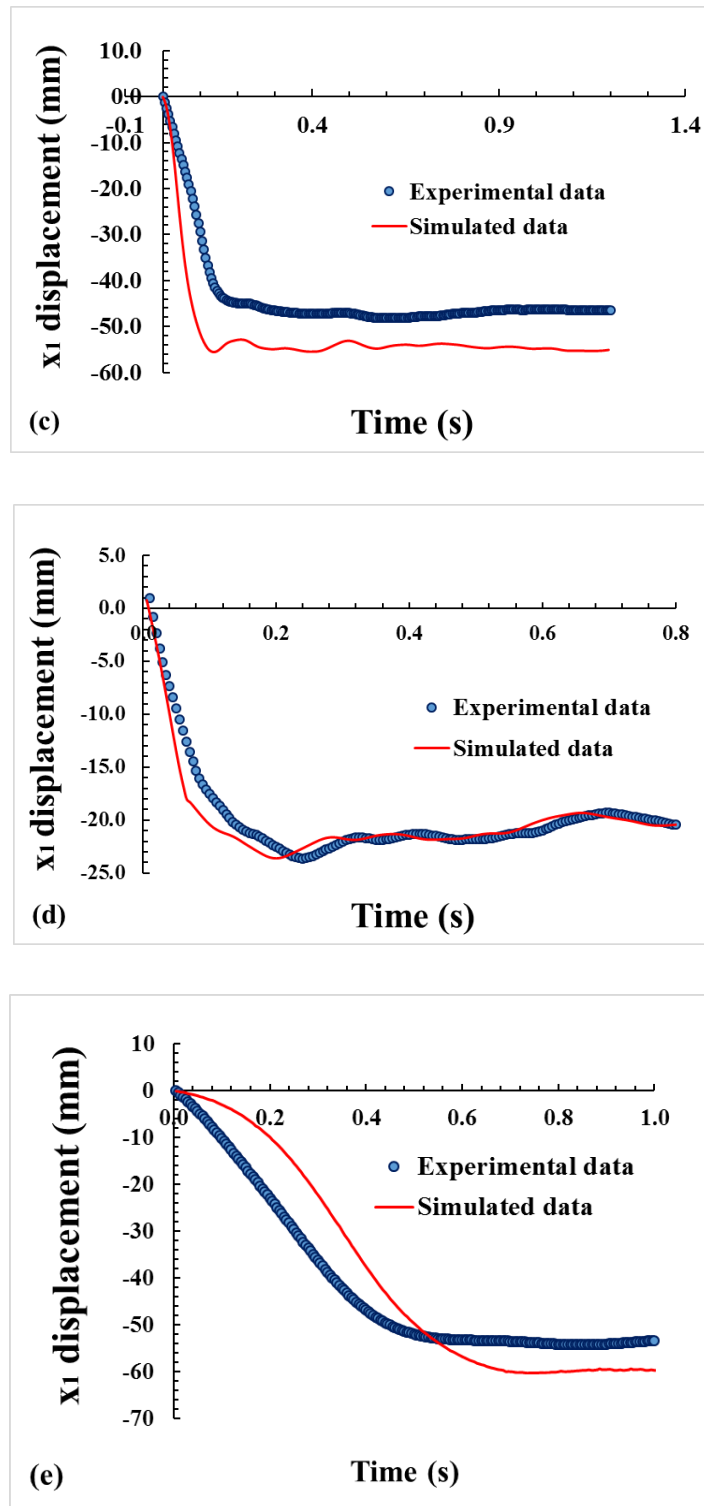
Figure 5.15. (a), (b), (c), (d), (e). Experimental and simulated data of the displacement of the Achilles tendon over time fitting the measured trajectories of the displacement over time of the Achilles tendon when plantar flexion of the right foot occurs for different volunteers.

(a)

(b)

(c)

149
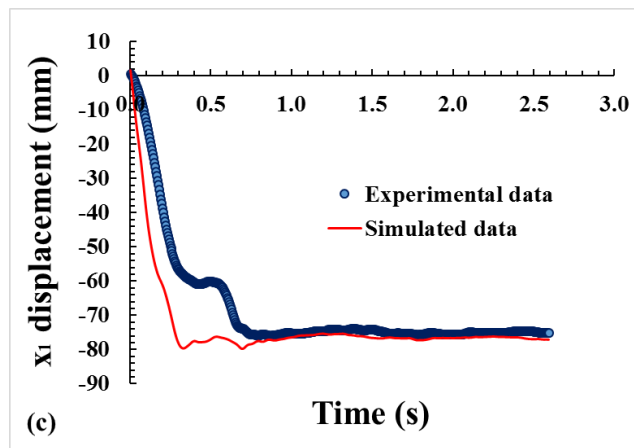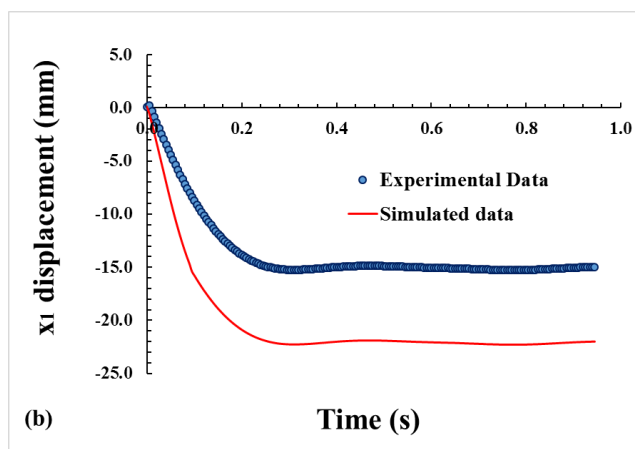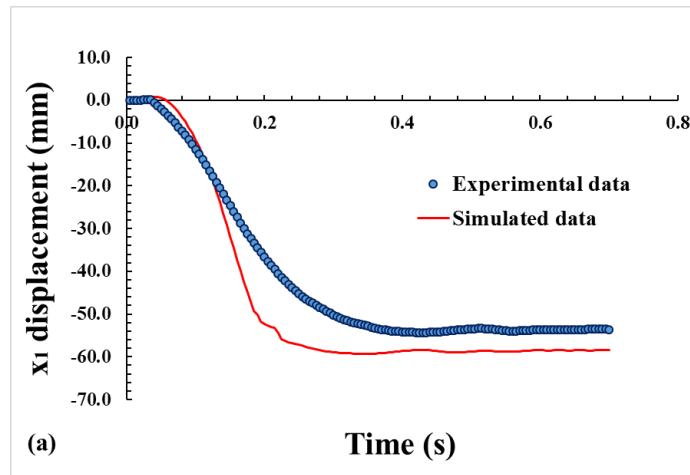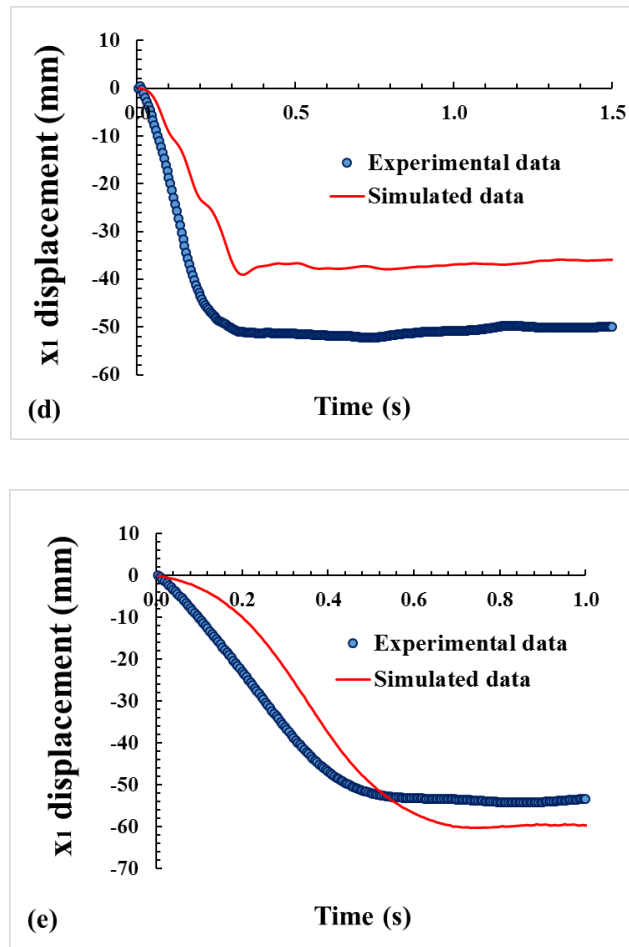
Figure 5.16. (a), (b), (c), (d), (e). Experimental and simulated data of the displacement of the Achilles tendon over time fitting the measured trajectories of the displacement over time of the Achilles tendon when plantar flexion of the left foot occurs for different volunteers.

In addition, the displacements of the Achilles tendon over time were plotted. As seen in Figures 5.13-5.16 the simulated responses approach the measured data for each volunteer. The curve for displacement over time has a similar form for each volunteer when they are dorsiflexing their foot. Left and right feet have similar curves. The curve for displacement over time has a similar form for each volunteer also when they are plantar flexing their foot. Again left and right feet follow similar curves. Volunteers with similar heights as seen in Figure 5.12 (a) and (e) have similar shapes of curves. The volunteer with the strongest background in sports/fitness training attains the highest maximum value of Achilles tendon displacement as

seen in Figures 5.12 (d) and 5.13 (d). This was volunteer 3, who had the lowest value of parameter k_2 in dorsiflexion and plantar flexion. A spring with a higher spring value needs more force to get the same amount of stretch than for a spring with lower spring value. Since the gastrocnemius muscle of volunteer 3 can shorten more with the same amount of force, their Achilles tendon can lengthen more and thus reach a maximum value of displacement that is larger than others.

The maximum strain of the Achilles tendon is suggested to be above 10% even though tendons in general begin to fail at strains from 6% to 10% [118]. Through experimental analysis it was found that the change in the total length of the Achilles tendon is not as large as the change in the total length of the gastrocnemius muscle. Thus, the Achilles tendon does not stretch as much as the muscle-tendon complex and its stiffness is considered to be greater than that of the gastrocnemius muscle [58]. This results in assuming that, when the contractile element (CE) is not active, the spring and damping elements of the muscle determine its dynamics. Furthermore, the values of the spring constants were assumed to lie within the range of 0-1000 N/m that were found in the literature. In the literature, a wide range of Achilles tendon stiffness is reported with values varying from 150 N/mm by Maganaris et al.[111], 188 N/mm by Lichtwark and Wilson [58], 201 N/mm by Morrison et al. [129] and 390 N/mm by Muroaka et al. [130]. The values from our model are consistent with the range presented in the literature. The values of the damping factors were considered to lie within the range of 0-100Ns/m [110] which are again consistent with those from the literature.

The causes of Achilles tendon injuries and ruptures were described in Section 2.2. The prevalence of Achilles tendon injuries is easy to understand when the enormous strain that is placed on the tendon is taken into consideration. For example, during the push-off phase of running, the Achilles tendon is exposed to a force of around seven times its body weight. This is close to the maximum strain the tendon can tolerate without rupturing. Furthermore, when

the high strain forces are coupled with the fact that the Achilles tendon significantly weakens as people get older, it is easy to see why this tendon is injured so frequently. A good mathematical and mechanical model when given certain input values from an individual, should be able to predict or identify potential tendency to injuries. In our model, if the elongation of the tendon is very large compared to its natural length, which means that the Achilles tendon stain is very large, or if the displacement vs time plot is not similar to the ones presented above, then the individual studied is prone to undergo an injury. However, this is a very general view, since each individual has a very distinct way of walking that is normal to them but could not be normal to the rest of the population. Therefore, before generalising and jumping to conclusions one must very carefully study each case.

5.3.2 Nonlinearity

Usually tendons are considered to be non-linear structures and their mechanical nonlinearity is shown through their stress strain-curves [58, 131]. At lower strains, Achilles tendon deforms nonlinearly, but at higher strains prior to yield and rupture it deforms linearly [131]. Although the Achilles tendon is commonly referred to as a viscoelastic material, recent studies performed in humans suggest that its elastic properties dominate [131]. Achilles tendon contains both elastic components, whose stress and strain occur in phase, and viscous components that display a 90-degree phase difference between stress and strain. These components store and release energy during loading to protect soft tissues from being damaged.

As mentioned in section 2.6, non-linear spring elements describing the Achilles tendon were also considered where α in Equation (4.11) equals 2 and 3. These two cases were investigated to see if the non-linear spring can describe the movement of the muscle-tendon complex in a more appropriate way than the linear spring [128]. The solution of the system of Equations (4.10) and (4.11) was studied where α in Equation (4.11) equals 2 initially:

$$F_{AT} = F_{CE} - b\frac{dx_2}{dt} - k_2 x_2 \text{ and } F_{AT} = k_1(x_2 - x_1)^2 .$$

Solving the system of equations symbolically in Matlab 2016a gives:

$$x_2 = \frac{F_{CE} - F_{AT} + e^{-\frac{k_2}{b}t}(F_{AT} - F_{CE})}{k_2} \qquad\qquad \text{(Eqn. 5.2)}$$

$$x_1 = x_2 + \frac{\sqrt{k_1 F_{AT}}}{k_1} \text{ or } x_1 = x_2 - \frac{\sqrt{k_1 F_{AT}}}{k_1} \qquad\qquad \text{(Eqn. 5.3)}$$

where x_2 and x_1 are the displacements described in Section 5.1.3 and seen in Figure 4.10. In order to examine if these equations can explain any of the movements studied, different values for parameters b, k_1, and k_2 were applied and values for the forces F_{AT} and F_{CE} were used according to the data obtained from the experiments conducted.
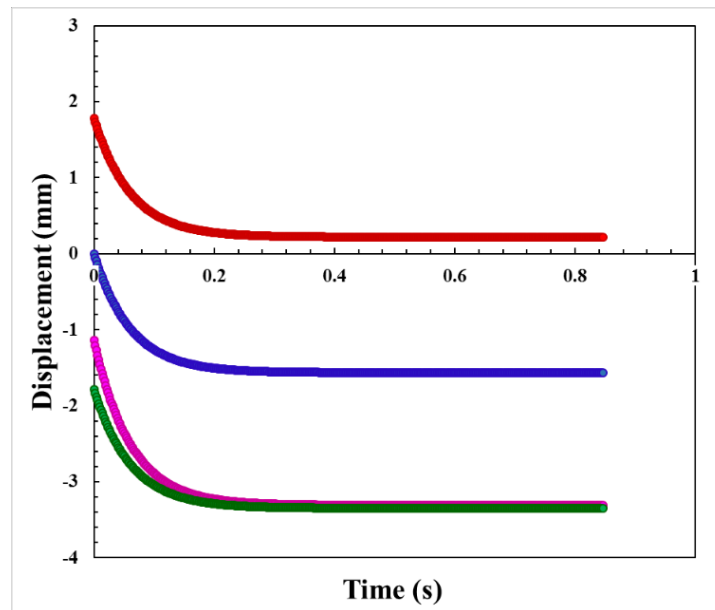
Figure 5.17. Displacement over time when volunteer is plantar flexing foot for the quadratic non-linear solution.

Figure 5.17 illustrates plantar flexion of the foot of one volunteer, where the blue line denotes the displacement x_2 over time. The magenta line symbolises the experimental data of the

153

displacement of the muscle-tendon complex over time. The red line represents the simulated displacement of the complex when $x_1 = x_2 + \sqrt{(k_1 F_{AT})/k_1}$ over time and the green line presents the simulated displacement of the complex when $x_1 = x_2 - \sqrt{(k_1 F_{AT})/k_1}$ over time. As seen from the plot, the simulated data approach the experimental data when $x_1 = x_2 - \sqrt{(k_1 F_{AT})/k_1}$.

The solution of the following system of equations was also studied where $\alpha=3$ in Equation (4.11):

$$F_{AT} = F_{CE} - b\frac{dx_2}{dt} - k_2 x_2 \text{ and } F_{AT} = k_1 x_2^3 - 3k_1 x_2^2 x_1 + 3k_1 x_2 x_1^2 - k_1 x_1^3.$$

The analytical solutions were generated symbolically in Matlab 2016a and gave Equation (5.4) as the solution of the ordinary differential equation:

$$x_2 = \frac{F_{CE} - F_{AT} + e^{-\frac{k_2}{b}t}(F_{AT} - F_{CE})}{k_2} \qquad \text{(Eqn. 5.4)}$$

and one real root and a complex conjugate pair of roots for the cubic equation. However, the mathematical solutions of the cubic equation for x_1 that are complex numbers cannot represent a displacement of a length. So further investigation was carried out only on the real root that is shown in (5.5):

$$x_1 = x_2 + C \text{, where } C = \left(-\frac{-k_1 x_2^3 + F_{AT}}{k_1} - x_2^3\right)^{1/3}. \qquad \text{(Eqn. 5.5)}$$

As described above for the quadratic equation, different values for parameters b, k_1, and k_2 were applied and values for the forces F_{AT} and F_{CE} were given according to the data obtained from the experiments conducted.

154
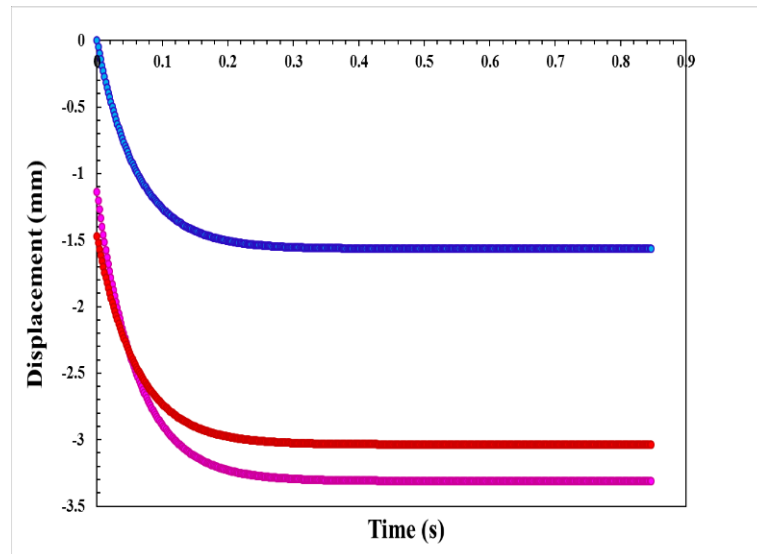
Figure 5.18. Displacement over time when volunteer is plantar flexing foot for the cubic non-linear solution.

Figure 5.18 illustrates plantar flexion of the foot of one volunteer. The blue line denotes the displacement x_2 over time. The magenta line symbolises the experimental data of the displacement of the muscle-tendon complex over time. The red line represents the simulated displacement of the complex when $x_1=x_2+C$. The simulated data approach the experimental but the two lines do not coincide as well as those in Figure 5.18. Simulations of both non-linear cases ($\alpha=2$ or 3) were performed using data from dorsiflexion experiments. However, the results did not correctly represent the displacements of the lengths of the Achilles tendon during dorsiflexion and thus are not shown in this study. As mentioned in Section 4.2.3 values for α greater than 3 were not studied because the solutions given when solving the equations could not represent the displacement of a length.

5.4 Interpretation of results obtained and discussion

The purpose of this study was to obtain more insight into how the muscle-tendon complex of the human gastrocnemius muscle-Achilles tendon behaves during plantar flexion, dorsiflexion and its resting position. Subsequently, a model of the complex was developed and

155

the patterns of the movements were determined through experiments conducted in a Gait Laboratory at the University of Warwick and at UHCW. An overview of the activities performed during this PhD so as to illustrate the steps needed to produce the various results obtained will be presented.

- Initially a mathematical/mechanical musculoskeletal model of the Achilles tendon and the gastrocnemius muscle that was anatomically meaningful was created. This was done to acquire mechanistic knowledge of the muscle-tendon complex behaviour during specific movements such as dorsiflexion and plantarflexion in humans through mathematical modelling.

- The unknowns in this musculoskeletal model were: a) the force the Achilles tendon could transmit from the leg to the foot and vice versa, b) the damping and spring elements characterising the gastrocnemius muscle behaviour in the complex and c) the spring element describing the Achilles tendon behaviour.

- Ultrasound experiments were conducted at the UHCW to validate the geometry of the Achilles tendon and calculate its length during the movements studied.

- The geometry and architecture of the gastrocnemius muscle and the Achilles tendon were also determined experimentally in the Gait Laboratory. Palpation of the legs of the volunteers before marker placement commenced, by feeling the origin and the end point of the muscles superficially was performed. Since the soleus muscle lies underneath the Achilles tendon and cannot be felt correctly by palpation, it was omitted in this study. This should be considered in future studies.

- A novel marker model was created based on the Vicon Nexus Plug-in Gait model to acquire the necessary data to compute the natural resting lengths and the elongation and shortening lengths of the muscle-tendon model.

- EMG experiments were performed to provide information about the activation of the muscles involved in the movements studied.

- Structural identifiability analysis of the modified Hill-type muscle model was performed and led to show identifiable parameters that can describe the movement of the muscle-tendon complex.

- Measurements from dorsiflexion and plantar flexion of the foot allowed us to uniquely identify the spring and damper elements of the gastrocnemius muscle-Achilles tendon unit model. Assumptions were made concerning the values of the damping and spring elements of the muscle and the tendon. However, these values lie within measured values found in the literature, where the dimensions and elastic behaviour of tendinous tissue in series with the muscle fibres were studied.

- Parameter estimation of the model was performed using Matlab 2016. It led to satisfactory agreement between measured and simulated data for the specific movements that were studied.

- Nonlinearity was studied to investigate if a linear or a non-linear spring can better describe the mechanical behaviour of the Achilles tendon. It was found that dorsiflexion can be better described by the linear case and plantar flexion can be well described by the linear and the quadratic non-linear case. This lies well in accordance with the findings from recent studies that the elastic properties of the Achilles tendon dominate its viscous properties.

The analyses of the results obtained from the experiments led to satisfactory agreement between measured and simulated data for the specific movements that were studied. Such a model and experimental approach offers the potential to be adapted to other joints, such as the hip joint and the knee. The approach developed for the upper limbs [45], was proven to be

suitable for the leg muscles, so we can speculate that other muscle groups can be parameterised and studied in a similar way. When investigating the non-linear model, the solution for the quadratic equation when simulated gave a better approach to the experimental data than the simulation of the solution of the cubic equation. The authors hope that by investigating tendons and muscles using a similar mathematical and experimental approach, doctors and researchers could be assisted in distinguishing a healthy individual from someone with a potential pathology or injury.

Chapter 6. Conclusions, discussion and future work

The main aim of this study described in this thesis has been the development of a mathematical/mechanical musculoskeletal model of the Achilles tendon that could distinguish a healthy individual from someone with a potential pathology or injury. A good mechanistic knowledge of the gastrocnemius muscle-Achilles tendon complex behaviour during specific movements in humans through mathematical modelling was required. Accurate model outcomes can be used to study how particular muscles contribute to movement coordination and propose or assess interventions to prevent foot injuries. Models that can predict how a tendon and a muscle should behave under 'normal' conditions, can be used to examine the effect of changes in the dynamics of individual components have in the anatomy and physiology on the whole dynamic system that is the human body.

Predictive models in general, help in the better understanding of how a pathology progresses, how rehabilitation works and what limitations there are in movements. Predictive models can also support the development of computer based mathematical models that could evolve the field of prostheses or orthoses used as part of movement rehabilitation. Muscle and tendon problems and their causes differ between individuals and populations. Thus, differences in the dynamics of components within the musculoskeletal system may appear [42]. In order to develop models that could help patients in rehabilitation and could predict movements and forces, the parameter values required in those models must be patient specific (i.e. tailored to the individual studied) in order to enable accurate predictions of the dynamics of their movements. Therefore, part of the model development described in this thesis was to ensure that the methods used could fully parameterise the models from in vivo measurements on an individual subject basis. Parameter values that were not directly measurable, were uniquely identified through parameter estimation experiments.

6.1 Achilles tendon model development

In Chapter 4 the development of the mathematical, mechanical, musculoskeletal model of the Achilles tendon was described. The model is anatomically meaningful; it describes the anatomy and physiology of the body components incorporated as realistically as possible. Inverse dynamics in conjunction with Newton's second and third laws were used in order to compute forces and moments of force indirectly from the kinematics and inertial properties of the lower bodies studied. The method used to numerically compute the internal kinetics of planar human movements was presented in Section 4.1. In order to calculate the forces and moments at specific joints, body kinematics and anthropometric data are applied. Three important principles were involved in this method; i) Newton's second law, ii) the principle of superposition and iii) a technique known as the method of sections. A single net force and a single moment of force, that can be measured from experiments, were produced in order to solve the unknown Achilles tendon force. Also forward dynamics were used to determine the resultant motion of bodies [41].

The present model is sensitive to its input data. Errors in marker locations, segment inertial properties, joint centre estimates, segment accelerations, joint forces and ground reaction forces affect the joint moment data. Some of these errors are less significant than others. An example mentioned in Robertson [41], states that ground reaction forces during locomotion tend to dominate stance-phase kinetics and measuring them accurately prevents the majority of accuracy problems. However, assumption made for the model and limitations that occurred do not invalidate the model data, but they do limit the extent of interpretation.

In Section 4.2, a two segment model of the human foot and leg was presented that describes the development of the musculoskeletal model of the Achilles tendon. Newton's laws and the method of link-segment modelling were used to derive the system equations necessary to

mathematically model the skeletal system along with the Achilles tendon. In Section 4.3 the method used to model human skeletal muscle dynamics using Hill-type muscle models was portrayed. A gastrocnemius muscle-Achilles tendon model was presented and the derivation of the system equations that characterise the muscle-tendon model were given. The purpose of this study is to acquire mechanistic knowledge of the gastrocnemius muscle-Achilles tendon complex behaviour during specific movements in humans through mathematical modelling. Accurate model outcomes were very important in order to study how particular muscles contribute to movement coordination and propose or assess interventions to prevent foot injuries. Therefore, a validated model of the Achilles tendon that could provide specific parameters for a specific person studied, was a main goal of this thesis. The derivation of the Achilles tendon force from the system equations for the musculoskeletal model of the Achilles tendon and the implementation of that force in the muscle-tendon model in order to derive the parameters of the model as well as the non-linear approach of the behaviour of the Achilles tendon studied through a motion capture system is, to the best of the authors knowledge, novel in the field of muscle-tendon research.

The variability in Achilles tendon stiffness between subjects strengthens the need for the development of experimentally measured subject-specific tendon properties. These properties would be the input parameters of the models that would help to improve the accuracy of musculoskeletal models. Hill-type muscle models and musculoskeletal simulations have broad application to biomechanical research and experimental investigations of musculoskeletal pathologies [129]. However, the accuracy of these simulations directly depends on the values used in the models, i.e. the natural resting length of muscles and tendons. Despite significant variability in these tendon properties between individuals many studies use generic values for the tendon properties. That is why in this thesis the model developed, used specific data for each individual that participated in the experiments conducted.

In order to obtain the appropriate specific inputs for each individual to then be incorporated in the model, anthropometric data were used. Ultrasound and Gait Laboratory experiments were used to obtain the natural resting lengths of the Achilles tendon and the gastrocnemius muscle as well as the change in length of the muscle and the tendon when an individual performed specific movements. A novel marker placement, which is a combination of the validated existing Plug-in Gait model with new markers added, was created in order to acquire the necessary data to compute the natural resting lengths and the elongation and shortening lengths of the muscle-tendon model. Cross validation of the lengths was performed through the lengths obtained from the Ultrasound experiments conducted at the UHCW. EMG experiments also provided information about the activation of the muscles involved in the movements studied. This information was valuable for the development of the model and the assumptions for the description of the contractile force input.

Structural identifiability analysis of the modified Hill-type muscle model was performed and concluded that all the parameters of the model are identifiable and can describe the movement of the muscle-tendon complex. Then, parameter estimation was performed in the time domain for each volunteer in order to acquire a set of fitted values for the parameters b, k_1, and k_2 that were the unknown ones in our model. Parameter estimation of the model led to satisfactory agreement between measured and simulated data for the specific movements that were studied. All results were found to lie in the accepted range of values mentioned in the literature. A non-linear model was also investigated which showed that the solution for the quadratic Equation (4.11) when simulated gave a better approach to the experimental data than the simulation of the solution of the cubic equation.

The general approach and the model developed was proven to be suitable for the leg muscles and the Achilles tendon, so we can speculate that other muscle groups can be parameterised and studied in a similar way.

6.2 Recommendations for future work

The foot in this thesis was represented as a rigid body. Since the Achilles tendon is not connected directly to the front part of the foot and the calcaneus-talus bone structures are much more rigid than the forefoot ones, the foot segment in this study was chosen to be represented as a whole [41]. When dividing the human body into segments, and at least one full-length bone such as the thigh or the leg is present in that segment then it is sensibly considered to be rigid since it can transmit forces well [1, 41]. In contrast, a non-rigid segment attenuates the forces that are applied to it. Therefore, in future work the foot needs to be segmented and the toe joint needs to be included for the gait model to be more accurate.

Absolute lengths and muscle velocities due to fascicle movement have been studied using ultrasound during walking and running [79, 118] and while joints are moved through a range of motion [111, 132, 133]. These studies provide important measurements of the absolute lengths and velocities of different muscles, including the gastrocnemius, the soleus, the biceps femoris and the vastus lateralis. However, ultrasound imaging alone does not determine normalized muscle fibre lengths or velocities. Normalized fibre lengths can be determined from measurements of sarcomere lengths that have been calculated in the upper extremity by using laser diffraction during surgery [79].

Isometric and isotonic contractions of the muscle-tendon complex and specific movements are important to be examined as an initial step. However, the way that muscles generate complex movements and behave during those complex movements is different from the way in which they behave in specific types of contractions (isotonic, isometric). Observations and analysis of the complex movements are also necessary which will hopefully lead to a more personalised analysis of the model generated. The material properties of the gastrocnemius muscle and the Achilles tendon should also be incorporated in future studies. In addition, a

spatio-temporal three-dimension description of the system would be an interesting approach to be investigated in the future.

A Finite Element Analysis (FEA) would greatly implement and validate the results of this study. When conducting a Finite Element Analysis, a subject specific geometry of the Achilles tendon can be inserted in an appropriate software to be further analysed. This geometry could be obtained from Ultrasound or MR Images so as to accurately design the Achilles tendon in a FEA environment. Material properties acquired from motion capture experiments or from experiments using cadaveric specimens could be used to define the mechanical properties of the Achilles tendon. Also, tendon material properties could be optimized by comparing and minimizing differences in uniaxial tension experimental results with model predictions. Predictions of tears and ruptures as to the specific locations along the length of the Achilles tendon can be given as well as the loads under which the tendons could rupture. This is very important information when studying a tendon and trying to understand whether geometry and material properties of a tendon are highly subject specific. Therefore, a Finite Element Analysis coupled with the mathematical/musculoskeletal analysis performed in this thesis could advance and validate the results of this research.

Lastly, a very interesting aspect to be studied in the future and compare with the results obtained from the current study, is the investigation of the same movements performed by individuals from 60 years old and onwards when the degradation of the cells has begun and fatigue in the muscles is more frequent.

References

[1]   D. A. Winter, *Biomechanics and Motor control of Human Movement*. NJ, 2005.

[2]   M. W. Whittle, "Chapter 2 - Normal gait," in *Gait Analysis (Fourth Edition)*, ed Edinburgh: Butterworth-Heinemann, pp. 47-100, 2007.

[3]   D. H. Sutherland, "The evolution of clinical gait analysis: Part II Kinematics," *Gait & Posture,* vol. 16, pp. 159-179, 10/ 2002.

[4]   D. H. Sutherland, "The evolution of clinical gait analysis part III – kinetics and energy assessment," *Gait & Posture,* vol. 21, pp. 447-461, 6/ 2005.

[5]   R. Baker, "Gait analysis methods in rehabilitation," *Journal of NeuroEngineering and Rehabilitation,* vol. 3, pp. 4-4, 03/02/2006.

[6]   J. P. Naomi Hartree. *Achilles Tendinopathy and Rupture*. Available: http://patient.info/doctor/achilles-tendinopathy-and-rupture, 2016.

[7]   S. de Jonge, C. van den Berg, R. J. de Vos, H. J. L. van der Heide, A. Weir, J. A. N. Verhaar*, et al.*, "Incidence of midportion Achilles tendinopathy in the general population," *British Journal of Sports Medicine,* vol. 45, pp. 1026-1028, October 1, 2011.

[8]   J. Wertz, M. Galli, and J. R. Borchers, "Achilles Tendon Rupture: Risk Assessment for Aerial and Ground Athletes," *Sports Health,* vol. 5, pp. 407-409, 2013.

[9]   I. Lantto, J. Heikkinen, T. Flinkkilä, P. Ohtonen, and J. Leppilahti, "Epidemiology of Achilles tendon ruptures: Increasing incidence over a 33-year period," *Scandinavian Journal of Medicine & Science in Sports,* vol. 25, pp. e133-e138, 2015.

[10]   M. R. Carmont, A. M. Highland, J. R. Rochester, E. M. Paling, and M. B. Davies, "An anatomical and radiological study of the fascia cruris and paratenon of the Achilles tendon," *Foot and Ankle Surgery,* vol. 17, pp. 186-192, 9/ 2011.

[11]   P. Szaro, G. Witkowski, R. Śmigielski, P. Krajewski, and B. Ciszek, "Fascicles of the adult human Achilles tendon – An anatomical study," *Annals of Anatomy - Anatomischer Anzeiger,* vol. 191, pp. 586-593, 11/20/ 2009.

[12]   e-medicine-health. *Achilles Tendon Injuries*. Available: http://www.emedicinehealth.com/script/main/art.asparticlekey=138768&ref=135864, 2015.

[13]   J. H. C. Wang, "Mechanobiology of tendon," *Journal of Biomechanics,* vol. 39, pp. 1563-1582, /2006.

[14]   A. D. Waggett, J. R. Ralphs, A. P. L. Kwan, D. Woodnutt, and M. Benjamin, "Characterization of collagens and proteoglycans at the insertion of the human achilles tendon," *Matrix Biology,* vol. 16, pp. 457-470, 3/ 1998.

[15]   A. Lesic and M. Bumbasirevic, "Disorders of the Achilles tendon," *Current Orthopaedics,* vol. 18, pp. 63-75, 2/2004.

[16]   A. Saxena and D. Bareither, "Magnetic resonance and cadaveric findings of the "watershed band" of achilles tendon," *The Journal of Foot and Ankle Surgery,* vol. 40, pp. 132-136, 5/ 2001.

[17]   P. Theobald, M. Benjamin, L. Nokes, and N. Pugh, "Review of the vascularisation of the human Achilles tendon," *Injury,* vol. 36, pp. 1267-1272, 11/ 2005.

[18]   C. C. van Gils, R. H. Steed, and J. C. Page, "Torsion of the human achilles tendon," *The Journal of Foot and Ankle Surgery,* vol. 35, pp. 41-48, 1/ 1996.

[19]   M. Ying, E. Yeung, B. Li, W. Li, M. Lui, and C.-W. Tsoi, "Sonographic evaluation of the size of achilles tendon: the effect of exercise and dominance of the ankle," *Ultrasound in Medicine & Biology,* vol. 29, pp. 637-642, 5/ 2003.

[20]   D. B. Tortora Gerard J., *Principles of Anatomy & Physiology*: John Wiley and Sons, 2011.

[21]   H. K. Marieb Elaine N., *Human Anatomy & Physiology*. San Fransisco: Pearson Benjamin Cummings, 2007.

[22]   Wikipedia. [Online]. Available: https://en.wikipedia.org/wiki/Ankle

[23]   K. Brandt. *Achilles tendon information*. Available: http://achillestendon.com/achilles-tendon-information/ 5th June 2015.

[24]   T. A. L. Wren, S. A. Yerby, G. S. Beaupré, and D. R. Carter, "Mechanical properties of the human achilles tendon," *Clinical Biomechanics,* vol. 16, pp. 245-251, 3/ 2001.

[25]   G. L. Caldwell Jr, "Achilles' tendon ruptures: Operative versus nonoperative management," *Operative Techniques in Orthopaedics,* vol. 5, pp. 290-294, 7/ 1995.

[26]   E. P. Mulligan, "20 - Lower Leg, Ankle, and Foot Rehabilitation," in *Physical Rehabilitation of the Injured Athlete (Fourth Edition)*, ed Philadelphia: W.B. Saunders, pp. 426-463, 2012.

[27]   Alila.   Available: http://www.123rf.com/photo_11347639_achilles-tendon-problems.html, 2008.

[28]   S. Malvankar and W. S. Khan, "Evolution of the Achilles tendon: The athlete's Achilles heel?," *The Foot,* vol. 21, pp. 193-197, 12/ 2011.

[29]   F. Benazzo, A. Todesca, and L. Ceciliani, "Achilles' tendon tendinitis and heel pain," *Operative Techniques in Sports Medicine,* vol. 5, pp. 179-188, 7/ 1997.

[30]   A. Neuhold, M. Stiskal, F. Kainberger, and B. Schwaighofer, "Degenerative Achilles tendon disease: assessment by magnetic resonance and ultrasonography," *European Journal of Radiology,* vol. 14, pp. 213-220, 5/ 1992.

[31]   M. A. Wessely, "MR imaging of the ankle and foot—A review of the normal imaging appearance with an illustration of common disorders," *Clinical Chiropractic,* vol. 10, pp. 101-111, 6/ 2007.

[32]   J. J. Rankine, "(iv) Imaging of foot and ankle disorders," *Orthopaedics and Trauma,* vol. 23, pp. 412-419, 12/ 2009.

[33]   J. Watkins and I. Mathieson, "Chapter 7 - Structure and function of the foot," in *The Pocket Podiatry Guide: Functional Anatomy*, ed Edinburgh: Churchill Livingstone, pp. 227-301, 2009.

[34]   S. Hitzmann. *Fine Anatomy: The lower leg and its functions and role in stabilization*. Available: http://www.ideafit.com/fitness-library/ankle-flexion, 01 February 2003.

[35]   O'Rahilly. *Basic Human anatomy - Chapter 17: The ankle and foot*. Available: http://www.dartmouth.edu/~humananatomy/part_3/chapter_17.html, 2009.

[36] T. L. Switaj and F. G. O'Connor, "Chapter 43 - Gait Analysis," in *The Sports Medicine Resource Manual*, ed Philadelphia: W.B. Saunders, pp. 536-542, 2008.

[37] L. Chaitow and J. DeLany, "Chapter 3 - Gait analysis," in *Clinical Application of Neuromuscular Techniques, Volume 2 (Second Edition)*, ed Oxford: Churchill Livingstone, pp. 61-84, 2011.

[38] C. Kirtley, "Introduction," in *Clinical Gait Analysis*, ed Edinburgh: Churchill Livingstone, pp. 201-222, 2006.

[39] C. Kirtley, "Chapter 3 - Three-dimensional gait analysis," in *Clinical Gait Analysis*, C. Kirtley, Ed., ed Edinburgh: Churchill Livingstone, pp. 53-71, 2006.

[40] A. V. Hill, "The Heat of Shortening and the Dynamic Constants of Muscle," *Proceedings of the Royal Society of London. Series B, Biological Sciences,* vol. 126, pp. 136-195, 1938.

[41] G. E. Robertson D., *Research Methods in Biomechanics*. USA: Edwards Brothers Malloy, 2014.

[42] T. F. Yu, "Musculo-Skeletal Modelling and Parameterisation in Vivo," PhD, Physics Department, University of Warwick, March 2014.

[43] D. F. B. Haeufle, M. Günther, A. Bayer, and S. Schmitt, "Hill-type muscle model with serial damping and eccentric force–velocity relation," *Journal of Biomechanics,* vol. 47, pp. 1531-1536, 4/11/ 2014.

[44] M. F. Bobbert, P. A. Huijing, and G. J. van Ingen Schenau, "A model of the human triceps surae muscle-tendon complex applied to jumping," *Journal of Biomechanics,* vol. 19, pp. 887-898, 1986.

[45] A. Freivalds, *Biomechanics of the upper limbs : mechanics, modeling, and musculoskeletal injuries*. USA: CRC press, 2004.

[46] A. M. Gordon, A. F. Huxley, and F. J. Julian, "The variation in isometric tension with sarcomere length in vertebrate muscle fibres," *The Journal of Physiology,* vol. 184, pp. 170-192, 1966.

[47] R. A. Zifchock and S. J. Piazza, "Investigation of the validity of modeling the Achilles tendon as having a single insertion site," *Clinical Biomechanics,* vol. 19, pp. 303-307, 3/ 2004.

[48] M. A. Townsend and A. Seireg, "The synthesis of bipedal locomotion," *Journal of Biomechanics,* vol. 5, pp. 71-83, 01/01 1972.

[49] H. Hemami, "A Feedback On-Off Model of Biped Dynamics," *IEEE Transactions on Systems, Man, and Cybernetics,* vol. 10, pp. 376-383, 1980.

[50] M. G. Pandy and N. Berme, "Synthesis of human walking: A planar model for single support," *Journal of Biomechanics,* vol. 21, pp. 1053-1060, 01/01 1988.

[51] M. A. Townsend, "Dynamics and coordination of torso motions in human locomotion," *Journal of Biomechanics,* vol. 14, pp. 727-738, 01/01 1981.

[52] E. Y.-S. Chao and K. Rim, "Application of optimization principles in determining the applied moments in human leg joints during gait," *Journal of Biomechanics,* vol. 6, pp. 497-510, 09/01 1973.

[53]   S. Onyshko and D. A. Winter, "A mathematical model for the dynamics of human locomotion," *Journal of Biomechanics,* vol. 13, pp. 361-368, 01/01 1980.

[54]   H. Hemami, Y.-F. Zheng, and M. J. Hines, "Initiation of walk and tiptoe of a planar nine-link biped," *Mathematical Biosciences,* vol. 61, pp. 163-189, 10/01 1982.

[55]   B.-R. Chen, M. J. Hines, and H. Hemami, "Dynamic modelling for implementation of a right turn in bipedal walking," *Journal of Biomechanics,* vol. 19, pp. 195-206, 01/01 1986.

[56]   S. J. Phillips, E. M. Roberts, and T. C. Huang, "Quantification of intersegmental reactions during rapid swing motion," *Journal of Biomechanics,* vol. 16, pp. 411-417, 01/01 1983.

[57]   H. M. J. Hemami H., Goddard R.E. , and Friedman B., "Biped Sway in the Frontal Plane with Locked Knees," *IEEE Transactions on Systems, Man, and Cybernetics,* vol. 12, pp. 577-582, 1982.

[58]   G. A. Lichtwark, & Wilson, A. M. , " In vivo mechanical properties of the human Achilles tendon during one-legged hopping," *Journal of Experimental Biology,* vol. 208(24), 2005.

[59]   E. Wallenböck, O. Lang, and P. Lugner, "Stress in the achilles tendon during a topple-over movement in the ankle joint," *Journal of Biomechanics,* vol. 28, pp. 1091-1101, 9/ 1995.

[60]   S. J. Obst, R. Newsham-West, and R. S. Barrett, "In Vivo Measurement of Human Achilles Tendon Morphology Using Freehand 3-D Ultrasound," *Ultrasound in Medicine & Biology,* vol. 40, pp. 62-70, 1/ 2014.

[61]   J. T.-M. Cheung, M. Zhang, A. K.-L. Leung, and Y.-B. Fan, "Three-dimensional finite element analysis of the foot during standing—a material sensitivity study," *Journal of Biomechanics,* vol. 38, pp. 1045-1054, 5/ 2005.

[62]   V. Juras, S. Apprich, C. Pressl, S. Zbyn, P. Szomolanyi, S. Domayer, *et al.*, "Histological correlation of 7T multi-parametric MRI performed in ex-vivo Achilles tendon," *European Journal of Radiology*, 19 September 2011.

[63]   L. E. DeFrate, A. van der Ven, P. J. Boyer, T. J. Gill, and G. Li, "The measurement of the variation in the surface strains of Achilles tendon grafts using imaging techniques," *Journal of Biomechanics,* vol. 39, pp. 399-405, 2006.

[64]   J. T.-M. Cheung and B. M. Nigg, "Clinical Applications of Computational Simulation of Foot and Ankle," *Sport-Orthopädie - Sport-Traumatologie - Sports Orthopaedics and Traumatology,* vol. 23, pp. 264-271, 1/24/ 2008.

[65]   J. Stebbins, M. Harrington, N. Thompson, A. Zavatsky, and T. Theologis, "Repeatability of a model for measuring multi-segment foot kinematics in children," *Gait & Posture,* vol. 23, pp. 401-410, 6/ 2006.

[66]   L. A. Gilchrist and D. A. Winter, "A multisegment computer simulation of normal human gait," *IEEE Trans Rehabil Eng,* vol. 5, pp. 290-9, Dec 1997.

[67]   L. A. Gilchrist and D. A. Winter, "A two-part, viscoelastic foot model for use in gait simulations," *Journal of Biomechanics,* vol. 29, pp. 795-798, 6/ 1996.

[68]   C. Bishop, G. Paul, and D. Thewlis, "Recommendations for the reporting of foot and ankle models," *Journal of Biomechanics,* vol. 45, pp. 2185-2194, 8/31/ 2012.

[69] C. J. Wright, B. L. Arnold, T. G. Coffey, and P. E. Pidcoe, "Repeatability of the modified Oxford foot model during gait in healthy adults," *Gait & Posture,* vol. 33, pp. 108-112, 1/ 2011.

[70] S. G. Seo, D. Y. Lee, H. J. Moon, S. J. Kim, J. Kim, K. M. Lee*, et al.*, "Repeatability of a multi-segment foot model with a 15-marker set in healthy adults," *Journal of Foot and Ankle Research,* vol. 7, p. 24, 2014.

[71] M. C. Carson, M. E. Harrington, N. Thompson, J. J. O'Connor, and T. N. Theologis, "Kinematic analysis of a multi-segment foot model for research and clinical applications: a repeatability analysis," *Journal of Biomechanics,* vol. 34, pp. 1299-1307, 10/ 2001.

[72] P. C. Dixon, H. Böhm, and L. Döderlein, "Ankle and midfoot kinetics during normal gait: A multi-segment approach," *Journal of Biomechanics,* vol. 45, pp. 1011-1016, 4/5/ 2012.

[73] M. Lord, D. P. Reynolds, and J. R. Hughes, "Foot pressure measurement: A review of clinical findings," *Journal of Biomedical Engineering,* vol. 8, pp. 283-294, 10/ 1986.

[74] S. van Hoeve, J. de Vos, P. H. E. Weijers, J. Verbruggen, P. Willems, M. Poeze*, et al.*, "Repeatability of the Oxford Foot Model for Kinematic Gait Analysis of the Foot and Ankle," *Clinical research on foot & ankle,* vol. 3, p. 171, 2015.

[75] J. T.-M. Cheung, M. Zhang, and K.-N. An, "Effect of Achilles tendon loading on plantar fascia tension in the standing foot," *Clinical Biomechanics,* vol. 21, pp. 194-203, September 2005.

[76] E. M. Arnold, S. R. Ward, R. L. Lieber, and S. L. Delp, "A Model of the Lower Limb for Analysis of Human Movement," *Annals of biomedical engineering,* vol. 38, pp. 269-279, 12/03 2010.

[77] J. R. Franz, L. C. Slane, K. Rasske, and D. G. Thelen, "Non-uniform in vivo deformations of the human Achilles tendon during walking," *Gait & Posture,* vol. 41, pp. 192-197, 1/ 2015.

[78] J. R. Franz and D. G. Thelen, "Imaging and simulation of Achilles tendon dynamics: Implications for walking performance in the elderly," *Journal of Biomechanics,* vol. 49, pp. 1403-1410, 6/14/ 2016.

[79] E. M. Arnold, S. R. Hamner, A. Seth, M. Millard, and S. L. Delp, "How muscle fiber lengths and velocities affect muscle force generation as humans walk and run at different speeds," *The Journal of Experimental Biology,* vol. 216, p. 2150, 2013.

[80] L. Mündermann, S. Corazza, and T. P. Andriacchi, "The evolution of methods for the capture of human movement leading to markerless motion capture for biomechanical applications," *Journal of NeuroEngineering and Rehabilitation,* vol. 3, pp. 6-6, 03/15/ 2006.

[81] A. Godfrey, R. Conway, D. Meagher, and G. ÓLaighin, "Direct measurement of human movement by accelerometry," *Medical Engineering & Physics,* vol. 30, pp. 1364-1386, 12/ 2008.

[82] Saunders. *Range of motion at the ankle joint.* Available: http://classconnection.s3.amazonaws.com/862/flashcards/749862/jpg/ankle_foot_rom 1319470990042.jpg, 2012.

[83] AOK-health. *Joint Range of Motion Data Using a Goniometer*. Available: www.aokhealth.com/.../Using%20a%20Goniometer%20Effectively.pdf

[84] L. J. Kleeblad, A. F. van Bemmel, I. N. Sierevelt, H. A. Zuiderbaan, and D. A. Vergroesen, "Validity and Reliability of the Achillometer®: An Ankle Dorsiflexion Measurement Device," *The Journal of Foot and Ankle Surgery,* vol. 55, pp. 688-692, 7/ 2016.

[85] N. Burr, A. L. Pratt, and D. Stott, "Inter-rater and Intra-rater Reliability when Measuring Interphalangeal Joints: Comparison between three hand-held goniometers," *Physiotherapy,* vol. 89, pp. 641-652, 11/ 2003.

[86] S. Milanese, S. Gordon, P. Buettner, C. Flavell, S. Ruston, D. Coe*, et al.*, "Reliability and concurrent validity of knee angle measurement: Smart phone app versus universal goniometer used by experienced and novice clinicians," *Manual Therapy,* vol. 19, pp. 569-574, 12/ 2014.

[87] Advanced-Mechanical-Technology, "AMTI Biomechanics Platform Instruction Manual Version 2.0," October 2004.

[88] Biometrics-LTD. Available: http://www.biometricsltd.com/gonio.htm

[89] E. Neil, "Gait Lab: Open Day Demo-Staff Briefing Notes," ed, 2011.

[90] Advanced-Mechanical-Technology. *OR6-7-1000 SPECIFICATIONS*. Available: http://www.amti.biz/AMTIpibrowser.aspx?__VIEWSTATE=%2FwEPDwULLTE0Nz Q1NDQ3OTNkZA%3D%3D&iListbox1=350&iListbox2=378&iListbox3=OR6-7, 2015.

[91] Advanced-Mechanical-Technology, "AMTI Biomechanics Force Plate Installation Manual Version 4.3," August 2012.

[92] Advanced-Mechanical-Technology. *AMTI Force and Motion Miniamp*. Available: http://www.amti.biz/AMTIpibrowser.aspx?__VIEWSTATE=%2FwEPDwULLTE0Nz Q1NDQ3OTNkZA%3D%3D&iListbox1=197&iListbox2=198&iListbox3=MSA-6, 2015.

[93] Advanced-Mechanical-Technology. *AMTI Force Platform Calculations*. Available: www.health.uottawa.ca/biomech/courses/apa6903/amticalc.pdf, 2015.

[94] D. A. Winter, A. E. Patla, S. Rietdyk, and M. G. Ishac, "Ankle Muscle Stiffness in the Control of Balance During Quiet Standing," *Journal of Neurophysiology,* vol. 85, pp. 2630-2633, 2001.

[95] M. Schmid, G. Beltrami, D. Zambarbieri, and G. Verni, "Centre of pressure displacements in trans-femoral amputees during gait," *Gait & Posture,* vol. 21, pp. 255-262, 4/ 2005.

[96] Vicon-Limited, "Plug-In Gait Manual," ed. Oxford UK.

[97] Vicon-Limited, "Oxford Foot Model 1.4 Release Notes," ed: Vicon Motion Systems, June 2012.

[98] Mathworks-Original. *Matlab*, 2014.

[99] A. Z. Richard Hartley, *Multiple View Geometry in Computer Vision Second Edition*. Cambridge, UK: Cambridge University Press, 2003.

[100] T.F.Yu,Available:
http://www2.warwick.ac.uk/fac/sci/physics/outreach/sciencesnaps/gallery/researcher-entries/tungfaiyu/, August 2010.

[101] Vicon-Limited, "Plug-in Gait Product Guide-Foundation Notes," ed. Oxford, UK: Vicon Motion systems, March 2010.

[102] C. Drewes, "Electromyography: Recording Electrical Signals from Human Muscle," ed Iowa State University, Department of Zoology and Genetics, pp. 248-270, 2000.

[103] P. Konrad, "The ABC of EMG: A Practical Introduction to Kinesiological Electromyography," March 2006.

[104] Tekscan-Inc, "Tekscan F-Scan User Manual," ed. Boston, USA, February 2014.

[105] R. A. Christman, "Chapter 16 - Overview of Special Imaging Studies," in *Foot and Ankle Radiology*, ed Saint Louis: Churchill Livingstone, pp. 317-343, 2003.

[106] C. Chillemi, A. Gigante, A. Verdenelli, M. Marinelli, S. Ulisse, A. Morgantini, *et al.*, "Percutaneous repair of achilles tendon rupture: ultrasonographical and isokinetic evaluation," *Foot and Ankle Surgery,* vol. 8, pp. 267-276, 2002.

[107] C. W. Heron, "Magnetic resonance imaging of the ankle and foot," *The Foot,* vol. 3, pp. 1-10, 3/ 1993.

[108] Siemens. *Achilles Tendon Tear*. Available: https://health.siemens.com/ct/image-contest/show/index/388/achilles-tendon-tear/1, 2010-2013.

[109] The-Bone-and-Joint-Journal. *The use of ultrasound in the assessment and treatment of Achilles tendinosis*. Available: http://www.bjj.boneandjoint.org.uk/content/91-B/11/1405/F2, 2015.

[110] C. N. Maganaris and J. P. Paul, "Tensile properties of the in vivo human gastrocnemius tendon," *Journal of Biomechanics,* vol. 35, pp. 1639-1646, 12/ 2002.

[111] C. N. Maganaris, "Tensile properties of in vivo human tendinous tissue," *Journal of Biomechanics,* vol. 35, pp. 1019-1027, 8/ 2002.

[112] N. Chatzistefani, M. J. Chappell, C. Hutchinson, and N. D. Evans, "A Mathematical Model of the Achilles tendon in humans," *IFAC-PapersOnLine,* vol. 48, pp. 429-434, 2015.

[113] J. Richards, *Biomechanics in Clinic and research*, 2008.

[114] N. K. Subhra Chowdhury "Estimation of Forces and Moments of Lower Limb Joints from Kinematics Data and Inertial Properties of the Body by Using Inverse Dynamics Technique," *Journal of Rehabilitation Robotics,* pp. 93-98, 2013.

[115] A. Crowe, "A mechanical model of muscle and its application to the intrafusal fibres of the mammalian muscle spindle," *Journal of Biomechanics,* vol. 3, pp. 583-592, 11/01 1970.

[116] G. L. Gottlieb and G. C. Agarwal, "Dynamic relationship between isometric muscle tension and the electromyogram in man," *Journal of Applied Physiology,* vol. 30, pp. 345-351, 1971.

[117] T. F. Yu and A. J. Wilson, "A passive movement method for parameter estimation of a musculo-skeletal arm model incorporating a modified hill muscle model," *Computer Methods and Programs in Biomedicine,* vol. 114, pp. e46-e59, 5/ 2014.

[118] G. A. Lichtwark and A. M. Wilson, "Is Achilles tendon compliance optimised for maximum muscle efficiency during locomotion?," *Journal of Biomechanics,* vol. 40, pp. 1768-1775, / 2007.

[119] M. D. Mann. *Chapter 14: Muscle Contraction.* Available: http://michaeldmann.net/mann14.html, 2011.

[120] D. Barrows. *The Difference Between an Isotonic and Isometric Contraction.* Available: http://www.livestrong.com/article/382348-the-difference-between-an-isotonic-and-isometric-contraction, 2013.

[121] S. Adhikari, J. Marx, and T. Crum, "Point-of-care ultrasound diagnosis of acute Achilles tendon rupture in the ED," *The American Journal of Emergency Medicine,* vol. 30, pp. 634.e3-634.e4, 5/ 2012.

[122] V. M. Systems, "Oxford Foot Model 1.4 release notes," June 2012.

[123] M. Ishikawa, P. V. Komi, M. J. Grey, V. Lepola, and G. P. Bruggemann, "Muscle-tendon interaction and elastic energy usage in human walking," *Journal of Applied Physiology,* vol. 99, pp. 603-608, 2005.

[124] W. Rose. *Electromyogram analysis/Mathematics and Signal Processing for Biomechanics.*Available: https://www1.udel.edu/biology/rosewc/kaap686/notes/EMG%20analysis.pdf, 2014.

[125] J. W. Bartlett and C. Frost, "Reliability, repeatability and reproducibility: analysis of measurement errors in continuous variables," *Ultrasound in Obstetrics and Gynecology,* vol. 31, pp. 466-475, 2008.

[126] M. J. Chappell and R. N. Gunn, "A procedure for generating locally identifiable reparameterisations of unidentifiable non-linear systems by the similarity transformation approach," *Mathematical Biosciences,* vol. 148, pp. 21-41, 2/ 1998.

[127] N. D. Evans and M. J. Chappell, "Extensions to a procedure for generating locally identifiable reparameterisations of unidentifiable systems," *Mathematical Biosciences,* vol. 168, pp. 137-159, 12/ 2000.

[128] N. Chatzistefani, M. J. Chappell, C. Hutchinson, S. Kletzenbauer, and N. D. Evans, "A mathematical model characterising Achilles tendon dynamics in flexion," *Mathematical Biosciences,* vol. 284, pp. 92-102, 2/ 2017.

[129] S. M. Morrison, T. J. M. Dick, and J. M. Wakeling, "Structural and mechanical properties of the human Achilles tendon: Sex and strength effects," *Journal of Biomechanics,* vol. 48, pp. 3530-3533, 15 June 2015.

[130] T. Muraoka, T. Muramatsu, T. Fukunaga, and H. Kanehisa, "Elastic properties of human Achilles tendon are correlated to muscle strength," *Journal of Applied Physiology,* vol. 99, pp. 665-669, 2005.

[131] B. R. Freedman, J. A. Gordon, and L. J. Soslowsky, "The Achilles tendon: fundamental properties and mechanisms governing healing," *Muscles, Ligaments and Tendons Journal,* vol. 4, pp. 245-255, 14/07 2014.

[132] C. Maganaris, "Imaging-based estimates of moment arm length in intact human muscle-tendons," *European Journal of Applied Physiology,* vol. 91, pp. 130-139, 03/01 2004.

[133] T. Fukunaga, M. Ito, Y. Ichinose, S. Kuno, Y. Kawakami, and S. Fukashiro, "Tendinous movement of a human muscle during voluntary contractions determined by real-time ultrasonography," *Journal of Applied Physiology,* vol. 81, pp. 1430-1433, 1996.

Appendix A

1. Biomedical & Scientific Research Ethics Committee (BSREC) Protocol Guidance

BIOMEDICAL & SCIENTIFIC RESEARCH ETHICS COMMITTEE (BSREC)

Title: Simulation of the Achilles tendon (Version 4)

Contact details:

Chief Investigator(s): DR MICHAEL CHAPPELL, DR NEIL EVANS

Principal Investigator(s): NEFELI CHATZISTEFANI

Summary:

This PhD research is on the Achilles tendon, its injuries and its rehabilitation. The basic aim of this research is to develop a musculoskeletal model of the Achilles tendon using motion capture data. To accomplish this, human gait and other everyday movements (e.g. climbing stairs) will be studied.

Gait can be defined as walking, as a method of movement that uses the two legs alternately and provides both propulsion and support [1]. Gait analysis in general helps us study different kinds of movement patterns as well as the forces involved in producing those movements and also measure and interpret kinematics and kinetics [2]. Gait analysis nowadays is more reliable since it uses computers and videography to capture, observe and interpret the different kinds of movements [2, 3]. Reflective markers are attached to the body of the subject. Cameras are positioned in a way that at least two of them can see each reflective marker at any given time. The original 3D trajectories can be reconstructed from these points giving us the ability to track the movement of the body in motion [3]. Experiments will be conducted in the Gait Laboratory of the University of Warwick to support and validate the simulation of the Achilles tendon.

Human volunteers will be asked to take part in gait laboratory sessions. They will be requested to walk at their normal pace while having reflective markers attached to them or while wearing a Tekscan plantar pressure insole device. The reflective markers will be positioned in non-intrusive locations on their lower body, torso and feet initially based on the Oxford Foot Model (OFM) guidelines. The Tekscan plantar pressure insole sensors will be placed in the volunteers'

BSREC Protocol guidance; version number: 2012-13.01; Version date: 01Oct12
Investigator's protocol issue date: 31March15
Investigator's protocol version number: [4]

1

174

own shoes or in shoes provided by the Gait Laboratory. Two Velcro ankle bands will be wrapped around the subjects' legs just above the ankle bones respectively to prevent slippage. A calf unit will be attached to each sensor and will then be placed on the ankle bands. All devices will be placed at non-intrusive locations and therefore will not inhibit any kind of movement. Measurements of the pressure forces of the different parts of the foot will be acquired using the Tekscan plantar pressure insole equipment. A small cohort (up to 10) volunteers will also be asked to undergo ultrasound scans at the University Hospitals Coventry and Warwickshire (UHCW). These will be normal subjects, including UHCW employees. A doctor or a sonographer - a specialist trained in the use of ultrasound - will perform the scans of the volunteers. These scans will assist in creating a more accurate mathematical model of the Achilles tendon in terms of the model geometry and parameterisation related to the anatomy and physiology.

Background:

The evolution of the Achilles tendon includes that i) it is the strongest tendon in the body, ii) it has an energy-saving mechanism for fast locomotion iii) it allows humans to walk, jump and run and iv) it is a spring and shock absorber during gait. A disadvantage is that the causes of its pathology are complicated [4]. Achilles tendon injuries can be caused by misalignment, overuse, medication side effects, accidents and sometimes by the use of improper footwear [5]. There has been observed an increase in Achilles tendon pathologies in recent years. When overused, the Achilles tendon is one of the two most commonly injured tendons and is the most frequently ruptured one. Changes in activity such as sudden increases in the duration or intensity of athletic training, or individuals engaging in irregular strenuous physical activities may cause overuse injuries and ruptures. The main goal of this PhD project is to provide a validated model of the Achilles tendon that could provide specific parameters for a patient studied and could be a first step towards creating a dynamic model of the human body. This could become a useful clinical tool that could evaluate gait pathologies, could help in preventing foot injuries and could assist rehabilitation of Achilles tendon injuries.

Musculoskeletal computer models are often created in order to understand and define the effects that pathological conditions and surgical procedures have on the movement and function of tendons. Typically, the Achilles tendon is modelled as having a single point

BSREC Protocol guidance; version number: 2012-13.01; Version date: 01Oct12
Investigator's protocol issue date: 31March15
Investigator's protocol version number: [4]

2

insertion on the posterior aspect of the heel. This model simplifies the geometry and structure of the tendon and needs alterations. Mathematical models have been used to describe stress in the Achilles tendon and acquire information about its loading during a motion [6]. However, all authors agree that modelling the Achilles tendon is a difficult and painful task given that its structure, kinetics and mechanisms cannot be easily defined [6-8].

Since numerous independent segments make up the structure of the foot and ankle complex, single-segment foot models are inadequate to reveal inter-segment foot kinematic changes during gait. A solution to this problem is the development of multi-segment foot models. Even though a number of kinematic foot and ankle models have been developed only the Milwaukee and the Oxford Foot Models seem to have external validity in the literature [9-11]. The Oxford Foot Model is the most widely accepted one since it has been validated and was able to evaluate the reliability of the protocol and the model.

There are not generally many measurements performed specifically for the Achilles tendon. There is a lack of accurate mathematical models describing the structure and behaviour of the Achilles tendon in the literature. A viscoelastic foot model has been developed by Gilchrist et al. [12]. This is a three-dimensional, two part model of the foot which has nine spring/damper systems as contact elements of the foot and the walking surface. The foot was modelled as two segments, the forefoot and the main foot with a revolute joint between them [12, 13]. This research project aims to produce a mechanical/mathematical model that will combine findings from the Gilchrist model and results from the Oxford Foot Model experiments conducted. The structure of this new model will depend upon the parameters identified from the measurements obtained from the Gait Laboratory sessions (i.e. the gait analysis, OFM and plantar pressure analysis sessions).

Aims and Objectives of the study:

The main objective of the project is a better understanding of the Achilles tendon, ways to prevent its injuries and how rehabilitation works through modelling of the tendon and its locality. This will help many individuals with Achilles tendon disorders that undergo short or long term therapies to i) understand the function of a healthy Achilles tendon ii) realise what limitations they have due to their injuries or disorders and iii) assist their gradual and painless rehabilitation.

3

The basic aim of developing a musculoskeletal model of the Achilles tendon using motion analysis data is that it can potentially become a useful clinical tool that could evaluate gait pathologies. Accurate model outcomes can be used to study how particular muscles contribute to movement coordination and propose or assess interventions to prevent foot injuries. Parameterised state space models will be used to characterise the Achilles tendon. Data collection to support parameterisation and validation of such models will be obtained through bibliographical research, ultrasound and MRI images obtained from project collaborators at UHCW hospital, but most importantly would be performed within the School of Engineering's Gait Laboratory, using volunteers obtained through Warwick Medical School, UHCW and colleagues at the University of Warwick. However, in this initial study, no patients from UHCW will be invited to take part in the experiments conducted and all the images obtained will abide with the UHCW ethics. Through analyzing the results obtained we will be able to understand how the Achilles tendon works and have an idea of what its interconnections with joints, musculature and soft tissues are. By understanding how normal gait works when using a "healthy" subject and by comparing it with pathological gait, we might be able to prevent Achilles tendon injuries and help patients with rehabilitation. Another aim of these experiments is to study the forces generated between the foot and the walking surface as well as the internal forces between the Achilles tendon and other adjacent tendons. This might assist in preventing injuries and ruptures as well as help with the recognition of any Achilles tendon pathologies at a fairly early stage.

Design/Methodology:

Experimental work and data collection will be performed in the Gait Laboratory and the surrounding area within the School of Engineering. A method called motion capture will be used. This allows joint motion in the foot to be measured quantitatively during normal function. Reflective markers will be placed on participants in order to study the motion, kinetics, forces etc. of the Achilles tendon. Twelve infra-red cameras will be used to "see" the reflective markers placed on the participant in a way that at least three of them can see each marker at any time. The system will then track these markers in time and 3D space. If the reflection of a marker appears in three or more camera's shots instantaneously, then its position can be calculated. The cameras are only capable of detecting the reflective markers. A force plate will be used to record the total force exerted on the plate during a dynamic experiment such as a

4

single step on it or a static one by just standing still on the force plate. The force plate provides the Ground Reaction Force (GRF) of the subject when they stand on it and this provides the external force necessary to perform some of the calculations. Two digital video (DV) cameras allow us to actually capture a video of any trials that run in the Gait Laboratory in a way that is synchronised with the rest of the system. Occasionally one or two trials might need to be recorded. This will help us understand and analyse the data obtained. In such cases, participants must agree and sign a consent form. These video captures will not be shared with anyone outside the members of the research group. There is a small likelihood that these videos or stills may be used for papers or posters presented to a scientific audience at conferences. All facial features of the participants will be masked and there will not be any possibility of them being recognised. All videos can be deleted at any time upon request.

In order to reconstruct the foot and its components, physical parameters such as body mass, height, leg length, knee width and ankle width will also need to be determined. Initially a new "subject" will be created by entering these parameters in the Gait Laboratory system. Then the markers will be placed on the participant. Forty-three (43) reflective markers need to be positioned in line with the Oxford Foot Model guidelines in order to conduct the same experiment on all participants. The Oxford Foot Model is a predetermined marker positioning system which is recognised by the gait laboratory software. This will permit comparison across all results. The markers will be attached to the skin or tight-fitting clothing using double-sided tape.

Upon completing this procedure, the trials will begin. A static trial will be performed and will be used to scale the underlying model appropriately for the "subject". The participant will stand on the force plate and stand still for a few seconds. Afterwards dynamic trials will be performed. The participant will be asked to walk in the Gait Laboratory room making sure to step on the force plate during the motion. She/he will not be required to make any violent or harmful movements. Participants might be asked to move quickly, stand up on toes or jump lightly in a way they feel will not cause discomfort or injury. At least three repetitions of each dynamic trial will be required. In order to investigate joint angles, torques, powers and moments all information and results obtained will be processed by the Vicon Nexus software. Further processing of the obtained data will be conducted by the use of other software tools such as MATLAB.

5

The most powerful muscle group in the body is the leg muscles where the Achilles tendon forms the thickest and strongest tendon. Its primary role is to plantarflex the ankle and therefore the Achilles tendon is essential for normal propulsion and gait. Any contraction of the calf muscles pulls the Achilles tendon, which results in pushing the foot downwards. This contraction enables walking, jumping, running and standing on the toes. When in movement, the Achilles tendon tends to be affected mostly by the tendons in the medial section of the foot that are the tibialis posterior, the flexor digitorum longus and the flexor hallusis longus ("Tom, Dick and Harry"). That is why it is important to examine the internal forces of the tendon and its interconnection with joints, musculature and soft tissues. To do that, measurement of the plantar pressure, i.e. the distribution of force over the sole of the foot, is useful as it provides detailed information specific to each region of contact of the foot. The Tekscan plantar pressure insole sensors will be placed in the participants' own shoes or in shoes provided by the Gait Laboratory. Two Velcro ankle bands will be wrapped around the subject's legs just above the ankle bones respectively. Two calf units will each be attached to a sensor and will then be placed on the ankle bands. After the calibration of the system, walking trials will take place and force distribution analysis results will be obtained. All devices will be placed in non-invasive positions of the participants' bodies and the use of any materials will not induce allergic reactions or otherwise harm the participants.

An electro-goniometer provides us with the means to measure the angles of the joints in real time. Participants might be asked to use such equipment outside the Gait laboratory with the assistance of a wireless EMG kit that will record the surface electrical activity of the skeletal muscles via pads placed on the skin. This will assist in understanding how the Achilles tendon is interconnected with the nearest joints and the influence they have on the way different individuals walk.

Ultrasound is the best tool for assessing tendons and ligaments due to its high resolution and ability to scan dynamically. It is used to evaluate chronic tendinopathy of the Achilles tendon, inflammation of its surrounding soft tissues (e.g., paratenon) and also to scan partial or complete tendon tears. Ultrasonography is a very safe procedure since it does not use a high magnetic field to produce an image, it is cost effective and can also evaluate a tendon in longitudinal as well as transverse projections, in both static and dynamic views. In this research we will only use the scans taken from the UHCW to measure the changes in length of the Achilles tendon and the gastrocnemius muscle in dorsiflexion and plantar flexion of the foot segment. This will

BSREC Protocol guidance; version number: 2012-13.01; Version date: 01Oct12
Investigator's protocol issue date: 31March15
Investigator's protocol version number: [4]

6

179

assist in learning the true elongation of the Achilles tendon under load when a person walks. These tests have been recommended by a clinician from UHCW; the measurements will not be invasive in any way; and because they will be part of a specific process which looks only into the anatomy of the Achilles tendon and not into any pathological issues, it will not clash with any medical confidentiality. A lubricating gel will be placed onto the skin of the volunteers by a doctor or a sonographer. A small handheld device called a transducer will be placed onto the skin, and moved over the Achilles tendon which is the only part of the body examined. The lubricating gel allows the transducer to move smoothly and ensures that there is continuous contact between the sensor and the skin. The transducer is connected to a computer and a monitor. Pulses of ultrasound will be sent from a probe in the transducer, through the skin and into the body. They will then bounce back from the structures of the body and will be displayed as an image on the monitor. Volunteers should not feel anything other than the sensor and gel on their skin which might feel a little cold, but should not cause any discomfort at all. Any volunteer is free to withdraw from the ultrasound scan procedure at any time. As stated above a doctor or a sonographer will perform the scans to the volunteers. Should the scan show anything unforeseen, the medical person will provide medical advice to the volunteer immediately. Those scans will not be used in the experiments if the volunteers do not wish to. All images obtained from UHCW will comply with NHS ethics approval for the collection and use of such images.

   The experimental phase of this study will be quantitative and prospective. Most of the published studies in journals use 15-20 participants when conducting experiments. So, approximately forty-five volunteers will be required to gain the necessary data for this project. They are likely to be between the ages of 18 and 65. Roughly 15 volunteers for each group age (18 to 30, 31 to 50, 51 to 65) will be needed. Participants must be capable of walking around the Gait Laboratory for up to ten minutes unaided. Both sexes will be requested to participate, but the sample of volunteers will not be divided according to gender, since there does not seem to be an anatomical difference of the Achilles tendon between men and women. A mass email inviting volunteers will be sent to the School of Engineering's students and staff, to all the members of the Sports Centre at the University of Warwick, to students and staff of the Medical School in Warwick, University House and to the Student Union so that students from all departments of the University of Warwick can take part in the study if they want to (see attached invitation email). A news item calling for volunteers will also be placed on the School

7

of Engineering's webpages. A Participant Information Leaflet will be given to each volunteer and they will be asked to read it carefully before taking part. They will be encouraged to ask any questions they might have concerning the experiment and the Gait Laboratory sessions. Subsequently they will be asked to sign a consent form which will enable their data to be used and analysed in this PhD research project. As people grow older, the morphology, the structure and the behaviour of the Achilles tendon deteriorates. We will divide our volunteers into age groups in order to see if there are any differences when the age changes. On the consent form they will be asked to tick a box stating if they are between 18 to 30 years old, 31 to 50 years old or 51 to 65 years old. They will also be asked to tick a box affirming if they have any Achilles tendon pathologies such as paratendonitis, paratendonitis with tendinitis, tendinitis with rupture, insertional tendinitis, tendinosis, haglung deformity inflammation and chronic disruption or if they have had an Achilles tendon rupture in the past. No volunteer having the above listed pathologies will be excluded from the study as long as he/she is capable of walking around the Gait Laboratory for up to ten minutes unaided. We are only asking about the presence of these pathologies in order to see if there are any differences in the way people walk and do their everyday movements if these pathologies are present. All completed consent forms will be safely stored in a locked cabinet in a locked office on the University premises away from the Gait Laboratory. Each consent form will contain a Subject Identifier which is an anonymously assigned number that will be used to label the data sets generated in the Gait Laboratory. It will not be possible to identify any participant since the only personal data collected will be the listed physical measurements necessary for the project.

Any participant is free to withdraw from the experiments at any time. Any collected data will be deleted and will not be used in any succeeding analyses. However, withdrawal from the study after 10 weeks may mean that results from a prior analysis of the data may have already been processed and added to the research report or may be published as a research paper. Such results will be utterly anonymous and by no means will they be traceable back to the participant. Any participant who wishes to withdraw can contact the investigator of this project. The consent forms will be retrieved from the secure location and the withdrawing participant's unique identifying number will be found. The corresponding data set will be deleted and the participant's consent form will be destroyed. These actions will be confirmed by any of the two chief investigators.

8

Ethical considerations:

Informed Consent

Participants will be asked to volunteer for the study willingly and will not be pressured into taking part. They will be given a Participant's Information Leaflet which will clearly state the purpose of this research project and they will be asked to read it carefully. All participants will be urged to ask any questions they might have about the project before completing any paperwork. If all of their questions are answered thoroughly and they are willing to participate in this study, they will be asked to complete a written consent form. No participant will be coerced into taking part by being promised reward or otherwise.

Participant Confidentiality and Data security

All data collected during this project will be confidential. No participant will be identified as Randomly Assigned Subject Identifiers will be used to anonymise the data obtained from each volunteer. All data will be collected, stored and processed by the principal and chief investigators. While conducting the experiments, all completed consent forms will be stored in a locked cabinet in a locked office on university premises away from the Gait Laboratory. The Consent Forms will be retained for the duration of the project and potentially after its completion if the data is to be reserved. If this is the case each participant will be contacted and they will be allowed to remove their data if desired. The final PhD thesis, which will include anonymous aggregated data, will be available through the University of Warwick Publication Service in electronic form. All data will be safely and securely stored for 10 years according to University policy.

Right of Withdrawal

Any participant can withdraw from the study at any time. Any collected data will be deleted and not be used in any succeeding analyses. However, withdrawal from the study after 10 weeks may mean that results from a prior analysis of the data may have already been processed and added in the research report or may be published as a research paper. Such results will be entirely anonymous and no participant will be identifiable. Any participant who wishes to withdraw can contact any member of the group conducting the experimenters, and all data

9

associated with that volunteer will be deleted immediately. If a participant has agreed to be video recorded and does not wish that any more, he/she can contact any of the investigators at any time and all of his/her videos will be deleted.

Benefits and Risks

No major risks can be identified with the conduction of these experiments. Since participants will be asked to walk around the Gait laboratory facilities, stand up on toes, step on a staircase and jump carefully, the main hazard associated with this study is the isolated risk of tripping whilst in the Gait Laboratory. Nevertheless, this is unlikely to happen and unlikely to result in serious injury. There also appears some potential for a participant to have an allergic reaction to the double sided tape which will be used to attach the reflective markers to their skin. This risk will be diminished by asking the participant if they know of any likely reaction before use.

No direct benefits to the volunteers are expected. However, their participation will help in the development of a new and reliable musculoskeletal model characterising the dynamics of the Achilles tendon and its interconnections with joints, musculature and soft tissues. This may help many individuals with Achilles tendon disorders that undergo short or long term therapies and can also potentially become a useful clinical tool that could evaluate gait pathologies.

Financing:

This is a PhD research project and is not funded externally. However, I am awarded a full scholarship from the School of Engineering at the University of Warwick.

Dissemination and Implementation:

At completion of the experiments, all collected data will be processed and used mainly in my PhD thesis. Some of these may be used in papers to be published in journals or posters to be presented at conferences. The PhD thesis will be available through the University of Warwick

10

Publication Service in electronic form. All data will be safely and securely stored for 10 years according to University policy.

References

[1] **M. W. Whittle, "Chapter 2 - Normal gait," in** *Gait Analysis (Fourth Edition)***, ed Edinburgh: Butterworth-Heinemann, 2007, pp. 47-100.**

[2] **T. L. Switaj and F. G. O'Connor, "Chapter 43 - Gait Analysis," in** *The Sports Medicine Resource Manual***, ed Philadelphia: W.B. Saunders, 2008, pp. 536-542.**

[3] **C. Kirtley, "Chapter 3 - Three-dimensional gait analysis," in** *Clinical Gait Analysis***, ed Edinburgh: Churchill Livingstone, 2006, pp. 53-71.**

[4] **S. Malvankar and W. S. Khan, "Evolution of the Achilles tendon: The athlete's Achilles heel?,"** *The Foot,* **vol. 21, pp. 193-197, 12// 2011.**

[5] **K. Brandt. (5th June).** *Achilles tendon information*

   Available: http://achillestendon.com/achilles-tendon-information/

[6] **E. Wallenböck, O. Lang, and P. Lugner, "Stress in the achilles tendon during a topple-over movement in the ankle joint,"** *Journal of Biomechanics,* **vol. 28, pp. 1091-1101, 9// 1995.**

[7] **J. H. C. Wang, "Mechanobiology of tendon,"** *Journal of Biomechanics,* **vol. 39, pp. 1563-1582, // 2006.**

[8] **R. A. Zifchock and S. J. Piazza, "Investigation of the validity of modeling the Achilles tendon as having a single insertion site,"** *Clinical Biomechanics,* **vol. 19, pp. 303-307, 3// 2004.**

11

[9]   C. Bishop, G. Paul, and D. Thewlis, "Recommendations for the reporting of foot and ankle models," *Journal of Biomechanics,* vol. 45, pp. 2185-2194, 8/31/ 2012.

[10]   C. J. Wright, B. L. Arnold, T. G. Coffey, and P. E. Pidcoe, "Repeatability of the modified Oxford foot model during gait in healthy adults," *Gait & Posture,* vol. 33, pp. 108-112, 1// 2011.

[11]   J. Stebbins, M. Harrington, N. Thompson, A. Zavatsky, and T. Theologis, "Repeatability of a model for measuring multi-segment foot kinematics in children," *Gait & Posture,* vol. 23, pp. 401-410, 6// 2006.

[12]   L. A. Gilchrist and D. A. Winter, "A multisegment computer simulation of normal human gait," *IEEE Trans Rehabil Eng,* vol. 5, pp. 290-9, Dec 1997.

[13]   L. A. Gilchrist and D. A. Winter, "A two-part, viscoelastic foot model for use in gait simulations," *Journal of Biomechanics,* vol. 29, pp. 795-798, 6// 1996.

Appendices (e.g. questionnaire(s), patient information leaflet(s), consent form(s), interview schedule(s), interview topic guide(s)):

Consent Form

Participant Information Leaflet

Invitation email

2. Participant Information Leaflet

THE UNIVERSITY OF
WARWICK

PARTICIPANT INFORMATION LEAFLET

Study Title: **Simulation of the Achilles tendon**

Investigator(s):   **Nefeli Chatzistefani, Dr Neil Evans (Academic Co-Supervisor),
Dr Mike Chappell (Academic Co-Supervisor)**

Introduction

You are invited to take part in a research study. Before you decide, you need to understand why the research is being done and what it would involve for you. Please take the time to read the following information carefully. Talk to others about the study if you wish.

(Part 1 tells you the purpose of the study and what will happen to you if you take part. Part 2 gives you more detailed information about the conduct of the study)

Please ask us if there is anything that is not clear or if you would like more information. Take time to decide whether or not you wish to take part.

PART 1

What is the study about?

The basic aim of this PhD research project is to develop a mathematical model of the Achilles tendon using motion capture data. To accomplish this, human gait and other everyday movements like climbing stairs or standing on ones' toes will be studied. Gait can be defined as the manner in which each person walks. Gait analysis in general helps us study different kinds of movement patterns as well as the forces involved in producing those movements. By understanding how normal gait works and then comparing it with changes in gait due to Achilles tendon injuries, we may be able to assist in prevention of injuries and help patients with rehabilitation. Another aim of these experiments is to study the forces generated between the foot and the walking surface as well as the internal forces between the Achilles tendon and other adjacent tendons. This may assist in preventing ruptures as well as help with the recognition of any Achilles tendon pathologies in a fairly early stage. We are searching for volunteers to take part in simple motion analysis experiments. Each

participant will be asked to walk around the University of Warwick's Gait Laboratory while wearing reflective markers placed on non-intrusive positions on their body. The markers will be positioned on the lower limbs of the participants, on the skin or on tight fitting clothing using double-sided tape. Infrared cameras can only see reflections and therefore will only record the position of these reflective markers, and from their motion, the participant's trajectory will be reconstructed and their gait pattern will be calculated. Specific physical parameters such as weight, height, knee width, ankle width and leg length are necessary for the system to analyse human motion and will need to be recorded prior to capturing the motion data.Measurements of the pressure forces of the different parts of the foot will be acquired using Tekscan plantar pressure insole equipment. To do this, Tekscan plantar pressure insole sensors will be placed in the volunteers' own shoes or in shoes provided by the Gait Laboratory. All devices will be placed at non-intrusive locations and therefore will not inhibit any kind of movement. Approximately forty-five volunteers in total will be needed for this study.

Do I have to take part?

It is entirely up to you to decide. We will describe the study and go through this information sheet, which we will give you to keep. If you choose to participate, we will ask you to sign a consent form to confirm that you have agreed to take part (if part of this study is an online or postal questionnaire/survey, by returning a completed questionnaire/survey, you are giving your consent for the information that you have supplied to be used in this study and formal signed consent will not be collected where postal or online questionnaires/surveys are concerned). You will be free to withdraw at any time, without giving a reason and this will not affect you or your circumstances in any way.

What will happen to me if I take part?

You will be asked to stand still, stand on your toes, walk and jump if possible in the Gait Laboratory, wearing reflective markers so that your gait can be analysed. You will also be asked to walk around the Gait Laboratory or the adjacent premises while wearing Tekscan insoles provided by our laboratory. The Tekscan plantar pressure insole sensors will be placed in your own shoes or in shoes provided by the Gait Laboratory. Two Velcro ankle bands will be wrapped around your legs just above the ankle bones respectively to prevent slippage. A calf unit will be attached to each sensor and will then be placed on the ankle bands. You will then be asked to walk at your normal pace in order for the system to take measurements of the plantar pressure, i.e. the distribution of force over the sole of the foot, which is useful as it provides detailed information specific to each region of contact of the foot.

An electro-goniometer provides us with the means to measure the angles of the joints in real time. You may be asked to use such equipment with the assistance of a wireless EMG kit that will record the surface electrical activity of the skeletal muscles via pads placed on the skin. This will assist in understanding how the Achilles tendon is interconnected with the nearest joints and the influence they have on the way different individuals walk.

All movements can be done at your own pace. You can take time to rest in-between if you need, as we understand that some people taking part in this study may struggle with certain activities.

The markers and the goniometer need to be precisely placed on your lower body, so the investigator will ask for your permission to put them on you. The markers, the electrogoniometers and the Tekscan insoles will not be placed anywhere intrusive and will not cause any form of discomfort.

As people grow older, the morphology, the structure and the behaviour of the Achilles

tendon deteriorates. We will divide you into age groups in order to see if there are any differences when the age changes. On the consent form you will be asked to tick a box stating if you are between 18 to 30 years old, 31 to 50 years old or 51 to 65 years old.
 You will also be asked to tick a box affirming if you have any Achilles tendon pathologies such as paratendonitis, paratendonitis with tendinitis, tendinitis with rupture, insertional tendinitis, tendinosis, haglung deformity inflammation and chronic disruption or if you have had an Achilles tendon rupture in the past. No volunteer having the above listed pathologies will be excluded from the study as long as he/she is capable of walking around the Gait Laboratory for up to ten minutes unaided. We are only asking about the presence of these pathologies in order to see if there are any differences in the way people walk and do their everyday movements if these pathologies are present.

You may be asked to undergo ultrasound scans at the University Hospitals Coventry and Warwickshire (UHCW). A doctor or a sonographer-a specialist trained in the use of ultrasound- will perform the scans to you. A lubricating gel will be placed onto your skin. A small handheld device called a transducer will be placed onto your skin, and moved over the Achilles tendon which is the part of the body being examined. The lubricating gel allows the transducer to move smoothly and ensures there is continuous contact between the sensor and the skin. The transducer is connected to a computer and a monitor. Pulses of ultrasound will be sent from a probe in the transducer, through the skin and into the body. They will then bounce back from the structures of the body and will be displayed as an image on the monitor. You should not feel anything other than the sensor and gel on your skin which might be a little bit cold, but does not cause any discomfort at all. You are free to withdraw from the ultrasound scan procedure at any time. These scans will assist in creating a more accurate mathematical model of the Achilles tendon. As stated above a doctor or a sonographer will perform the scans to you. Should the scan show anything unforeseen, the medical person will provide medical advice to you immediately. Your scans will not be used in the experiments if you do not wish to.

You may be asked to allow us to capture a digital video of your walking trial. This will help us understand and analyse the data obtained   from the trial. Only if you agree to be recorded, will you be asked to sign a consent form. These video captures will not be shared with anyone outside the members of the research group. There is a small likelihood that these videos or stills may be used for papers or posters presented to a scientific audience at conferences. All facial features will be masked and there will not be any possibility of you being recognised. All videos can be deleted at any time upon request. If you have any questions about these videos and their necessity please feel free to ask the investigators about them.

What are the possible disadvantages, side effects, risks, and/or discomforts of taking part in this study?

The experiments appropriate for this study involve walking and doing everyday activities such as standing on ones' toes or climbing a stair. Therefore, there are not any disadvantages, side effects, risks and/or discomforts that the participant might experience while doing the movements.There appears to be some potential for a volunteer to have an allergic reaction to the double sided tape which will be used to attach the reflective markers to their skin. This risk will be diminished by asking the participant if they know of any likely reaction before use.

What are the possible benefits of taking part in this study?

No personal benefits are expected. However, your participation will help in the development of a new and reliable mathematical model characterising the dynamics of the Achilles

tendon and its interconnections with joints, musculature and soft tissues. The basic aim of developing such a model is that it can potentially become a useful clinical tool that could evaluate gait abnormalities. By understanding how normal gait works and by comparing it with changes in gait that occur due to Achilles tendon injuries, we might be able to assist in preventing injuries and ruptures, help with the recognition of any Achilles tendon abnormalities in a fairly early stage and help patients with rehabilitation.

Expenses and payments

You will not receive any reimbursement for taking part in this study.

What will happen when the study ends?

At completion of the experiments, all collected data will be processed and used mainly in my PhD thesis. Some of those may be used in papers to be published in journals or posters to be presented at conferences. The PhD thesis will be available through the University of Warwick Publication Service in electronic form.

Will my taking part be kept confidential?

Yes. We will follow strict ethical and legal practice and all information about you will be handled in confidence. Further details are included in Part 2.

What if there is a problem?

Any complaint about the way you have been dealt with during the study or any possible harm that you might suffer will be addressed. Detailed information is given in Part 2.

This concludes Part 1.

If the information in Part 1 has interested you and you are considering participation, please read the additional information in Part 2 before making any decision.

PART 2

Who is organising and funding the study?

This is a PhD research project and is not funded externally. However, I am fully funded by a scholarship from the Engineering department of the University of Warwick.

What will happen if I don't want to carry on being part of the study?

Participation in this study is entirely voluntary. Refusal to participate will not affect you in any way. If you decide to take part in the study, you will need to sign a consent form, which states that you have given your consent to participate.

If you agree to participate, you may nevertheless withdraw from the study at any time without affecting you in any way.

You have the right to withdraw from the study completely and decline any further contact by study staff after you withdraw.

Any participant is free to withdraw from the experiments at any time. Any collected data will be deleted and will not be used in any succeeding analyses. However, withdrawal from the study after 10 weeks may mean that results from a prior analysis of the data may have already been processed and added to the research report or may be published as a research paper. Such results will be utterly anonymous and by no means will they be traceable back to the participant.

If a participant has agreed to be video recorded and does not wish that any more, he/she can contact any of the investigators at any time and all of his/her videos will be deleted.

Any participant is free to withdraw from the ultrasound scans at any time. Any collected data will be deleted and will not be used in any succeeding analyses. Withdrawal from the study will not affect the participant's usual care or any benefits to which they would otherwise be entitled.

What if there is a problem?

This study is covered by the University of Warwick's insurance and indemnity cover. If you have an issue, please contact the Chief Investigator of the study:

Nefeli Chatzistefani (PhD student)
N.Chatzistefani@warwick.ac.uk
+44 (0) 74 496 40785

Who should I contact if I wish to make a complaint?
Any complaint about the way you have been dealt with during the study or any possible harm you might have suffered will be addressed. Please address your complaint to the person below, who is a senior University of Warwick official entirely independent of this study:

Director of Delivery Assurance

Registrar's Office

University House

University of Warwick

Coventry

CV4 8UW

Complaints@Warwick.ac.uk

024 7657 4774

Will my taking part be kept confidential?

All completed consent forms will be safely stored in a locked cabinet in a locked office on the University premises away from the Gait Laboratory. Each consent form will contain a Subject Identifier which is a randomly associated number that will be used to label the data sets generated in the Gait Laboratory. All data will be anonymised with a Randomly Assigned Subject Identifier and it will not be possible to identify any participant. All data will be safely and securely stored for 10 years according to University policy.

What will happen to the results of the study?

The results of this study will be used in order to create and design a mathematical model of the Achilles tendon. All data collected will support parameterisation (the process of deciding and defining the parameters necessary for a complete or relevant specification of a model) and validation of such a model. Hence some or all of the results will appear in my PhD thesis, in papers submitted to any journals for publication and in posters to be presented in conferences.

Who has reviewed the study?

This study has been reviewed and given favourable opinion by the University of Warwick's Biomedical and Scientific Research Ethics Committee (BSREC): REGO-2013-578 AM01 17th March 2015

What if I want more information about the study?

If you have any questions about any aspect of the study, or your participation in it, not answered by this participant information leaflet, please contact:

Nefeli Chatzistefani (PhD student)
N.Chatzistefani@warwick.ac.uk
+44 (0) 74 496 40785

Dr Michell Chappell (Academic Supervisor)
M.J.Chappell@warwick.ac.uk
+44(0)24 765 24309

and

Dr Neil Evans (Academic Supervisor)
Neil.Evans@warwick.ac.uk
+44 (0)24 765 22062

Thank you for taking the time to read this participant information leaflet.

3. Consent form signed by all participants

THE UNIVERSITY OF
WARWICK

CONSENT FORM

(Biomedical and Scientific Research Ethics Committee) Study Number:

Patient Identification Number for this study:

Title of Project: Simulation of the Achilles tendon

Name of Researcher(s): Nefeli Chatzistefani (PhD student), Dr Neil Evans (Academic Supervisor), Dr Michael Chappell (Academic Supervisor)

Please initial all boxes by printing Y if the answer is yes or N if the answer is No

1. I confirm that I have read and understand the information sheet dated **[31March15]** (version **[4]**) for the above study. I have had the opportunity to consider the information, ask questions and have had these answered satisfactorily.

2. I understand that my participation is voluntary and that I am free to withdraw at any time without giving any reason.

3. I have Achilles tendon pathologies such as paratendonitis, paratendonitis with tendinitis, tendinitis with rupture, insertional tendinitis, tendinosis, haglung deformity inflammation and chronic disruption.

4. I have had an Achilles rupture in the past.

5. I agree to take part in the above study.

6. I am between 18 to 30 years old.

7. I am between 31 to 50 years old.

8. I am between 51 to 65 years old.

193

9. I consent to having my trials digitally captured and to having these videos or stills used for papers or posters presented to a scientific audience at conferences.

_____	_____	_____
Name of Participant	Date	Signature

_____	_____	_____
Name of Person	Date	Signature

Page 1 of 1

4. BSREC Approval letter

The following is the letter from the BSREC committee granting me full approval to perform my experiments that comply with the research code of practice of the University of Warwick.

1st April 2015

Warwick
Medical School

PRIVATE
Miss Nefeli Chatzistefani
School of Engineering
University of Warwick
Coventry
CV4 7AL
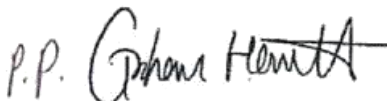
Dear Miss Chatzistefani,

Study Title and BSREC Reference: *Simulation of the Achilles Tendon* REGO-2013-578 AM01

Thank you for submitting the revised substantial amendment application for the above-named project to the University of Warwick's Biomedical and Scientific Research Ethics Sub-Committee.

I am pleased to confirm that the changes that you wish to make to this study have been approved.

Please keep a copy of the signed version of this letter with your study documentation.

Yours sincerely

P.P. (signature)

Professor Scott Weich
Chair
Biomedical and Scientific
Research Ethics Sub-Committee

**Biomedical and Scientific
Research Ethics Sub-Committee**
A010 Medical School Building
Warwick Medical School,
Coventry, CV4 7AL.
Tel: 02476-528207
Email: BSREC@warwick.ac.uk

Medical School Building

The University of Warwick
Coventry CV4 7AL United Kingdom
Tel: +44 (0)24 7657 4880
Fax: +44 (0)24 7652 8375

THE UNIVERSITY OF
WARWICK